University of Alberta

STABILITY OF HAPTIC VIRTUAL ENVIRONMENTS AND TELEOPERATION SYSTEMS : EFFECT OF SAMPLED-DATA CONTROL, COMMUNICATION DELAY AND ACTIVE OPERATOR

by

NOUSHIN MIANDASHTI

A thesis submitted to the Faculty of Graduate Studies and Research
in partial fulfillment of the requirements for the degree of

Master of Science
in
Biomedical Engineering

Department of Electrical and Computer Engineering

Fall 2013
Edmonton, Alberta

Family is not an important thing. It's everything.

This thesis is dedicated to Ali Farshchi Tabrizi, Negin Miandashti, Nahid Nabatian and Nemat Miandashti for their unconditional love and support throughout the course of my M.Sc.

ABSTRACT

Three factors can jeopardize the stability of haptic virtual environments (HVE)s and teleoperation systems: (a) delayed communication channel, (b) controller discretization and (c) active operator intervention. This thesis studies the stability of these systems and investigates the simultaneous effect of all three de-stabilizing factors via a proposed unified framework. The conditions that ensure the stability of these systems are derived and reported. This thesis also addresses the stability problem in the context of teleoperation systems in the four-channel architecture in a passivity-based framework. While it is assumed that the teleoperation system operates in continuous-time and the terminations are passive, the communication delay is compensated for and the stability conditions are derived.

ACKNOWLEDGMENTS

I would like to express my gratitude to my supervisor Dr. Mahdi Tavakoli for the inspiring guidance and engagement and invaluable support throughout my research.

Furthermore I would like to thank all my friends and colleagues who have helped and supported me throughout my journey here at University of Alberta. At last but not least I wish to extend my gratitude to my loved ones, who have supported me throughout the entire process, both by keeping me harmonious and helping me putting pieces together. I will be grateful forever for their love.

CONTENTS

LIST OF FIGURES

LIST OF TABLES

LIST OF ABBREVIATIONS

HVE Haptic virtual environment

PEB Position-error-based

DFR Direct force reflection

4CH Four-channel

ISP Input strictly passive

EOP Excess of passivity

SOP Shortage of passivity

MCU Master control unit

SCU Slave control unit

2PN Two-port network

SLF Single-loop feedback

MLF Multi-loop feedback

ZOH Zero-order-hold

DOF Degree of freedom

1 INTRODUCTION

German philosopher and psychologist Max Dessoir was the first to propose the term haptic to comprehensively encircle all different aspects of sense of touch and its study [26]. Haptic technology relates to a technology that interfaces with a user through the sense of touch. Many applications of haptic enabled interfaces can fall into two main categories: Haptic Virtual Environment (HVE) systems, and Teleoperation systems. A single-user HVE system consists of a human operator and a virtual environment and a haptic interface that acts as a link between them and conveys a kinesthetic sense of presence in the virtual environment to the operator. Surgical simulation [5, 50, 59, 72], VR-based gaming [9, 52], and telerehabilitation [14, 34, 60] are only a few applications of HVE systems. A teleoperation system comprises of a human operator interacting with a master robot, thus remotely controlling a slave robot to perform a task in a remote environment. Ideally, from a performance perspective, the slave robot exactly reproduces the master's position trajectory while the master robot reproduces the slave-environment contact force for the human operator; this is called bilateral teleoperation. Bilateral teleoperation has applications including telesurgery and remote underwater and space exploration. Surveys on bilateral teleoperation can be found in [3, 58, 64].

1.1 THESIS ORGANIZATION AND SYNOPSIS

The main focus of this dissertation is the analysis of stability of HVE and teleoperation systems. Stability is a vital issue and can be jeopardized due to several factors. Here, we narrow the research to three main factors: controller discretization, communication channel delay and operator and/or environment activity. The following presents a brief summary of each chapter in this thesis and how they are connected to each other.

Chapter 3 investigates the stability of HVE systems. An HVE system is a sampled-data system in the sense that it includes a virtual environment simulated in a digital computer while the human operator and the haptic interface are actual physical systems. For this sampled-data, system a stability criterion is given under delayed communication channel and also while allowing the operator to

behave actively. The proposed stability criterion is verified through simulations and experiments involving a Phantom Premium 1.5A robot.

In the study of bilateral teleoperation systems stability, two approaches have been taken in this dissertation. Chapter 4 studies the stability in the context of a sampled-data teleoperation system. It gives a criterion for stability of the teleoperation system when the controllers are modeled by discrete-time systems while the rest of the system is in continuous-time. This stability analysis considers communication delay and active operator/environment. The proposed stability criterion is verified through simulations and experiments involving a pair of Phantom Premium 1.5A robots.

In Chapter 5, the stability of bilateral teleoperation systems is studied when the entire system is assumed to operate in continuous-time. A passivity-based stability criterion is given for a bilateral teleoperation system under the general four-channel (4CH) architecture. The delay in the communication channel is compensated for via wave operation blocks. Also, the stability of 4CH trilateral teleoperation systems is investigated under the architecture proposed in [39].

Finally, the conclusions are discussed in Chapter 6. Also, in this chapter directions for future work are proposed. These include extension of the proposed framework for HVE systems to the case where the robots have more than one degree of freedom. For the bilateral teleoperation system in the sample-data approach, the future work can be the extension to the 4CH architecture. Another extension in both sample-data and continuous-time approaches is to consider multilateral teleoperation systems in the presence of both active terminations and delayed communication channel.

1.2 CONTRIBUTIONS OF THE THESIS

In Chapters 3 and 4, the main contribution is the proposed unified framework using which stability can be investigated in the presence of both delay and active operator/environment while considering the sampled-data nature of HVE and bilateral teleoperation systems. Although the stability of sampled-data HVE systems have been studied extensively in the literature, the effect of active operator has been neglected. The assumption of operator passivity is not always valid and much depends on the task being performed by the operator. This proposed framework enables us to study the stability of both HVE and bilateral teleoperation systems in the

presence of active terminations (operator or environment). Another advantage of this framework over previously proposed methods is that it can be easily applied to m-user HVE systems where $m \geq 2$. This framework also enables us to compare the relative effects of delay, sampling and activity on the stability of HVE and bilateral teleoperation systems. For instance, in the context of sampled-data HVE systems, it has been shown that the effect of communication time-delay on jeopardizing the stability is twice the effect of the sampling period.

Previous studies in the literature tend to model the teleoperation systems via 2-port (teleoperator) and 1-port (operator and environment) networks to address the stability using the physical interpretation of system passivity. In Chapter 5 we propose a transfer matrix based approach to modeling and stability analysis which is easier to follow compared to traditional two-port network based passivity analyses and requires no need for physical interpretation of the signals that are involved in a delay-compensated 4-channel teleoperation system.

In the literature, the passivity-based stability analysis for a delayed teleoperation system under 4CH architecture has mostly been narrowed down to only compensating for the delay in the communication channel while assuming the rest of the system is passive. In Chapter 5, we show that although the master and slave robots are passive systems, when combined with their controllers the passivity may be jeopardized, thus a set of conditions imposed on the controllers are derived.

2

BACKGROUND

In recent years, haptic interfaces have been successfully integrated into a wide range of fields. The many applications of haptic interfaces can fall into two wide categories: haptic virtual environment systems and teleoperation systems. In Section 2.1, we start with a brief overview of haptic virtual environment systems and their applications in recent years. In Section 2.1.1, the passivity and absolute stability of single and multi-user virtual environment systems are briefly discussed. In Section 2.2, a brief overview of bilateral and trilateral teleoperation systems is given, followed by their contemporary applications. In Section 2.2.1, common controller architectures for bilateral and trilateral teleoperation systems are discussed. Then, stability and absolute stability of bilateral and trilateral teleoperation system are discussed in Section 2.2.2. Finally a brief introduction is given to the main three chapters of this thesis.

2.1 HAPTIC VIRTUAL ENVIRONMENT SYSTEMS

A haptic interface acts as a link between a human operator and a virtual environment and conveys a kinesthetic sense of presence in the virtual environment to the operator. Collaborative haptic interaction has gained great attention in recent years both in gaming and medical applications [19, 25, 63, 74]. As an application example, virtual reality (VR) based surgical simulation has opened up new opportunities in medical training and education. The surgeon is provided with both a scene of modeled organs on the computer screen and haptic feedback at the tool handle of the haptic interface. Scheduling various training situations, repeating identical training scenarios, and tracking surgical gestures for future evaluation or replay are only a few advantages of VR-based, haptics-assisted surgical training over the traditional training methods. As another applicaton, VR-based gaming has received massive attention in relation to adding the sense of touch for bringing more realistic feeling to users. It is well-known that gaming experience has four aspects: physical, mental, social, and emotional [57]. Haptic feedback improves emotional and mental aspects while enhancing the physical feeling sensed by the player, making the game more immersive and realistic.

Another emerging application of haptic virtual environment systems is in telerehabilitation. According to the World Health Organization, by the end of 2050 a 73 and a 203 percent increase will be seen in the number of persons over 65 in industrialized countries and worldwide, respectively. People in this age range are particularly prone to stroke, since the relative incidence of stroke doubles every decade after age 55. Stroke is the leading cause of permanent disability in industrialized nations. In addition to stroke, other age-related diagnoses such as orthopedics and arthritis will likely increase. Therefore, rehabilitation facilities must keep pace with these changes by providing effective, less costly services. Robotic-assisted and VR-assisted telerehabilitation have received huge attention in recent years since they provides innovative, interactive, and precisely reproducible therapies that can be performed for an extended duration and implemented remotely from hospitals.

Collaboration is possible through a shared virtual environment with which operators interact through their haptic interfaces. The common architectures for creating shared virtual environments (SVE) over the Internet are [81]:

- Server-Client (Hierarchical): A single virtual environment runs on a server and clients pass local information to the server. The server updates the virtual environment and sends graphic and haptic (force command) updates to the clients.
- Peer-to-Peer: Each client runs its own virtual environment. The clients update their own graphics and haptic loads and exchange the local updates with each other.

A few implementations of the client-server architecture in creating SVEs in telerehabilitation applications can be found in [14].

2.1.1 *Stability in HVE Systems*

The stability and passivity of single-user HVE systems have been studied extensively in the literature. Assuming that the operator is passive, conditions on the controller (the virtual coupling between the operator and the virtual wall) are reported for ensuring passivity and absolute-stability of single-user HVE systems. As described later, this operator passivity assumption may be violated depending on the task being performed. A thorough introduction on this topic is given in Section 3.2.

Stability analysis in the context of multi-user HVEs depending on the architecture chosen, server-client or peer-to-peer, may take

different approaches. In [74], a multi-rate control strategy is proposed for multi-user haptic cooperation under server-client architecture. In [19], for both server-client and peer-to-peer architectures, stability conditions are derived.

In this thesis, because of rising applications of cloud computing designed under the client-server architecture, the stability analysis for the multi-user HVEs is done under the client-server architecture.

In Chapter 3, the stability of both single-user and multi-user HVE systems are studied, and using a unified framework, the conditions for ensuring stability are derived.

2.2 TELEOPERATION SYSTEMS

A teleoperation system consists of human operator(s) interacting with master robot(s) in order to extend the human operator's sensing and manipulation capability to remote site(s) [3, 55, 58, 62]. The many applications of teleoperation systems are in handling hazardous materials [73], undersea and space manipulation [20, 76], mobile robotics [48], remote delivery of health care [31] including tele-surgery [49], etc. Basically, when the task environment is hazardous, has a large distance from the operator or has a considerably different scale compared to the human hand's natural range of motion, a teleoperation system can be useful.

The first teleoperation system was developed in 1945 in order to handle hazardous materials remotely [65]. Soon after landing on the surface of the moon in 1966, the research in teleoperation system boosted vastly and motivated the need for dealing with time delay in the communication channel between the master and the slave robots. Delay causes instability and the need to design stable teleoperation systems which can handle time-varying communication delay has been felt by researchers. Since 1980's, control systems theory has influenced the theoretical and controller design aspects of teleoperation systems in the presence of delay [53]. To deal with delay, in 1990, Bejczy and Kim proposed a predictive display where the human operator was able to see the slave-sides response in a predictive manner [10]. Since 1990's, with the use of Internet as communication channel, time-varying delay and packet loss in the channel had to be considered [54]. Recent advances in teleoperation systems has made remote surgery possible. In 2001, a surgeon in New York, U.S., performed a robot-assisted minimally invasive surgery in which he remotely removed gall-

bladder of a patient in Strasbourg, France, using a ZEUS surgical robot [12, 21].

2.2.1 *Controllers for Teleoperation Systems*

Three common control architectures for bilateral teleoperation systems are:

- position error-based (PEB) control architecture in which the position of each robot is transmitted to the opposite robot in the teleoperation system.
- direct force reflecting (DFR) control architecture where the position of the master robot is sent to the slave robot and contact force of the slave/environment is transmitted to the master robot.
- 4-channel (4CH) architecture where both positions and forces of the master and the slave are transmitted to the other end of the teleoperation system [46, 75].

The possible control architectures for a trilateral teleoperation system consisting of two master robots for two operators and one slave robot to perform a task on an environment are:

- force-position: A weighted sum of positions of the two master robots is sent to the salve robot while the force of contact between the slave and environment is sent back to the master robots. The force feedback to each master robot is a weighted sum of the environment contact force and the other operator's hand force applied to his/her master device. The weights are specified by a dominance factor, α, which determines the supremacy of each user over the slave [41].
- position-position: A weighted sum of positions of the two master robots is sent to the slave robot while position of the salve robot is sent back to the master robots. The position for each master robot is a weighted sum of the slave position and the other master device's position. Again the weights are specified by a dominance factor, α [40].
- 4-channel (4CH): The desired position and force for each robot are a weighted sum of positions and forces of the other two robots, realizing a four-channel multilateral shared control architecture. The weights are again specified by a dominance

factor, α, which determines the supremacy of each user over the slave [39].

In the design of teleoperation system controllers, two objectives are to be met. First, the system stability must be ensured in the sense that all the signals within the system must be bounded. Second in a bilateral teleoperation system, positions/forces of the master and the slave should be similar, meaning that the human operator should receive an undistorted perception of the environment properties – this is called transparency and is a performance measure. There is a tradeoff between transparency and stability of teleoperation systems [18,46]. The best transparency is achieved by the least-conservative stabilizing controller [28].

2.2.2 *Stability and Passivity in Teleoperation Systems*

Since the dynamic parameters of human operators are largely unknown, and the dynamic parameters of environments are also usually uncertain, time-varying and/or nonlinear, analyzing the closed-loop stability of teleoperation systems using conventional stability analysis methods is not possible. In order to overcome this problem and stabilize the system in spite of unknown models for human operators and environments, two main approaches have been proposed in literature: passivity-based stability analysis and absolute stability analysis. For a bilateral teleoperation system in both approaches the system is modeled as three main blocks two of which are 1-port networks (human operator an environment) while a 2-port network block represents the *teleoperator*. The combination of the master robot, the communication channel, the slave robot and local controllers is defined as the teleoperator. The concern in passivity-based stability analysis is to to ensure that teleoperator does not generate any net energy. If so, with the assumption of having a passive human operator and a passive environment, the overall teleoperation system will be passive (the concatenation of three passive blocks is passive). Absolute stability, on the other hand, is concerned with the stability of the overall teleoperation system for any passive or otherwise arbitrary operator and environment.

In the stability analysis of teleoperation systems in the literature, the entire system is assumed to be in continuous-time. While the human operator, the environment, and the robots operate in continuous-time, the controllers involved in teleoperation system are implemented via discrete-time components, we cannot neglect the discrete-time nature of the controller and the energy leaks caused

by the Zero-Order-Hold (ZOH) [47, 70]. The ZOH also accounts for half-sample delay (distinct from the communication channel delay) and has energy-instilling effects [4, 24, 47]. In our work, to fully account for the continuous-time and the discrete-time nature of various signals in the stability analysis of a teleoperation system, a sampled-data analysis is applied (Chapter 4).

The stability analysis of delayed teleoperation systems is usually meant to passify the communication channel and assumes that the rest of the system is passive. In reality, however, passifying the communication channel alone does not guarantee the stability of the entire teleoperation system. The reason for this is that although the master and slave robots by themselves are passive, when combined with their corresponding controllers their passivity will no longer be guaranteed. The detailed stability analysis of delayed 4CH bilateral and trilateral teleoperation systems while examining the effect of local controller on the passivity of robots are provided in Chapter 5.

3

STABILITY OF SAMPLED-DATA, DELAYED HAPTIC INTERACTION IN A VIRTUAL ENVIRONMENT UNDER PASSIVE OR ACTIVE OPERATOR

3.1 SUMMARY

This chapter studies the absolute stability of a sampled-data, m-user haptic virtual environment (HVE) system based on the discrete-time circle criterion. Depending on the task being performed by an operator, the passivity of the operator is influenced. We provide a framework for the system stability analysis in which the operators are allowed to exhibit passive or active behavior. In this chapter, the well-known Colgate's stability condition for a 1-user haptic system with a passive operator is reproduced and then extended to the m-user case while allowing each or all of the operators to behave actively. Another extension to Colgate's condition comes by allowing communication delays to exist in the system. Simulations and experiments confirm the validity of the proposed conditions for stability of sampled-data, m-user HVE systems.

3.2 INTRODUCTION

A haptic interface acts as a link between a human operator and a virtual environment and conveys a kinesthetic sense of presence in the virtual environment to the operator. The combined system is *sampled-data* as it includes a virtual environment simulated in a digital computer and a human operator and a haptic interface that are actual physical systems. For this system, stability is a prime concern because it may be jeopardized by the discrete-time simulation of the virtual environment due to its inherent sampling effects. Investigations done on energy leaks caused by the sample-and-hold in sampled-data haptic interaction has shown that a zero-order-hold (ZOH) accounts for a half-sample delay and has energy-instilling effects [69]. To qualitatively explain this, consider haptic interaction with a finite-impedance virtual object where the interaction forces are sampled and fed back to the user. As the virtual object is penetrated by the virtual tool, the sampled forces will be

less than the real forces during each sampling intervals, resulting in the forces reflected to the user to be too low. By contrast, as the virtual tool moves out of the object, the reflected forces will be too high compared to reality. Thus, the user's legitimate expectation that a passive object would not generate energy is violated. Indeed, as the user utilizes the haptic device to probe the virtual object by pushing and letting go of the user interface, the energy-instilling sampled-data coupling presents the object to the user as one emitting energy and causing vibrations, an effect never observed when touching the same object directly by hand.

3.2.1 *Literature Survey*

A number of authors have considered the issue of stability in sampled-data haptic interaction in the virtual space. Minsky et al. [51] were the first to study this problem. As shown in Figure 3.1, they considered a continuous-time model of a one degree-of-freedom (DOF) haptic device interacting with a discretely-simulated virtual wall. The robot (haptic interface) was modeled as a mass m and a damping b connected to the virtual wall by a virtual coupling (digital controller) modeled by a stiffness K. In their study, system instabilities were attributed to the time delay introduced by the hold operation; in fact, the hold operation is absent from Figure 3.1 because it was replaced by a time delay of one sampling period T approximated by a second-order Taylor series expansion. It was shown that the system in Figure 3.1 is stable if

$$b > KT \tag{3.1}$$

They argued that the above condition is approximate and in reality there is a constant C approximately equal to $1/2$ for which $b > C * KT$ is the true stability condition. Also, they showed via experiments that with the operator's mass m_h, damping b_h and stiffness k_h, and with a virtual damping B complementing the virtual stiffness K, the stability condition will become

$$B + b + b_h > \frac{(K + k_h)T}{2} \tag{3.2}$$

A more rigorous examination of stability was performed by Colgate and Schenkel [15]. They again considered a 1-DOF haptic interface to derive necessary and sufficient conditions under which a sampled-data haptic display system would exhibit passive behavior. For a common discrete-time implementation of the virtual en-

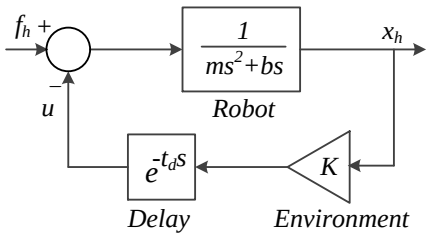

Figure 3.1: A continuous model for a single-user HVE system

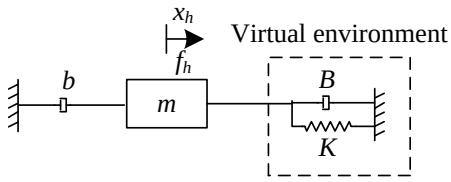

Figure 3.2: A single-user HVE system

vironment composed of a spring and a damper in parallel as in Figure 3.2, which is essentially a discrete-time PD controller, the necessary and sufficient condition for passivity and absolute stability[1] of the sampled-data HVE system was derived as

$$b > \frac{KT}{2} + B \tag{3.3}$$

This result shows that some physical dissipation in the haptic interface (i.e., $b > 0$) is essential to achieving passivity and absolute stability. On the other hand, high robot damping causes poor performance. The upper limit on the environment stiffness imposed by the stability condition implies that in order to implement a highly stiff, dissipative wall constraint, it is imperative to lower the sampling period T as much as possible. Another approach to the stability analysis of a similar HVE system was provided by Gil et al. In [22], using the Routh-Hurwitz criterion, the closed-loop stability problem of the 1-DOF HVE system was addressed directly; this is distinct from the absolute stability and passivity analysis in [15].

1 Since the human operator model is unknown, there is interest in absolute stability and passivity methods instead of conventional stability method. A common assumption in absolute stability and passivity methods is that the operator behaves passively.

The environment was modeled as a virtual spring and damper in mechanical parallel and the stability condition was derived as

$$b + B > \frac{KT}{2} \tag{3.4}$$

The above condition was shown to be valid only for low values of the virtual damping B. Comparing Colgate's and Gil's condition, it is easily seen that the passivity criterion is more conservative than the stability criterion. As for the human operator model, it has been argued in [22], [32] and [16] that the operator only contributes positively to stability (i.e., the absence of a user amounts to a worst-case scenario for stability) as long as it is passive, thus the operator effect is neglected in the stability analysis; note that the operator is simply modeled as an external input force f_h. However, as mentioned later, passivity of the operator is case-dependent and that is why that in this chapter we will introduce a new method that will allow us to account for active operators as well

The stability of time-delayed HVE systems has been inspected in [33], once again assuming that the operator is passive and that the virtual damping B is small. For a delay t_d, which can be the sum of several effects (computations, communications, etc), the stability condition was found to be

$$K < \frac{B + b}{T + t_d} \tag{3.5}$$

The passivity of the operator is simply a convenient assumption used in all of the above work for stability analysis of a teleoperation system independent of the typically uncertain, time-varying and/or unknown dynamics of the operator. However, given that the operator voluntarily manipulates the master robot and thereby has the capacity to inject energy into the teleoperation system, this assumption may not always be valid depending on the task. Active behavior of the operator in a haptic system has been reported in [17]. In this chapter, a discrete-time circle criterion based framework to find the stability condition for a sampled-data, delayed haptic system for passive or active operator is proposed. This chapter derives Colgate's stability condition for passive operator in a new and simplified way and extends it to the case of an active operator. Also, while because of the nature of Colgate's or Gil's methods, it is difficult to extend them to multiple-operator collaborative HVE systems, our proposed method is easily extended to the m-user case where $m \geq 2$. The many applications of multi-user collaborative HVEs in surgical training [77, 78], telerehabilitation [79, 80],

gaming [81, 82], etc. have been reported in literature. This chapter studies the stability of multi-user HVEs based on the client-server architecture (see Section 2 for client-server architecture). When considering client-server architecture, we should also account for the transmission delay of the visual and haptic commands. With this another extension to Colgate's stability condition comes by allowing communication delays to exist in the system. The rest of the chapter is organized as follows. Section 3.3 provides mathematical preliminaries required for the rest of the chapter. Section 3.4 is divided into two subsections 3.4.1 and 3.4.2. In Section 3.4.1, for the single-user haptic system in Figure 3.5a, stability conditions for both passive and active operators as well as under delayed or non-delayed channels are derived. In Section 3.4.2, a model for a sampled-data, m-user collaborative HVE is proposed and its stability conditions is derived. In Section 3.5, the simulation results are described. Experimental results are presented in Section 3.6 and Section 3.7 presents the conclusions.

3.3 MATHEMATICAL PRELIMINARIES

Definition 3.3.1. *The output of a sampler can be represented as a Dirac comb weighted by the sampled signal, i.e.,*

$$x^*(t) = \sum_{k=0}^{\infty} x(kT)\delta(t - KT)$$

and the representation of the sampled signal in the Laplace domain is

$$X^*(s) = \mathcal{L}x^*(t) = \sum_{k=0}^{\infty} x(kT)e^{-skT} \tag{3.6}$$

The z-domain equivalent of (3.6) is

$$X(z) = \mathcal{Z}x^*(t) = X^*(s)|_{s=\frac{1}{T}lnz}$$

Definition 3.3.2. *[44] The memory-less system*

$$y = h(t, u)$$

is passive if

$$u^T y \geq 0$$

Otherwise, it is active.

Lemma 3.3.1. *[44] The LTI minimal realization*

$$x(i+1) = Ax(i) + Bu(i) \tag{3.7}$$
$$y(i) = Cx(i) + Du(i) \tag{3.8}$$

with $G(z) = C(zI - A)^{-1}B + D$ is

- *passive if $G(z)$ is positive real;*
- *strictly passive if $G(z)$ is strictly positive real.*

Definition 3.3.3. *[44] An $m \times m$ proper rational transfer function matrix $G(z)$ is positive real if*

- *poles of all elements of $G(z)$ are inside or on the unit circle*
- *for all real ω for which $e^{j\omega}$ is not a pole of any element of $G(z)$, the matrix $G(e^{j\omega}) + G^T(e^{-j\omega})$ is positive semidefinite, and*
- *the poles of any element of $G(z)$ on $|z| = 1$ are simple and the associated residue matrices of these poles are positive semidefinite.*

Definition 3.3.4. *[44] Let A be a Hermitian symmetric matrix. A is positive semidefinite, if all its leading principle minors are non-negative. We say that A is positive definite if all its leading principle minors are positive.*

Definition 3.3.5. *Consider a system with input $u(t)$ and output $y(t)$. If there exists constant β such that for all $t \geq 0$,*

$$\int_0^t y(\tau)u(\tau)d\tau \geq \beta + \delta \int_0^t u(\tau)u(\tau)d\tau \tag{3.9}$$

then for $\delta > 0$ the system is input strictly passive (ISP) with excess of passivity (EOP) of δ [13], [29]. For $\delta < 0$, the system is active with shortage of passivity (SOP) of δ.

Passivity of an LTI system is equivalent to having the system's Nyquist diagram entirely in the right half plane Figure 3.3a. The Nyquist diagram of an ISP system with transfer function $G(s)$ and EOP of $\delta > 0$ is in the right hand side of the vertical line at δ, i.e. $\Re G(s) \geq \delta$ (Figure 3.3b). Similarly, for a non-passive transfer function $G(s)$ with SOP of $\delta > 0$ the Nyquist diagram is in $\Re G(s) \geq -\delta$ (Figure 3.3c).

Theorem 3.3.1. *[45] Consider a sampled-data multivariable control system that consists of an LTI system in the forward path and the nonlinearity*

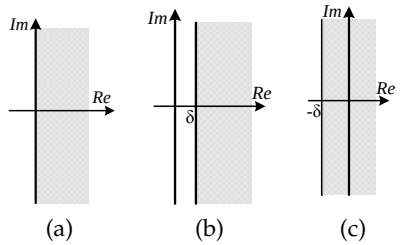

Figure 3.3: Nyquist diagrams of (a) a passive system, (b) an *ISP* system with excess of passivity of δ, (c) an active system with shortage of passivity of δ

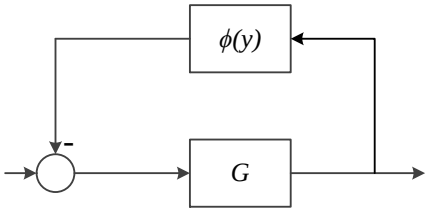

Figure 3.4: The model of a sampled-data feedback system with LTI system G in the forward path and the nonlinearity $\phi = \phi(y)$ in the feedback path

$\phi = \phi(y)$ in the feedback path as shown in Figure 3.4. Such a system can be presented by the difference equation

$$x(i+1) = Ax(i) - B\phi(y) \tag{3.10}$$

$$y(i) = Cx(i), \;\; y \in R^m \tag{3.11}$$

$$\phi(y) = [\phi_1(y_1), \phi_2(y_2), ..., \phi_m(y_m)]^T \tag{3.12}$$

If there exists $K = diag(k_1, ..., k_m) > 0$ such that

$$K^{-1} + C(zI - A)^{-1}B \tag{3.13}$$

is positive real then $G(z)$ is absolutely stable for any ϕ satisfying

$$\phi(0) = 0, \; 0 < y_i\phi(y_i) \leq y_i^2 k_i \tag{3.14}$$

Thus, the sampled-data system (3.10)-(3.12) will be stable. For a passive ϕ, $k_i \to \infty$ and condition (3.13) will change to $G(z)$ being positive real.

3.4 STABILITY ANALYSIS OF HAPTIC VIRTUAL ENVIRONMENTS

This section comprises of two subsections. In Section 3.4.1, the stability of the single-user 1-DOF HVE system in Figure 3.2 is studied. When there is no delay, Colgate's stability condition is arrived at using the proposed framework and based on the discrete-time circle criterion in Theorem 3.3.1. Also, the stability condition in the presence of delay is derived. In both cases, the effect of an active operator on the stability condition is studied. Later in Section 3.4.2, a multi-user 1-DOF HVE system is considered and for both non-delayed and delayed cases the stability condition is derived while accounting for possible operator activity.

3.4.1 *A Sampled-Data Single-User HVE System*

In this section two methods for stability analysis of single-user HVE systems are provided. The first method is the based on discrete-time circle criterion and is the proposed method in this thesis and is explained in Section 3.4.1.1. In Section 3.4.1.2 the previously proposed method in [15] is extended to the cases where the communication time-delay can exist in the system while the operator is allowed to behave actively. It is shown that both methods result in the same stability conditions for single-user HVE systems.

3.4.1.1 *Discrete-Time Circle Criterion Based Method*

The block diagram of the single-user HVE system in Figure 3.2 is shown in Figure 3.5a, where $Z_h(s)$ is the unknown human operator model and $H(z)$ is the known discrete-time model of the environment (i.e., the digitally-implemented virtual coupling between the haptic interface and the virtual wall). As before, the haptic interface is a rigid manipulator and is modeled as a mass m and a damper b. The input and output of $H(z)$ pass through a sampler and a ZOH with a sampling period of T, respectively. Simple manipulations in the block diagram in Figure 3.5a will result in the one in Figure 3.5b. The equations governing the resulting system in Figure 3.5b will be

$$f_h - u = bv_h \tag{3.15}$$

$$x_h = \frac{v_h}{s} \tag{3.16}$$

$$u^* = z^{-n} H(z) x_h^* \tag{3.17}$$

With the assumption that $n = t_d/T$ is an integer (t_d represents the communication delay), the discrete-time equivalent of (3.15) is

$$f_h^* - u^* = bv_h^*$$

and with the help of (3.17) we get

$$f^* - z^{-n}H(z)x_h^* = bv_h^*$$

The above can be written in the z-domain as

$$F(z) - z^{-n}H(z)X_h(z) = bV_h(z)$$

where

$$X_h(z) = \mathcal{Z}\{\frac{v_h}{s}\}$$

It is important to note that $\mathcal{Z}\{\frac{v_h}{s}\} \neq \mathcal{Z}\{\frac{1}{s}\}V_h(z)$. To be able to derive the transfer function from f_h to v_h, we need to approximate $\mathcal{Z}\{\frac{v_h}{s}\}$. We can do so based on one of the following approximation methods:

- Forward Difference

$$\begin{gathered} x_h(kT+K) = x_h(kT) + T\dot{x}_h(kT) \xrightarrow{\mathcal{Z}} zX_h(z) = X_h(z) + TV_h(z) \\ \Longrightarrow X_h(z) = \tfrac{T}{z-1}V_h(z) \end{gathered}$$

- Backward Difference

$$\begin{gathered} x_h(kT) = x_h(KT-T) + T\dot{x}_h(kT) \xrightarrow{\mathcal{Z}} X_h(z) = z^{-1}X_h(z) + TV_h(z) \\ \Longrightarrow X_h(z) = \tfrac{Tz}{z-1}V_h(z) \end{gathered}$$

- Tustins Transformation

$$\begin{gathered} x_h(kT+T) = x_h(kT) + T\dot{x}_h(kT) + (\dot{x}_h(kT+T) - \dot{x}_h(kT))\tfrac{T}{2} \\ \xrightarrow{\mathcal{Z}} zX_h(z) = X_h(z) + TV_h(z) + (zV_h(z) - V_h(z))\tfrac{T}{2} \\ \Longrightarrow X_h(z) = \tfrac{T}{2}\tfrac{z+1}{z-1}V_h(z) \end{gathered}$$

In previous related works [15, 23, 32, 33] the impedance of the environment in the z domain has been approximated as $H(z) = K + \frac{B(z-1)}{Tz}$ and, we will use the same model. In the following, we consider four cases for operator passivity and communication delay.

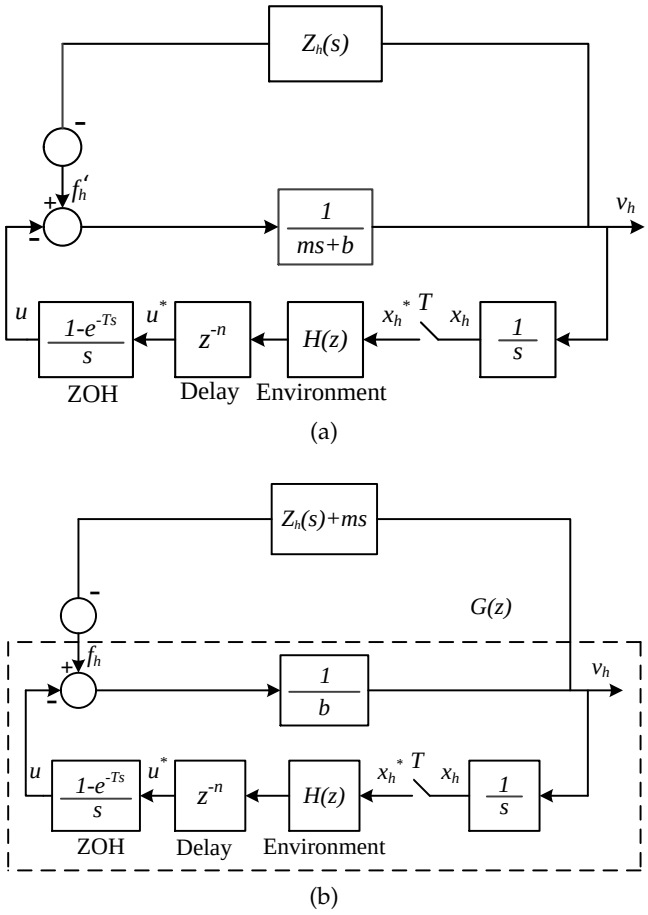

Figure 3.5: Model of a 1-DoF sampled-data HVE system

PASSIVE OPERATOR, NO DELAY Assuming that $t_d = 0$, depending on which approximation is chosen, the f to v mapping will be one of the following:

$$F_h(z) = bV_h(z) + (K + \frac{B(z-1)}{Tz})\frac{T}{z-1}V_h(z) = G_1^{-1}(z)V_h(z)$$
$$F_h(z) = bV_h(z) + (K + \frac{B(z-1)}{Tz})\frac{Tz}{z-1}V_h(z) = G_2^{-1}(z)V_h(z)$$
$$F_h(z) = bV_h(z) + (K + \frac{B(z-1)}{Tz})\frac{T}{2}\frac{z+1}{z-1}V_h(z) = G_3^{-1}(z)V_h(z)$$

The above correspond to forward difference, backward difference and Tustin approximations, respectively. Based on Theorem 3.3.1 for $m = 1$, since $Z_h(s) + ms$ is passive, the system in Figure 3.5b is stable if $G(z)$ is positive real. Based on Lemma 3.3.1 and using the fact that passivity of $G(z)$ is equal to $G^{-1}(z)$ being passive [6],

the stability of the system is ensured if $G^{-1}(z)$ is positive real. The first condition for positive realness of $G^{-1}(z)$ is satisfied since it can be clearly seen that the poles of $G_i^{-1}(z)$, $i = 1, 2, 3$, lie inside or on the unit circle. Since $z = 1$ is a simple pole and its residue for each $G_i^{-1}(z)$ is positive semidefinite, KT, the only remaining condition to check is the second condition in the Definition 3.3.3, which for $m = 1$ will reduce to $\Re\{G_i^{-1}(z)\} \geq 0$. In this way, the conditions for stability of the single-user HVE system based on the three approximations are found as follows:

$$b > \frac{KT}{2} - B\cos(\omega T) \tag{3.18}$$

$$b + \frac{KT}{2} + B > 0 \tag{3.19}$$

$$b + B\frac{1 + \cos(\omega T)}{2} \tag{3.20}$$

From (3.18)-(3.20), the worst-case condition is (3.18). In turn, (3.18) assumes its worst-case $\cos(\omega T = -1$, when we will have

$$b > \frac{KT}{2} + B \tag{3.21}$$

This is identical to Colgate's condition. As shown, forward difference approximation method resulted in the worst-case condition for stability of the single-user HVE system. As a result, in the rest of the chapter, the $\frac{1}{s}$ is approximated using the forward difference approximation method.

PASSIVE OPERATOR, DELAY The previous condition was found assuming no delay in the system. For a delayed single-user HVE system, the stability condition will take a different form depending on the virtual environment model. Here again, it can be shown that forward difference approximation method for $\frac{1}{s}$ will lead us to the worst-case condition. The f to v mapping in the z domain will then be

$$F_h(z) = bV_h(z) + z^{-n}(K + \frac{B(z-1)}{Tz})\frac{T}{z-1}V_h(z) \tag{3.22}$$

Since the passivity of $G(z)$ is equal to $G^{-1}(z)$ being passive, the delayed sampled-data HVE system is stable if (3.23) is positive real:

$$G^{-1}(z) = b + z^{-n}(K + \frac{B(z-1)}{Tz})\frac{T}{z-1} \tag{3.23}$$

The first and third conditions in Definition 3.3.3 are readily satisfied leaving us with the third condition which requires $\Re\{G^{-1}(z)\} \geq 0$. Substituting $z = \cos(\omega T) + j\sin(\omega T)$ in (3.23) the real part of $G(j\omega)^{-1}$ must satisfy:

$$b + B\cos(\omega t_d - T) - \frac{KT}{2}\cos(\omega t_d) - KTS > 0 \tag{3.24}$$

where, $S = \frac{\sin(\omega t_d)\sin(\omega T)}{2(1-\cos(\omega T))}$. With the assumption that $t_d/T = n$ and B is small, the worst-case condition will happen if $\cos(\omega T) = 1$. Then, we have

$$\lim_{\cos(\omega T)\to 1} KTS = \lim_{\cos(\omega T)\to 1} KT\frac{\sin(\omega t_d)\sin(\omega T)}{2(1-\cos(\omega T))} = Kt_d$$

and (3.24) will simplify to

$$b + B - \frac{KT}{2} - t_d/T\cos(\omega T/2) > 0 \tag{3.25}$$

For $\cos(\omega T/2) = 1$ the passivity condition for a delayed single-user HVE system will be derived as follow:

$$b + B > \frac{KT}{2} + Kt_d \tag{3.26}$$

Interestingly, the above condition is identical to the condition reported in [33].

ACTIVE OPERATOR, NO DELAY The same approach will also enable us to inspect the stability of sampled-data HVE systems with an active operator. Note that previously in Figure 3.5b, in order to simplify the system, the mass m of the master device was moved to the operator impedance $Z_h(s)$ without affecting the overall system or the passivity of the new operator $Z_h(s) + ms$. Now, employing a similar technique, given that we want to allow the operator to be active, we will move enough of damping b of the master device to the operator impedance $Z_h(s)$ to render it passive. Let's name the real part of the operator impedance Z_h to be $-z_a$. When $z_a > 0$, it represents the shortage of passivity of an active operator. Let us transfer z_a units of the master device damping b, to $Z_h(s)$ to neutralize this shortage of passivity and make the new operator passive. As a result, based on (3.21) and after replacing b by $b - z_a$, the sta-

bility condition after accounting for the active operator effect will be

$$b - z_a > \frac{KT}{2} + B \tag{3.27}$$

Evidently, the proposed condition (3.28) extends the condition in [15] by both allowing the operator to be active and for the delay to exist, and extends the condition in [33] by allowing the operator to be active. The above shows an inevitable trade-off faced when allowing for active operators. Although higher robot dampings go against conventional wisdom due to the associated performance degradations, we see that it is the price to be paid for allowing active intervention of the operators.

ACTIVE OPERATOR, DELAY In the case of a delayed HVE system in which the operator has shortage of passivity of z_a, again the approach is the same as for active operator without delay. We will transfer z_a units of the master device damping b, to $Z_h(s)$ to neutralize the shortage of passivity and make the new operator passive. Based on (3.26) and after replacing b by $b - z_a$, the stability condition for a delayed single-user HVE system with active operator will be

$$b - z_a + B > Kt_d + \frac{KT}{2} \tag{3.28}$$

3.4.1.2 *Small-Gain Theorem Approach*

The above results, which were derived using the proposed simplified framework, can also be derived using the method in [15], which did not allow for the operator to be passive or for a delay to exist. The closed-loop characteristic equation of the sampled-data HVE system in Fig. 3.5a is $1 + H(e^{sT})G_T{}^*(s) = 0$ where $G_T{}^*(s) = \frac{1}{T}\Sigma_{k=-\infty}^{\infty} G_T(s + jk\omega_s)$ and $G_T(s) = \frac{1-e^{-Ts}}{s^2}\frac{1}{ms+b+Z_h(s)}$. Note that the feedback interconnection of $\frac{1}{ms+b}$ and $Z_h(s)$ results in $\frac{1}{ms+b+Z_h(s)}$. In order to understand the following analysis, Figure 3.6 is key. The human operator with impedance Z_h in Figure 3.6a is allowed to be active with a shortage of passivity equal to $z_a \geq 0$. In Figure 3.6b, this impedance is shifted to the right by b (it is assumed that $b > z_a$). It is easy to see that the feedback interconnection of the operator impedance Z_h and the robot impedance $\frac{1}{ms+b}$ will span the complex plane region R_1 shown in Figure 3.6c. In a manner similar to [15],

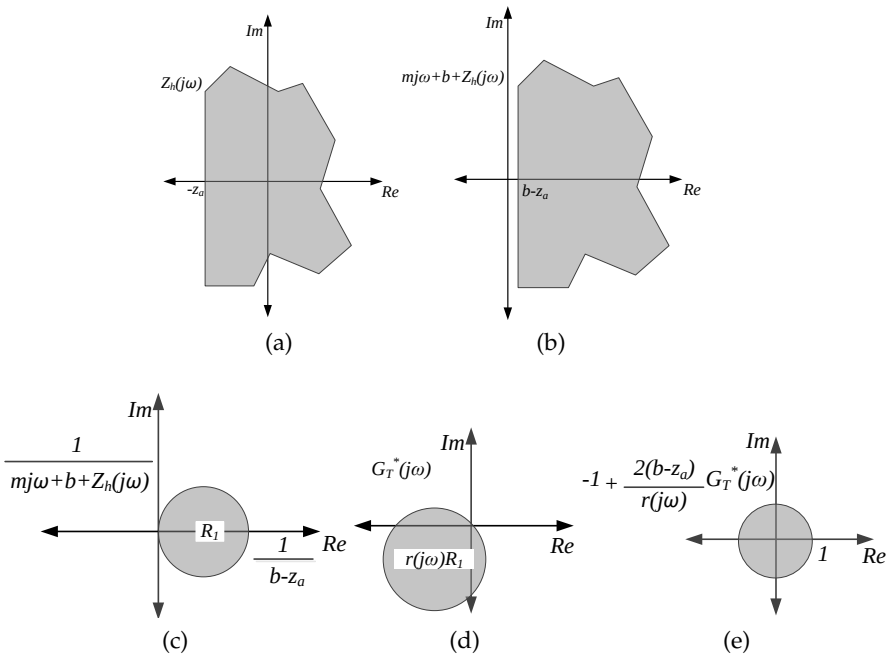

Figure 3.6: The Nyquist plots of (a) operator impedance with shortage of passivity of z_a, (b) the inverse closed-loop transfer function of the operator and robot impedances, (c) the closed-loop transfer function of the operator and robot impedances, (d) ${G_T}^*(s)$ and (e) the mapping of ${G_T}^*(s)$ into the unit circle.

it can be shown that ${G_T}^*(s)$ covers the region $R_{{G_T}^*}(\omega) = r(j\omega)R_1$ shown in Figure 3.6d, where

$$r(j\omega) = e^{-j\omega t_d}\frac{T}{2}\frac{e^{-j\omega T}-1}{1-\cos(\omega T)} \tag{3.29}$$

once we assume that t_d is an integer multiple of T.

Theorem 3.4.1. *The sampled-data system in Figure 3.5a will be stable if*

$$\|\mathcal{M}\mathcal{N}\|_\infty < 1 \tag{3.30}$$

where $\mathcal{M}$ and $\mathcal{N}$ are linear fractional tranformations defined as

$$\mathcal{M}\{s, {G_T}^*(s)\} = -1 + \frac{2(b-z_a)}{r(s)}{G_T}^*(s) \tag{3.31}$$

$$\mathcal{N}\{s, {G_T}^*(s)\} = \frac{r(s)H(e^{sT})}{2(b-z_a)+r(s)H(s))} \tag{3.32}$$

Proof. For the absolute stability of a single-user HVE system in Figure 3.5a, it is necessary and sufficient that the closed-loop char-

acteristic equation of the system $(1 + H(e^{sT})G_T{}^*(s) = 0)$ has all of its roots in the left half of the complex plane. Let us find $\mathcal{M}$ and $\mathcal{N}$ can be found such that the transformed characteristic equation

$$1 + \mathcal{M}\mathcal{N} = 0 \tag{3.33}$$

has the same roots as the original characteristic equation of the sample-data single-user HVE system $1 + H(e^{sT})G_T{}^*(s) = 0$. As it can be seen in Figure 3.6e, the appropriate linear fractional transformation applied to $G_T{}^*(s)$ that will provide the appropriate translation and scaling to map $R_{G_T{}^*}(\omega)$ to the unit disk in Figure 3.6e will be

$$\mathcal{M}\{s, G_T{}^*(s)\} = -1 + \frac{2(b - z_a)}{r(s)} G_T{}^*(s) \tag{3.34}$$

By replacing $\mathcal{M}$ in (3.33) and comparing with $1 + H(e^{sT})G_T{}^*(s) = 0$, $\mathcal{N}$ will be

$$\mathcal{N}\{s, G_T{}^*(s)\} = \frac{r(s)H(e^{sT})}{2(b - z_a) + r(s)H(s))} \tag{3.35}$$

Since, $\mathcal{M}$ is already in the unit disk, by applying small-gain theorem the condition for stability of the delayed single-user HVE system with active operator will be

$$\left| \frac{r(j\omega)H(e^(j\omega T)}{2(b-z_a)+r(j\omega)H(e^{j\omega T})} \right| < 1 \tag{3.36}$$

Straightforward manipulation then leads to the following condition:

$$b - z_a > \frac{T}{2} \frac{1}{1 - \cos(\omega T)} \Re\{e^{-j\omega t_d}(1 - e^{-j\omega T})H(e^{j\omega T})\} \tag{3.37}$$

For the virtual wall $H(z) = K + B\frac{z-1}{Tz}$ and assuming that B is small enough, this stability condition will again reduce to (3.28), where if $z_a = 0$ the condition will be identical to that reported in [33].

3.4.2 *A Sampled-Data Multi-User HVE System*

Based on the sampled-data single-user HVE system modeled in Figure 3.2, the model of a multi-user system can be presented as in Figure 3.7. Since each operator affects one master device only, the block diagram of the multi-user system can be modified to Figure 3.8a. A slight manipulation in Figure 3.8a will result in Fig-

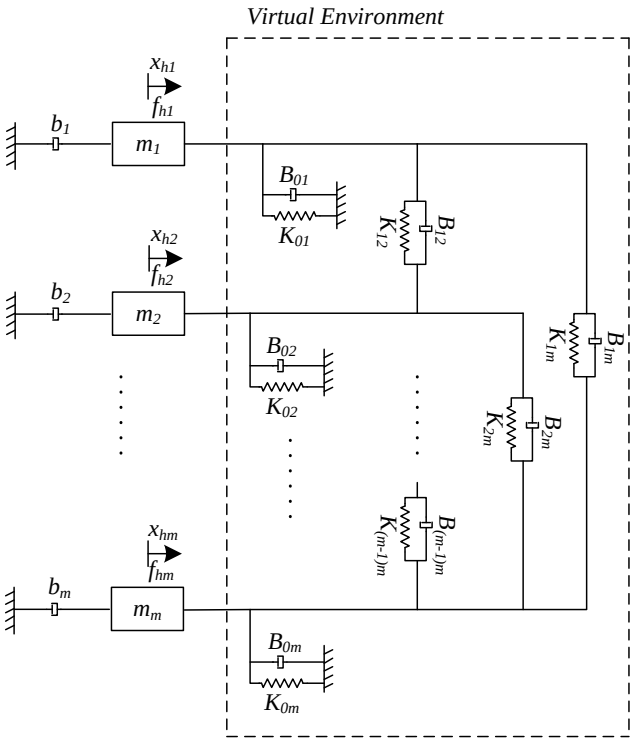

Figure 3.7: An m-user HVE system

ure 3.8b without affecting the overall system. The dynamics of the system in Figure 3.8b are as

$$b_i V_{hi}(z) = F_{hi}(z) - U_i(z), \quad i = 1, \cdots, m \tag{3.38}$$

where $V_{hi}(z) = \mathcal{Z}\{v_{hi}\}$, $F_{hi}(z) = \mathcal{Z}\{f_{hi}\}$, $U_i(z) = \mathcal{Z}\{u_i\}$. Note that

$$U(z) = z^{-n_i} H(z) X_h(z)$$

where $n_i = t_{di}/T$ is an integer and

$$H_{ii}(z) = K_{0i} + \Sigma_{k=1,k\neq i}^{m}(K_{ik} + \frac{(B_{0i} + \Sigma_{k=1,k\neq i}^{m} B_{ik})(z-1)}{Tz})$$

$$H_{ij}(z) = -(K_{ij} + \frac{B_{ij}(z-1)}{Tz}), \quad j \neq i$$

As a result, we have

$$U_i(z) = (K_{0i} + \Sigma_{k=1,k\neq i}^{m} K_{ik} + \frac{(B_{0i} + \Sigma_{k=1,k\neq i}^{m} B_{ik})(z-1)}{Tz}) X_{hi}(z) - \Sigma_{j=1,j\neq i}^{m} (K_{ij} + \frac{B_{ij}(z-1)}{Tz}) X_{hj}(z) \tag{3.39}$$

Substituting the forward difference approximation for $\frac{1}{s}$ in (3.39)

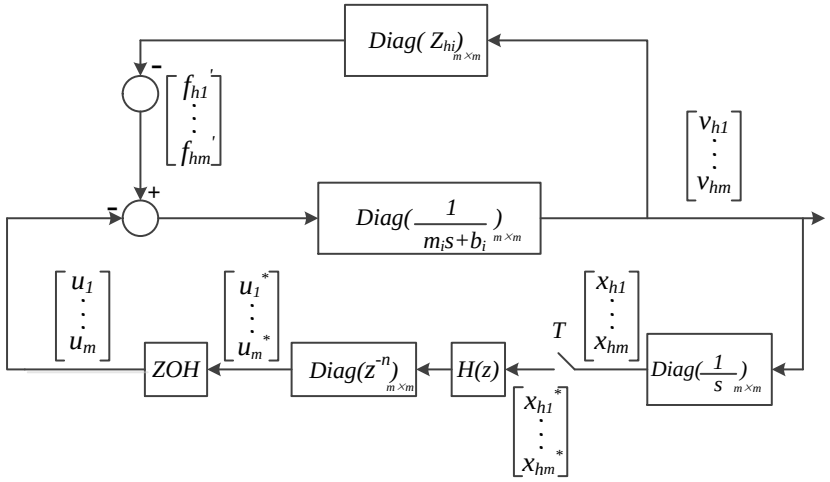

(a)

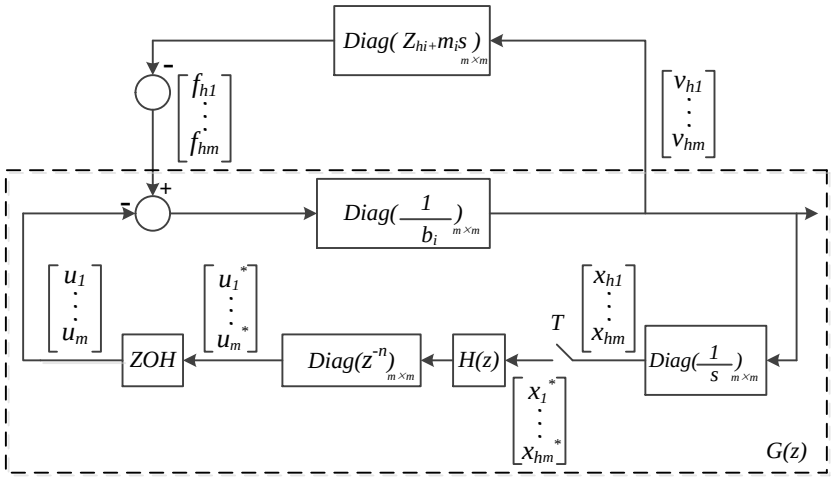

(b)

Figure 3.8: Model of a 1-DOF multi-user HVE system

and then combining the result with (3.38), the relationship between the force vector F_h and the velocity vector V_h can be written as

$$F_h(z) = G^{-1}(z)V_h(z) \tag{3.40}$$

where $G(z)$ is the $m \times m$ transfer matrix of the multi-user system. Again, we distinguish the following four cases.

PASSIVE OPERATORS NO DELAY Based on the multivariable discrete circle criterion, Theorem 3.3.1, $G(z)$ needs to be positive real for the system in Figure 3.8b to be stable assuming that the operators are passive. Again, since passivity of $G(z)$ is equal to $G^{-1}(z)$ being passive, based on Lemma 3.3.1, the positive realness of $G^{-1}(z)$ will ensure the passivity of $G(z)$. Since the expression for $G(z)$ is involved for a general m-user system, let us begin by considering the special case of $m = 2$:

$$G^{-1}(z) = \tag{3.41}$$
$$\begin{bmatrix} b_1 + \frac{(K_{01}+K_{12})T}{z-1} + \frac{(B_{01}+B_{12})}{z} & -(\frac{K_{12}T}{z-1} + \frac{B_{12}}{z}) \\ -(\frac{K_{12}T}{z-1} + \frac{B_{12}}{z}) & b_2 + \frac{(K_{02}+K_{12})T}{z-1} + \frac{(B_{02}+B_{12}}{z} \end{bmatrix}$$

The first condition in Definition 3.3.3 for positive realness of $G^{-1}(z)$ requires all poles of the matrix elements to lie inside the unit disk, which is clearly the case here. The third condition in Definition 3.3.3 for positive realness of $G^{-1}(z)$ requires the poles on the $|z| = 1$ to be simple and have positive semidefinite residue matrices. As it can be clearly seen in (3.41), $z = 1$ is a simple pole and the residue matrix for this pole is

$$R_0 = \begin{bmatrix} (K_{01} + K_{12})T & -K_{12}T \\ -K_{12}T & (K_{02} + K_{12})T \end{bmatrix} \tag{3.42}$$

As it can be seen R_0 is a Hermitian matrix and based on Definition 3.3.4 it is positive semidefinite since

$$(K_{01} + K_{12})T > 0 \tag{3.43}$$
$$det(R_0) = (K_{01}K_{02} + (K_{01} + K_{02})K_{12})T^2 > 0 \tag{3.44}$$

Substituting $z = e^{j\omega T} = \cos(\omega T) + j\sin(\omega T)$, the second condition in Definition 3.3.3 for positive realness of $G^{-1}(z)$ will lead to the following two conditions:

$$b_1 - \frac{(K_{01} + K_{12})T}{2} + (B_{01} + B_{12})\cos(\omega T) > 0 \tag{3.45}$$

$$\begin{aligned} &det(G(e^{j\omega T}) + G^T(e^{-j\omega T})) = \\ &(2b_1 - K_{01}T + 2B_{01}\cos(\omega T))(2b_2 - K_{02}T + 2B_{02}\cos(\omega T)) \\ &+ ((2b_1 + 2b_2) - (K_{01} + K_{02})T + 2(B_{01} + B_{02})\cos(\omega T)) \\ &(-K_{12}T + 2B_{12}\cos(\omega T)) > 0 \end{aligned} \tag{3.46}$$

The worst-case for (3.45)-(3.46) occurs when $\cos(\omega T) = -1$. With $b = \min(b_1, b_2)$, $B_0 = \max(B_{01}, B_{02})$ and $K_0 = \min(K_{01}, K_{02})$, the above two conditions will hold if

$$(2b - K_0T - 2B_0)^2 + 2(2b - K_0T - 2B_0)(-K_{12}T - 2B_{12}) > 0 \tag{3.47}$$

After simplifying (3.47), the stability condition for this sampled-data, dual-user HVE system will be

$$b > \frac{K_0T}{2} + K_{12}T + B_0 + 2B_{12} \tag{3.48}$$

Having found the stability condition for $m = 2$, let us know proceed to the case of $m = 3$. The matrix $G^{-1}(z)$ for the corresponding sampled-data, tri-user HVE system is

$$G^{-1}(z) = \begin{bmatrix} b_1 + \frac{K_1T}{z-1} + \frac{B_1}{z} & -(\frac{K_{12}T}{z-1} + \frac{B_{12}}{z}) & -(\frac{K_{13}T}{z-1} + \frac{B_{13}}{z}) \\ -(\frac{K_{12}T}{z-1} + \frac{B_{12}}{z}) & b_2 + \frac{K_2T}{z-1} + \frac{B_2}{z} & -(\frac{K_{23}T}{z-1} + \frac{B_{23}}{z}) \\ -(\frac{K_{13}T}{z-1} + \frac{B_{13}}{z}) & -(\frac{K_{23}T}{z-1} + \frac{B_{23}}{z}) & b_3 + \frac{K_3T}{z-1} + \frac{B_3}{z} \end{bmatrix}$$

where $K_1 = K_{01} + K_{12} + K_{13}$, $K_2 = K_{02} + k_{12} + K_{23}$, $K_3 = K_{03} + k_{13} + K_{23}$, $B_1 = B_{01} + B_{12} + B_{13}$, $B_2 = B_{02} + B_{12} + B_{23}$ and $B_3 = B_{03} + B_{13} + B_{23}$. Again, $G^{-1}(z)$ needs to be positive real. The first condition in Definition 3.3.3 for positive realness of $G^{-1}(z)$ requires all poles of the matrix elements to lie inside the unit disk, which is clearly the case here. The third condition in Definition 3.3.3 for positive realness of $G^{-1}(z)$ requires the poles on the $|z| = 1$ to be simple and have positive semidefinite residue matrices. As it can be

clearly seen in (3.49), $z = 1$ is a simple pole and the residue matrix for this pole is

$$R_0 = \begin{bmatrix} (K_{01}+K_{12}+K_{13})T & -K_{12}T & -K_{13} \\ -K_{12}T & (K_{02}+K_{12}+K_{23})T & \\ -K_{13}T & -K_{23}T & (K_{03}+K_{13}+K_{23}) \end{bmatrix} \tag{3.49}$$

R_0 is a Hermitian matrix and based on Definition 3.3.4 it is positive semidefinite since

$$(K_{01}+K_{12}+K_{13})T > 0 \tag{3.50}$$

$$((K_{01}+K_{13})(K_{02}+K_{23})+K_{12}(K_{01}+K_{02}+K_{13}+K_{23}))T^2 > 0 \tag{3.51}$$

$$\begin{aligned} det(R_0) &= K_{01}K_{02}K_{03}+(K_{01}+K_{02}+K_{03})(K_{12}K_{13}+K_{12}K_{23}+K_{13}K_{23}) \\ &+ K_{01}K_{02}(K_{13}+K_{23})+K_{01}K_{03}(K_{12}+K_{23}) \\ &+ K_{02}K_{03}(K_{12}+K_{13}) > 0 \end{aligned} \tag{3.52}$$

Substituting $z = e^{j\omega T} = \cos(\omega T) + j\sin(\omega T)$, the second condition in Definition 3.3.3 for positive realness of $G^{-1}(z)$ will lead to the following conditions:

$$b_1 - \frac{(K_{01}+K_{12}+K_{13})T}{2} + (B_{01}+B_{12}+B_{13})\cos(\omega T) > 0 \tag{3.53}$$

$$\begin{aligned} &det(G(e^{j\omega T}) + G^T(e^{-j\omega T})) = \\ &(2b_1 - (K_{01}+K_{12}+K_{13})T + 2(B_{01}+B_{12}+B_{13})\cos(\omega T)) \\ &(2b_2 - (K_{02}+K_{12}+K_{23})T + 2(B_{02}+B_{12}+B_{23})\cos(\omega T)) \\ &(2b_3 - (K_{03}+K_{13}+K_{23})T + 2(B_{03}+B_{13}+B_{23})\cos(\omega T)) \\ &- 2(K_{12}T+2B_{12})(K_{13}T+2B_{13})(K_{23}T+2B_{23}) - \\ &(2b_1 - (K_{01}+K_{12}+K_{13})T + 2(B_{01}+B_{12}+B_{13})\cos(\omega T)) \\ &(K_{23}T+2B_{23})^2 - (2b_2 - (K_{02}+K_{12}+K_{23})T + 2(B_{02} \\ &+ B_{12}+B_{23})\cos(\omega T))(K_{13}T+2B_{13})^2 - (2b_3 - (K_{03}+K_{13} \\ &+ K_{23})T - 2(B_{03}+B_{13}+B_{23})\cos(\omega T))(K_{12}T+2B_{12})^2 > 0 \end{aligned} \tag{3.54}$$

The worst-case for the above conditions occurs when $\cos(\omega T) = -1$. With $B = \min(B_{12}, B_{13}, B_{23})$, $B_0 = \max(B_{01}, B_{02}, B_{03})$, $K_0 =$

$\min(K_{01}, K_{02}, K_{03})$, $K = \min(K_{12}, K_{13}, K_{23})$ and $b = \min(b_1, b_2, b_3)$, the above two conditions will hold if

$$(2b - K_0T - 2B_0 - 4B)^3 - 2(KT + 2B)^3 - 3(KT + 2B)^2(2b - K_0T - 2B_0 - 4B) > 0 \tag{3.55}$$

After simplifying (3.55), the stability condition for this sampled-data, tri-user HVE system will be

$$b > \frac{K_0T}{2} + \frac{3KT}{2} + B_0 + 3B \tag{3.56}$$

In a similar way, it is possible to show that the stability condition for any m will be

$$\min_i b_i > \max_i\{\frac{K_{0i}T}{2} + B_{0i}\} + m \max_{i,j\neq i}\{\frac{K_{ij}T}{2} + B_{ij}\} \tag{3.57}$$

As it can be seen from (3.57), when only one user is involved, the condition will reduce to Colgate's condition for sampled-data, single-user HVE system.

ACTIVE OPERATORS, NO DELAY The above method also allows us to inspect the system stability in the presence of active operators. This is a marked advantage over the method in [15], which leads to involved equations when there is more than one user in the system making it very difficult to derive the stability conditions for active operators. But here, the circle criterion based method enables us to readily account for active operators. Assuming that operator Z_{hi} has shortage of passivity of z_{ai}, the stability condition in (3.57) will change into

$$\min_i\{b_i - z_{ai}\} > \max_i\{\frac{K_{0i}T}{2} + B_{0i}\} + m \max_{i,j}\{\frac{K_{ij}T}{2} + B_{ij}\} \tag{3.58}$$

The above condition can be derivd in a manner similar to (3.27), so the details are not shown. Again, for only one operator, (3.58) will reduce to (3.27).

PASSIVE OPERATORS AND DELAY For a delayed m-user HVE system, assuming that $t_{di}/T = n_i$ is an integer and B_{0i} and B_{ij} are small enough, the stability condition will be derived below. Again, for simplicity, let us start with the special case of $m = 2$. The matrix

$G^{-1}(z)$ for the corresponding sampled-data, dual-user HVE system is

$$G^{-1}(z) = \begin{bmatrix} b_1 + z^{-n_1}(\frac{K_1 T}{z-1} + \frac{B_1}{z}) & -z^{-n_1}(\frac{K_{12} T}{z-1} + \frac{B_{12}}{z}) \\ -z^{-n_2}(\frac{K_{12} T}{z-1} + \frac{B_1 2}{z}) & b_2 + z^{-n_2}(\frac{K_2 T}{z-1} + \frac{B_2}{z}) \end{bmatrix} \tag{3.59}$$

where $K_1 = K_{01} + K_{12}$, $B_1 = B_{01} + B_{12}$, $K_2 = K_{02} + K_{12}$ and $B_2 = B_{02} + B_{12}$. As before, based on Theorem 3.3.1 and Lemma 3.3.1, we require $G^{-1}(z)$ to be positive real assuming that the operators are passive. The first condition in Definition 3.3.3 for positive realness of $G^{-1}(z)$ requires all poles of the matrix elements to lie inside the unit disk, which is clearly the case here. The residue matrix for the delayed system is the same as non-delayed system explained before. Therefore, the third condition of Definition 3.3.3 is met. Substituting $z = e^{j\omega T} = \cos(\omega T) + j\sin(\omega T)$, the second condition in Definition 3.3.3 for positive realness of $G^{-1}(z)$ will lead to the following three conditions:

$$t_{d1} = t_{d2} \tag{3.60}$$

$$b_1 + (B_{01} + B_{12})\cos(\omega(t_d - T)) - \frac{(K_{01} + K_{12})T}{2}\cos(\omega t_d) - (K_{01} + K_{12})TS > 0 \tag{3.61}$$

$$\begin{aligned} &det(G(e^{j\omega T}) + G^T(e^{-j\omega T})) = (b_1 + B_{01}\cos(\omega(t_d - T)) - \\ &\frac{K_{01}T}{2}\cos(\omega t_d) - K_{01}TS)(b_2 + B_{02}\cos(\omega(t_d - T)) \\ &- \frac{K_{02}T}{2}\cos(\omega t_d) - K_{02}TS) + (B_{12}\cos(\omega(t_d - T)) \\ &- \frac{K_{12}T}{2}\cos(\omega t_d) - K_{12}TS)(b_1 + B_{01}\cos(\omega(t_d - T)) \\ &- \frac{K_{01}T}{2}\cos(\omega t_d) - K_{01}TS) + (B_{12}\cos(\omega(t_d - T)) \\ &- \frac{K_{12}T}{2}\cos(\omega t_d) - K_{12}TS)(b_2 + B_{02}\cos(\omega(t_d - T)) \\ &- \frac{K_{02}T}{2}\cos(\omega t_d) - K_{02}TS) > 0 \end{aligned} \tag{3.62}$$

where $S = \frac{\sin(\omega t_d)\sin(\omega T)}{2(1-\cos(\omega T))}$. As it can be seen form the first condition, $t_{d1} = t_{d2}$ (which in general will be $t_{di} = t_d$), the limitation of this method is that it cannot allow for different delay values in the multi-user architecture. Assuming that $t_d/T = n$ is an integer and B_{0i} and B_{ij} are sufficiently small and with $b = \min(b_1, b_2)$, $B_0 = \min(B_{01}, B_{02})$, and $K_0 = \max(K_{01}, K_{02})$ the worst-case for

(3.60) and (3.62) occurs when S has its maximum value. Therefore, solving the $\frac{d}{d\omega}S = 0$ will lead us to $cos(\omega T) = 1$, which is confirmed to give the maximum value of S by checking the sign of the second derivative of S for $cos(\omega T) = 1$. The maximum value of S will then be

$$\lim_{\cos(\omega T)\to 1} \frac{\sin(\omega t_d)\sin(\omega T)}{2(1-\cos(\omega T))} = \frac{t_d}{T}$$

Then,

$$\begin{aligned} &det(G(e^{j\omega T}) + G^T(e^{-j\omega T})) = \\ &(2b + 2B_0 + 2B_{12} - (K_{01} + K_{12})T - 2(K_0 + K_{12})t_d)^2 - \\ &(2B_{12} - K_{12}T - 2K_{12}t_d)^2 > 0 \end{aligned} \tag{3.63}$$

Simplifying (3.63) will give us

$$b + B_0 + 2B_{12} > \frac{K_0 T}{2} + K_{12}T + K_0 t_d + 2K_{12}t_d \tag{3.64}$$

In a similar way, the stability condition for a delayed m-user HVE system will be

$$\begin{aligned} \min_i\{b_i + B_{0i}\} + m\min_{i,j\neq i} B_{ij} > \max_i\{K_{0i}t_d + \frac{K_{0i}T}{2}\} \\ + m\max_{i,j\neq i}\{K_{ij}t_d + \frac{K_{ij}T}{2}\} \end{aligned} \tag{3.65}$$

Again, for a single-user system, condition (3.65) will reduce to (3.28).

ACTIVE OPERATORS, DELAY Finally, with the addition of active operators to the delayed system and assuming that $t_d/T = n$ is an integer and B_{0i} and B_{ij} are small enough, the stability condition will be

$$\begin{aligned} &\min_i\{b_i - z_{ai} + B_{0i}\} + m\min_{i,j\neq i} B_{ij} > \\ &\max_i\{K_{0i}t_d + \frac{K_{0i}T}{2}\} + m\max_{i,j\neq i}\{K_{ij}t_d + \frac{K_{ij}T}{2}\} \end{aligned} \tag{3.66}$$

3.5 SIMULATION STUDY

In this section, the conditions derived throughout the chapter are tested using MATLAB/Simulink. Since having an operator with a

desirable amount of shortage of passivity is quite difficult to robustly implement in practice, experimental resultswill not be provided for conditions that allow operator activity; instead, such cases are tested in simulations. This is the main reason for reporting both simulations and experiments in this chapter.

In order to test conditions (3.27) and (3.28), the sampled-data single-user HVE system in Figure 3.5a is simulated in MATLAB/ Simulink. To determine the stability of the system, the system outputs are monitored for boundedness at all times -- if any output goes unbounded, the system is unstable. The master robot has been modeled with $m =$ and $b =$.

For the non-delayed single-user HVE system with $m = 0.015$, $b = 0.02$ and $B = 0$, simulations have been conducted for three cases where the shortage of passivity z_a of the operator is either 0, $0.5b$, or $0.8b$. To this end, the operator model was considered to be $-z_a + \frac{1}{s}$; note that $\Re\{\frac{1}{s}\} = 0$ makes it a least-passive operator corresponding to a worst-case scenario for the coupled system stability.

During the simulations, the sampling time is increased by steps of $1ms$. For each sampling time, the controller gain K is changed to find the largest gain value for which the system remains stable. In Figure 3.9a, each of these maximum controller gain values at a given sampling period is represented by a star. Evidently, these simulation data points are very close to the solid lines, which correspond to the theoretical borderline given by (3.27). Therefore, the simulations confirm the theoretical condition (3.27). Also, as expected from (3.27), an increase in the shortage of passivity z_a will cause the stable region to shrink.

For the delayed single-user HVE system with $m = 0.15$, $b = 0.2$ and $B = 0$, the delay t_d is set to $10T$ and again simulations are conducted for the three cases involving shortages of passivity z_a of 0, $0.2b$, and $0.5b$. The simulation procedure is the same as before. As shown in Figure 3.9b, again the simulation data points represented by stars are close to the theoretical borderline (3.28). This time, there is a small gap between the simulation data points and the theoretical borderline, which corresponds to cases where condition (3.28) is conservative for detecting the system instability. The conservatism of condition (3.28) was predictable due to the fact that it was found as a sufficient condition for stability. Also, as before, any increase in the shortage of passivity z_a decreases the stability region as predicted by the theoretical condition (3.28).

It is also educational to compare the stability regions for a single-user HVE system with and without the time delay. As shown in Figure 3.10, for the same shortage of passivity of the operator, de-

lay causes the stability region to shrink. This was predictable if one compares the theoretical conditions (3.27) and (3.28) for $B = 0$. Similar simulations are conducted for a sampled-data dual-user HVE system. Using MATLAB/Simulink the system in Figure 3.8a is simulated and conditions (3.58) and (3.65) are tested for $m = 2$. The simulations for both non-delayed dual-user HVE system with environment parameters $K_{01} = K_{02} = K_{12} = \frac{K}{2}$, $B_{01} = B_{02} = B_{12} = 0$, $m_1 = m_2 = 0.015$, and $b_1 = b_2 = 0.01822$ and delayed dual-user HVE system ($t_d = 5T$) with $K_{01} = K_{02} = K_{12} = \frac{K}{2}$, $B_{01} = B_{02} = B_{12} = 0$, $m_1 = m_2 = 0.15$, and $b_1 = b_2 = 0.1822$, are done for three cases with shortages of passivity z_a of 0, $0.2b$, and $0.5b$ (See Figures 3.11a and 3.11b). As before, there is a good match between the simulation results and the theoretically-derived stability borderlines.

3.6 EXPERIMETAL RESULTS

To verify the stability conditions (3.21) and (3.28), experiments involving a single-user HVE system consisting of a Phantom Premium 1.5A robot (Geomagic, Wilmington, MA) with a JR3 force sensor (JR3, Inc., Woodland, CA) at its end-effector are conducted. The mass and damping for the Phantom Premium 1.5A robot are $m = 0.015$ and $b = 0.01822$, respectively. The robot can move in three Cartesian directions and can be modeled as first-order transfer functions from the end-effector force input to the end-effector velocity output along each of these directions. Out of the three Cartesian axes, the x axis is used in the experiment while the y and z axes are locked using high-gain controllers. In agreement with the literature, the virtual environment composed of a spring and a damper in parallel as in Figure 3.2 has been implemented in discrete-time using the backward-difference method.

In the experiments, the robot is initially in free space and at some distance (initial condition) from the virtual wall. The initial condition is the difference in the position of the robot from its rest position, which is chosen to be co-located with the wall edge. Since a passive system should remain stable regardless of its initial condition, when investigating the stability of the system, the initial condition has been changed over a series of trials in a large span only limited by the physical constraints of the experimental setup. If the system becomes unstable in one trial (corresponding to a particular initial condition), it can be indicated that the system with the chosen parameters is unstable. If in none of the trials of an ex-

periment with the controller gain K and the sampling time T the system becomes unstable, then it is identified as stable.

The procedure for experimentally determining the stability/instability borderline is as follows. The objective of the experiment is to determine the largest and smallest values of the controller gain K with which the system is stable and unstable, respectively. At different sampling times apart by steps of $1ms$ in a given range, the controller gain is altered gradually until the above-mentioned maximum and minimum gains are found. The exact experimental protocol for this process of changing the controller gain is described below. Starting with a value of K close to the value obtained from conditions (3.21) and (3.28) for a given sampling time T, if no instability is seen, the experiment is repeated with a larger initial condition while keeping the same controller gain K. If the system stays stable for all initial conditions tested in the robot workspace, the corresponding data point is considered as being stable in the $K-T$ plane. Then, K is increased (by steps of 0.1) and the previous procedure involving changing the robot initial condition is repeated. Increasing the value of K is continued until the system becomes unstable. The last data point for which the system is stable is marked as stable (represented by a star) in the $K-T$ plane. Also, the data point corresponding to the unstable experiment with the smallest controller gain K is marked by a circle in the $K-T$ plane.

The results of the above procedure form a stability borderline in the $K-T$ plane. The experimentally-obtained borderlines found for the non-delayed and delayed single-user HVE system with a passive operator are shown in Figure 3.12a and 3.12b, respectively. For each case, the theoretical regions of stability and instability obtained from conditions (3.21) and (3.28) are separated by the theoretical borderline (blue line). As explained before, the result of each experiment is indicated either as a star or a circle, which correspond to largest and the smallest controller gains for which the system will be stable or unstable, respectively. Note that for each sampling time, many more tests were conducted but they are not shown in Figures 3.12a and 3.12b; only those data points corresponding to the smallest and largest controller gains for unstable and stable systems are shown. From both Figures 3.12a and 3.12b, it is seen that the theoretical absolutely stable/potentially unstable borderline is more conservative than the experimentally-obtained borderline.

3.7 CONCLUSION

This chapter studied the absolute stability of an m-user haptic virtual environment system based on the discrete-time circle criterion. In practice, depending on the task being performed by the human operator, the operator might behave passively or actively. The proposed stability analysis method enables a unified framework in which the human operators can demonstrate active or passive behavior. The same unified framework can be applied to study the stability with or without time delay. Simulation results and experiments confirm the validity of the proposed stability conditions.

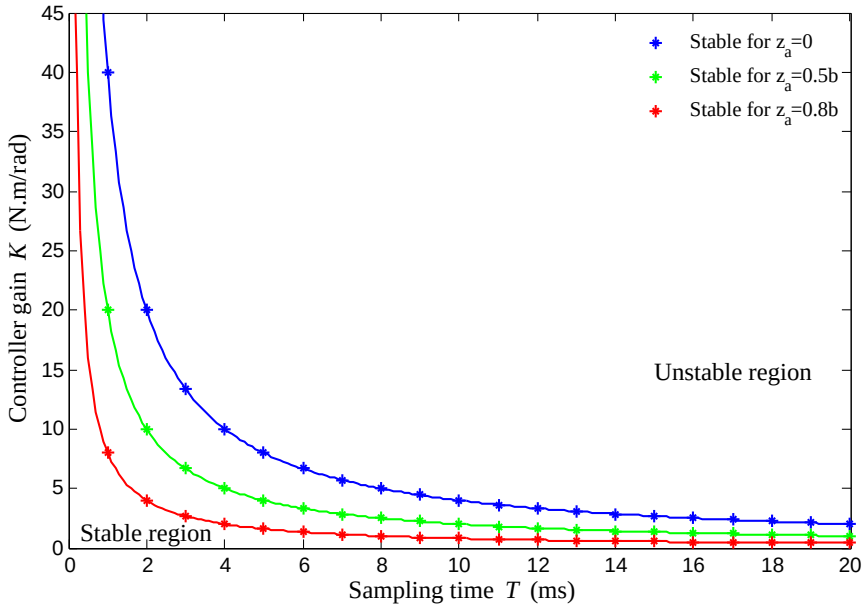

(a)

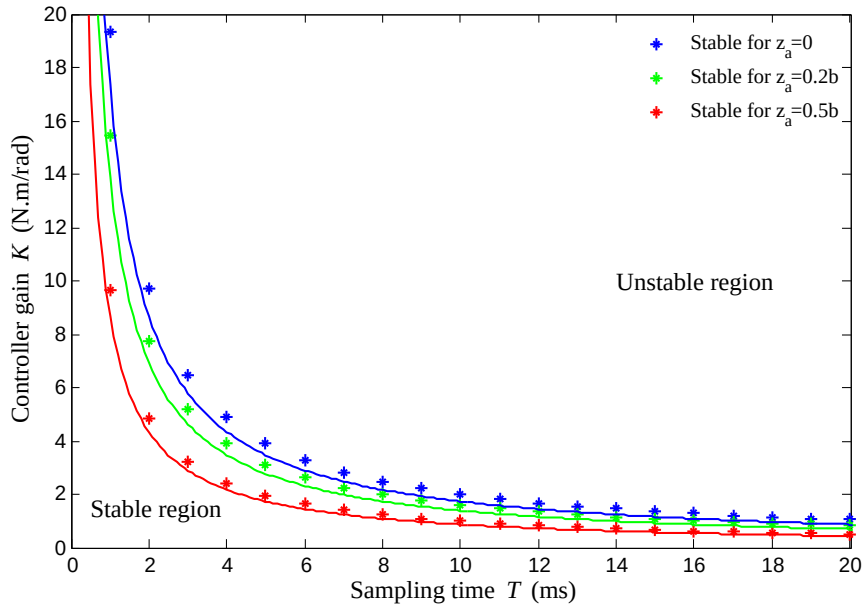

(b)

Figure 3.9: Simulation data points and corresponding theoretical borderlines for (a) a no-delay single-user HVE system, and (b) a delayed ($t_d = 10T$) single-user HVE system

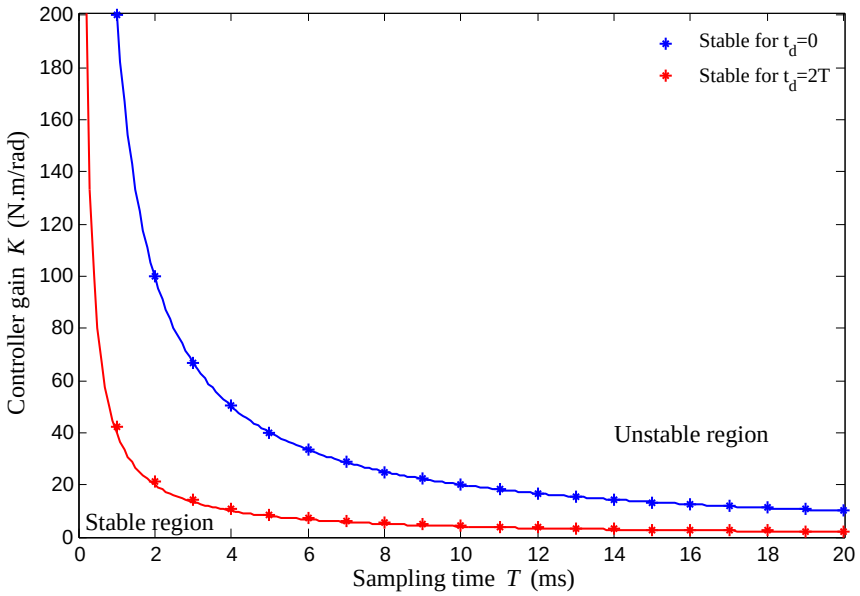

Figure 3.10: Simulation data points and corresponding theoretical borderlines for non-delayed (blue) and delayed (red) single-user HVE system when the operator is allowed to have $z_a = 0.5b$ shortage of passivity

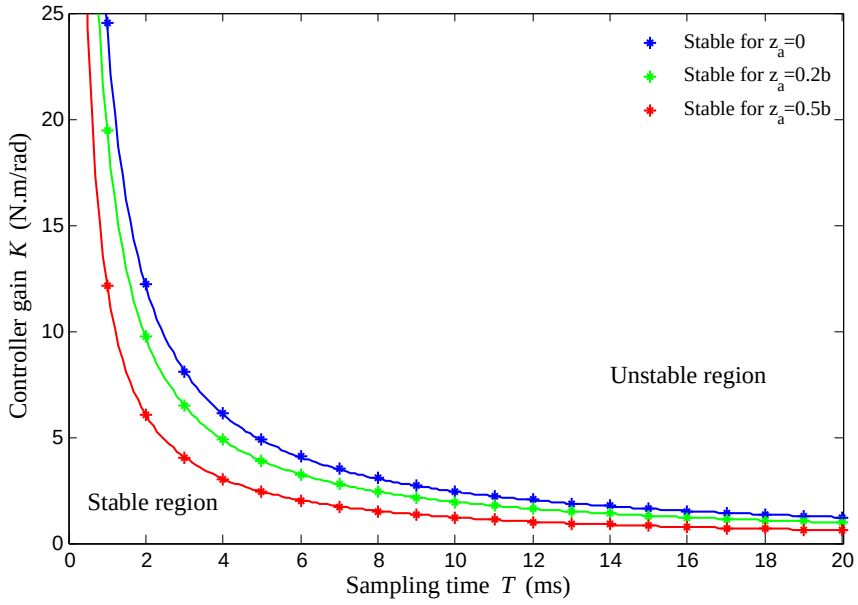

(a)

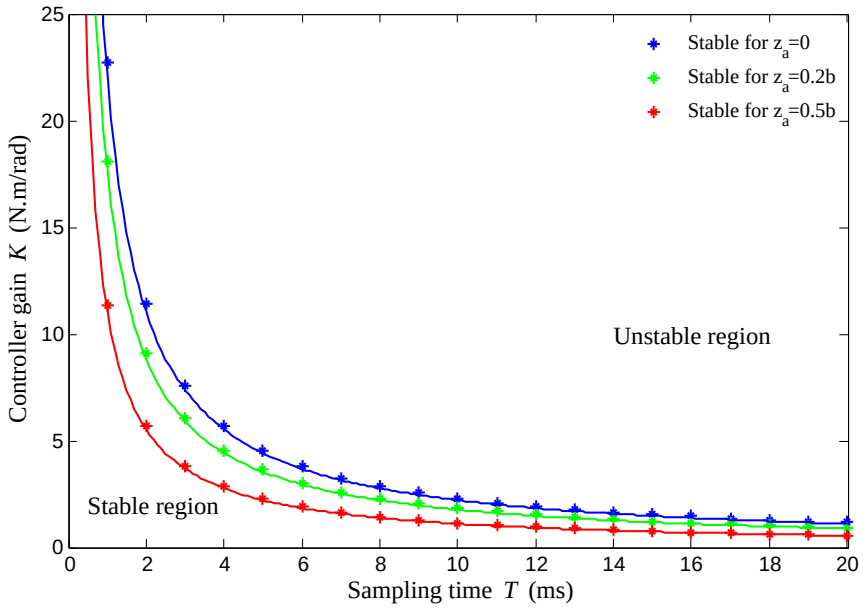

(b)

Figure 3.11: Simulation data points and corresponding theoretical borderlines for (a) a no-delay dual-user HVE system , and (b) a delayed ($t_d = 5T$) dual-user HVE system

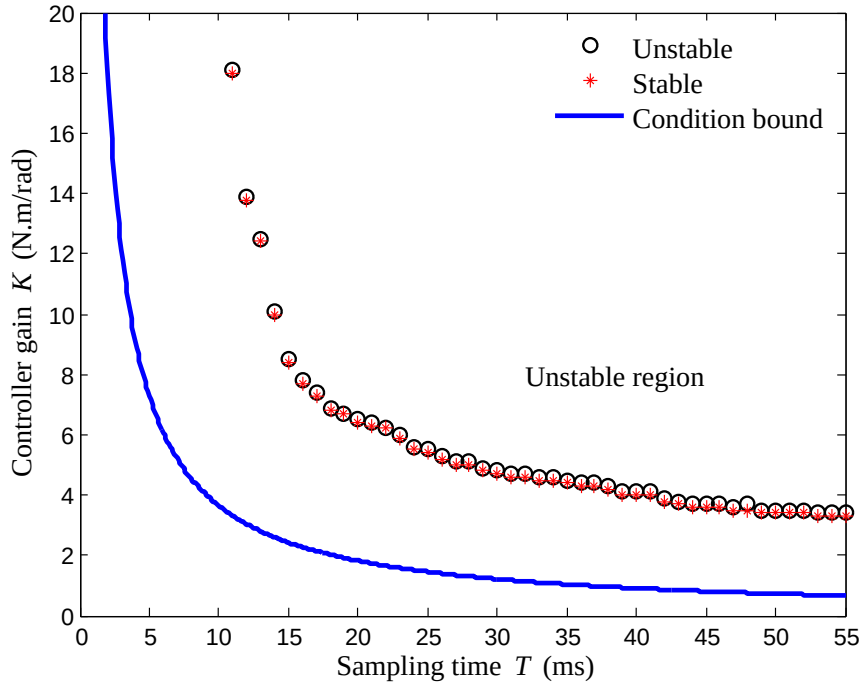

(a)

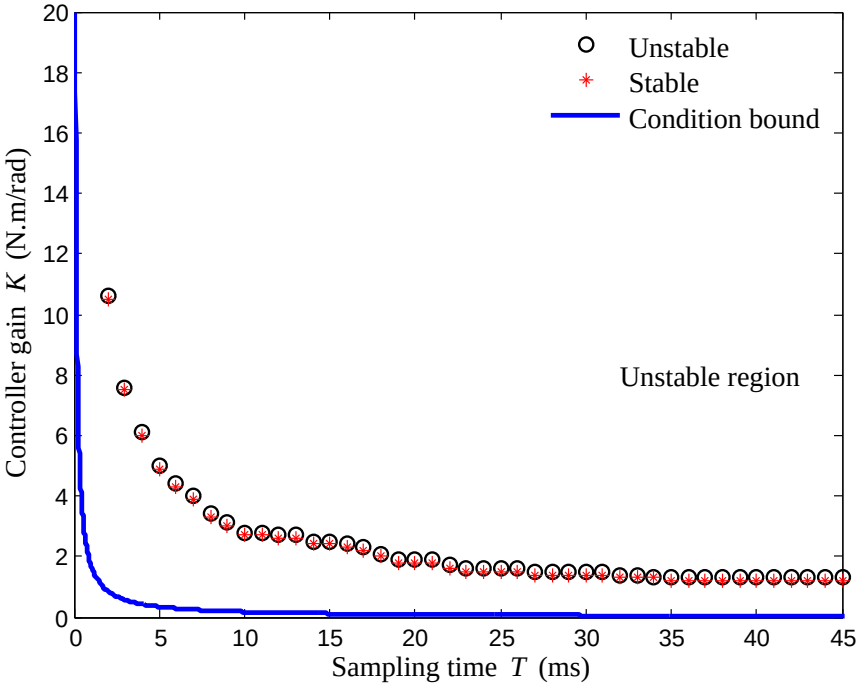

(b)

Figure 3.12: Experimental data points and theoretical borderlines for (a) a non-delayed single-user HVE system, and (b) a delayed ($t_d = 10T$) single-user HVE system

4

STABILITY ANALYSIS OF A TELEOPERATION SYSTEM VIA CIRCLE CRITERION: EFFECTS OF CONTROL SAMPLING, COMMUNICATION DELAY, AND ACTIVE OPERATOR AND ENVIRONMENT

4.1 SUMMARY

This chapter studies the absolute stability of a sampled-data, position-error-based (PEB) bilateral teleoperation systems using the discrete-time circle criterion. We pay attention to the fact that depending on the task being performed by an operator through the master robot, the passivity of the operator is influenced -- i.e., the operator may behave actively in some cases. The environment of the slave robot can also behave passively or actively. The use of circle criterion in this chapter provides a framework for system stability analysis in which the operator and the environment are allowed to exhibit passive or active behavior. In this chapter, the stability criterion previously derived in [37] for a sampled-data bilateral teleoperation system is re-generated and then extended to the case where the operator and the environment behave actively. Another extension to past work comes in the form of allowing for the communication delay. The proposed stability criterion not only unifies the analysis of stability under control sampling, communication delay, and operator/environment activity in a single framework, it also allows for comparing the relative effect of each of these non-idealities. Simulation results and experiments confirm the validity of the proposed stability conditions.

4.2 INTRODUCTION

In the design of controllers for a teleoperation system, stability is a vital issue that can be jeopardized by time delay in the communication channel, controller discretization, and active intervention of the operator and/or the environment. While the impacts on teleoperation system stability of delay [2, 55], of control sampling [36, 37], and of operator/environment activity [35] have been studied by and large individually, it is interesting to study the combined impact of these effects on stability. Below, we briefly review selected

literature concerning the effect of each of the above three factors on the stability of haptic teleoperation systems.

A stabilizing continuous-time controller does not necessarily preserve the stability after being discretized [24, 47]. Because of the energy-instilling effects of the ZOH [24], the stability of the system may be jeopardized. In the context of bilateral teleoperation, Stramigioli et al. proposed a geometric framework allowing both continuous-time and discrete-time signals in a teleoperation system [68]. In more recent studies involving sampled-data bilateral teleoperation systems, the effects of discretized controllers on teleoperation system passivity and stability have been investigated [36, 37]. Moreover, if the sampling time is comparable to the fast dynamics of the controlled system the resulting sampled-data system will perform poorly.

Given that the human operator in a teleoperation system voluntarily manipulates the master robot, and has the capacity to inject energy into the teleoperation system, the stability of the teleoperation system might be jeopardized. Active behavior of the operator has been reported in [17]. As such, the stability of bilateral teleoperation systems under active operator has been studied in [7, 35], albeit assuming continuous operation of the teleoperation system controllers. Communication delays have long been recognized as a main cause of instability in bilateral teleoperation systems. Time delay compensation in teleoperation has been studied extensively in the literature including for discrete-time implementation of the communication channel [11]. Reviews of time delay compensation techniques for teleoperation systems can be found in [3, 58, 64].

In this chapter, the absolute-stability of a sampled-data, PEB bilateral teleoperation system based on the discrete-time circle criterion is investigated. The main contribution of the chapter is in proposing a unified framework that allows inspecting the effects of various de-stabilizing factors including controller discretization, time delay and active behavior of the operator and/or the environment at the same time. This framework for stability analysis leads to conditions involving the control parameters and other system parameters for preserving the stability of the teleoperation system when coupled to an operator and an environment. In this chapter, the stability criterion for sampled-data teleoperation systems previously derived in [37] is re-generated and then extended to the case where the operator and environment are allowed to behave actively and delays are allowed to exist in the communication channel. The resulting conditions also provide a way to compare the relative effects of all of the three de-stabilizing factors.

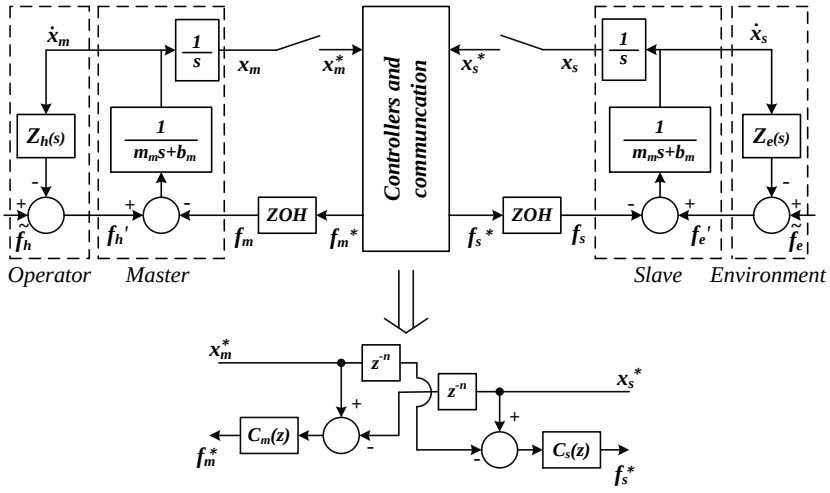

Figure 4.1: Model of a sampled-data bilateral teleoperation system

The rest of the chapter is organized as follows. Section 3.3 provides mathematical preliminaries required in the rest of the chapter. In section 4.3, the model of a sampled-data, delayed teleoperation system is presented and used to derive stability condition for passive or active operator/environment under a delayed or non-delayed communication channel. The simulation results are presented in Section 4.4 and the experimental setup and results are presented in Section 4.5. Section 4.6 includes the concluding remarks.

4.3 SYSTEM MODELING

A sampled-data teleoperation system with PEB architecture is modeled in Figure 4.1. The master and slave robots are modeled as 1-DOF, mass-damper, LTI systems with the following dynamics:

$$\begin{aligned} f_h^{'} - f_m &= m_m \ddot{x}_m + b_m \dot{x}_m \\ f_e^{'} - f_s &= m_s \ddot{x}_s + b_s \dot{x}_s \end{aligned} \tag{4.1}$$

In the above, $f_h^{'}$ and $f_e^{'}$ are the human operator and the environment forces. Also, f_m and f_s are the control actions from the master and the slave discrete-time controllers $C_m(z)$ and $C_s(z)$. The parameters b_m and b_s are the dampings and m_m and m_s are the masses of the master and slave robots, respectively. In the force-velocity domain, the operator and the environment are modeled as LTI impedances $Z_h(s)$ and $Z_e(s)$, respectively. In Figure 4.1, $\tilde{f}_h$ is the exogenous in-

put force from the operator and $\tilde{f}_e$ is the exogenous input force from the environment. As shown in Figure 4.1, the positions of the master and robots are discretized using sampler blocks. The superscript * denotes sampled signals. ZOH blocks convert the sampled signals back to the continuous-time domain. The output of the sampler can be mathematically represented as a Dirac comb weighted by the sampled signal, i.e., $x^*(t) = \Sigma_{k=0}^{\infty} x(kT)\delta(t-kT)$. Thus, mathematical representation of the sampling operation in the Laplace domain is

$$X^*(s) = \mathcal{L}\{x^*(t)\} = \sum_{k=0}^{\infty} x(kT)e^{-skT} \tag{4.2}$$

Conversely, mathematical representation of the ZOH operation in the Laplace domain is

$$X(s) = \frac{1-e^{-sT}}{s} X^*(s) \tag{4.3}$$

The LTI models of the environment and the operator can be written in the Laplace domain as

$$\begin{aligned} \tilde{F}_h(s) - F_h^{'}(s) &= Z_h(s) s X_m(s) \\ \tilde{F}_e(s) - F_e^{'}(s) &= Z_e(s) s X_s(s) \end{aligned} \tag{4.4}$$

The dynamics of the master and slave robots in (4.1) are also as follows in the Laplace domain:

$$\begin{aligned} sX_m(s) &= \frac{1}{m_m s + b_m}(F_h(s) - F_m(s)) \\ sX_s(s) &= \frac{1}{m_s s + b_s}(F_e(s) - F_s(s)) \end{aligned} \tag{4.5}$$

The PEB controller blocks in Fig 4.1 apply forces based on the master/slave position difference while considering the time delay incurred when each position signal travels to the other end of the teleoperation system. Thus, the discrete-time controllers of the master and the slave implement the following laws:

$$\begin{aligned} F_m^*(s) &= C_m(z)|_{z=e^{sT}}[X_m^*(s) - z^{-n}X_s^*(s)] \\ F_s^*(s) &= C_s(z)|_{z=e^{sT}}[X_s^*(s) - z^{-n}X_m^*(s)] \end{aligned} \tag{4.6}$$

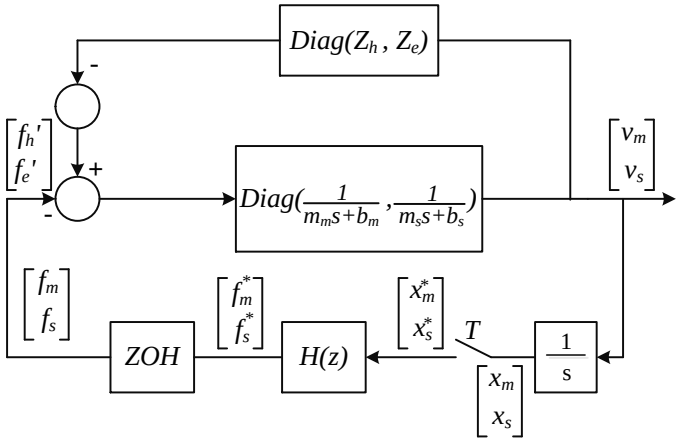

(a)

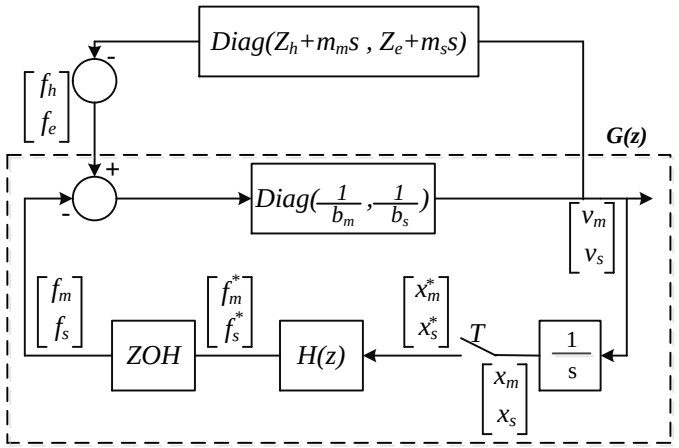

(b)

Figure 4.2: Block diagram of a teleoperation system, which includes discretized controller models

The system in Figure 4.1 can be represented as the block diagram in Figure 4.2a where delay $n = \frac{t_d}{T}$ is an integer and

$$H(z) = \begin{bmatrix} C_m(z) & -z^{-n}C_m(z) \\ -z^{-n}C_s(z) & C_s(z) \end{bmatrix} \tag{4.7}$$

Simple manipulation in Figure 4.2a will result in Figure 4.2b. Note that by moving the masses of the master and slave robots m_m and m_s to the operator and environment impedances, the closed-loop transfer matrix will not change. Then, the mapping for the system in Figure 4.2b can be written as:

$$\begin{bmatrix} F_h(z) \\ F_e(z) \end{bmatrix} = \begin{bmatrix} b_m & 0 \\ 0 & b_s \end{bmatrix} \begin{bmatrix} V_m(z) \\ V_s(z) \end{bmatrix} + H(z)\mathcal{Z}\begin{bmatrix} \frac{V_m(s)}{s} \\ \frac{V_s(s)}{s} \end{bmatrix}^* \tag{4.8}$$

Note that $\mathcal{Z}[\frac{v}{s}] \neq \mathcal{Z}[\frac{1}{s}]V(z)$. To be able to derive the transfer function from force to velocity we need to approximate $\mathcal{Z}[\frac{v}{s}]$ based on one of the three approximation methods (forward difference, backward difference and tustin transformation) discussed in Section 3.4.1.1. In this chapter it is assumed that $C_m = K_m + B_m s$ and $C_s = K_s + B_s s$. In agreement with [36, 37], to have the z domain equivalent of C_m and C_s, the backward difference is used to approximate s:

$$C_m(z) = K_m + \frac{B_m(z-1)}{Tz} \quad C_s(z) = K_s + \frac{B_s(z-1)}{Tz} \tag{4.9}$$

PASSIVE TERMINATIONS, NO DELAY Assuming that $t_d = 0$, depending on which approximation is chosen, the force to velocity mapping will be one of the following:

$$\begin{bmatrix} F_h(z) \\ F_e(z) \end{bmatrix} = \left(\begin{bmatrix} b_m & 0 \\ 0 & b_s \end{bmatrix} + H(z)\frac{T}{z-1} \right) \begin{bmatrix} V_m(z) \\ V_s(z) \end{bmatrix}$$
$$= G_1^{-1}(z)V(z) \tag{4.10}$$
$$\begin{bmatrix} F_h(z) \\ F_e(z) \end{bmatrix} = \left(\begin{bmatrix} b_m & 0 \\ 0 & b_s \end{bmatrix} + H(z)\frac{Tz}{z-1} \right) \begin{bmatrix} V_m(z) \\ V_s(z) \end{bmatrix}$$
$$= G_2^{-1}(z)V(z) \tag{4.11}$$
$$\begin{bmatrix} F_h(z) \\ F_e(z) \end{bmatrix} = \left(\begin{bmatrix} b_m & 0 \\ 0 & b_s \end{bmatrix} + H(z)\frac{T}{2}\frac{z+1}{z-1} \right) \begin{bmatrix} V_m(z) \\ V_s(z) \end{bmatrix}$$
$$= G_3^{-1}(z)V(z) \tag{4.12}$$

The above correspond to the forward difference, the backward difference and the Tustin approximation methods, respectively. Based on Theorem 3.3.1, the sampled-data PEB bilateral teleoperation system is absolutely stable if $G(z)$ is positive real. Since passivity of $G(z)$ is equal to $G^{-1}(z)$ being passive, it suffices to show that $G^{-1}(z)$ is positive real. The first condition in Definition 3.3.3 requires all poles of $G^{-1}(z)$ to lie inside or on the unit circle, which obviously is the case here. As it can be clearly seen in (4.10)-(4.12), $z = 1$ is a simple pole and in order to satisfy the second condition for positive realness the residue matrix corresponding to this

pole must be positive semidefinite. For all three approximation, the residue matrix is

$$R_0 = \begin{bmatrix} K_m T & -K_m T \\ -K_s T & K_s T \end{bmatrix} \tag{4.13}$$

which is clearly positive semidefinite since $K_m, K_s, T > 0$ and $det(R_0)$ is zero. The only remaining condition is the second condition in Definition 3.3.3, which requires $G(e^{j\omega}) + G^T(e^{-j\omega})$ to be positive semidefinite. Starting with the forward approximation method and substituting $z = \cos(\omega T) + j\sin(\omega T)$, leading principle minors of $G(e^{j\omega}) + G^T(e^{-j\omega})$ need to be positive semidefinite. Therefore,

$$b_m - \frac{K_m T}{2} + B_m \cos(\omega T) > 0 \tag{4.14}$$

$$\begin{aligned} &det(G_1^{-1}(e^{j\omega T}) + G_1^{T-}(e^{-j\omega T})) = \\ &(2b_m - K_m T + 2B_m \cos(\omega T))(2b_s - K_s T + 2B_s \cos(\omega T)) - \\ &((\frac{K_m + K_s}{2})T - (B_m + B_s)\cos(\omega T))^2 - \\ &((\frac{K_m - K_s}{2})T \cot(\frac{\omega T}{2}) + (B_m - B_s)\sin(\omega T))^2 > 0 \end{aligned} \tag{4.15}$$

It can been shown that condition (4.15) is valid for $C_m = C_s = K + \frac{B(z-1)}{Tz}$ if

$$\frac{b_m b_s}{b_m + b_s} > \frac{KT}{2} - B\cos(\omega T) \tag{4.16}$$

Condition (4.16) is dependent on the frequency ω and since $\cos(\omega T)$ can vary between -1 and 1, the worst-case for conditions (4.14) and (4.16), assuming $C_m = C_s = K + \frac{B(z-1)}{Tz}$, will be

$$b_m > \frac{KT}{2} + B \tag{4.17}$$

$$\frac{b_m b_s}{b_m + b_s} > \frac{KT}{2} + B \tag{4.18}$$

For $b = \min\{b_m, b_s\}$, a sufficient condition for absolute stability of a non-delayed sampled-data PEB bilateral teleoperation system will be

$$b > KT + 2B \tag{4.19}$$

Now, proceeding to the backward approximation method, the same procedure is applied on $G_2^{-1}(z)$. Again for $C_m = C_s = K + \frac{B(z-1)}{Tz}$, the absolute stability condition will be

$$b_m + \frac{KT}{2} + B > 0 \quad , \quad \frac{b_m b_s}{b_m + b_s} + \frac{KT}{2} + B > 0 \tag{4.20}$$

Finally, applying the same procedure for the tustin transformation approximation method the absolute stability condition will be

$$b_m + B > 0 \quad , \quad \frac{b_m b_s}{b_m + b_s} + B > 0 \tag{4.21}$$

From (4.19), (4.20) and (4.21), it can clearly be seen that the forward difference approximation method returns the worst-case condition (4.19) for absolute stability of sampled-data PEB bilateral teleoperation system.

ACTIVE TERMINATIONS, NO DELAY The above approach also enables us to inspect the stability of sampled-data PEB bilateral teleoperation system with active terminations. Note that previously in Figure 4.2b, in order to simplify the system, the masses m_m and m_s of the master and slave devices were moved to the operator and environment impedances $Z_h(s)$ and $Z_e(s)$ without affecting the overall system or the passivity of the new operator $Z_h(s) + m_m s$ and the new environment $Z_e(s) + m_s s$. Now, given that we want to allow the operator and environment to be active, we will move enough of dampings bm and b_s of master and slave devices to the new operator and the new environment impedances. Let's name the real part of the operator impedance Z_h to be $-z_a$ and the real part of environment impedance to be $-z_b$. When $z_a > 0$ and $z_b > 0$, they show the shortage of passivity of an active operator and an active environment. We will transfer z_a units of the master device damping b_m, and z_b units of the slave device damping b_s to $Z_h(s)$ and $Z_e(s)$, respectively, to neutralize the shortages of passivity and make the new operator and the new environment passive. As a result, based on (4.17)-(4.18) and after replacing b_m by $b_m - z_a$ and b_s by $b_s - z_b$, the stability condition after accounting for the active operator and environment will be

$$b_m - z_a > \frac{KT}{2} + B \tag{4.22}$$

$$\frac{(b_m - z_a)(b_s - z_b)}{(b_m - z_a) + (b_s - z_b)} > \frac{KT}{2} + B \tag{4.23}$$

With $b_d = \min\{b_m - z_a, b_s - z_b\}$, the absolute stability condition for a non-delayed sampled-data teleoperation system under active terminations will be

$$b_d > KT + 2B \tag{4.24}$$

PASSIVE TERMINATIONS, DELAY For a delayed sampled-data PEB bilateral teleoperation system, again the three approximation methods are compared and the worst-case condition is chosen as the absolute stability condition. For brevity, only the procedure using the forward approximation method is shown here becuase it returns the worst-case condition for the stability of the delayed sampled-data PEB bilateral teleoperation system. The resulting inverse transfer matrix will be

$$G^{-1}(z) = \tag{4.25}$$
$$\begin{bmatrix} b_m + (\frac{K_m T}{z-1} + \frac{B_m}{z}) & -z^{-n}(\frac{K_m T}{z-1} + \frac{B_m}{z}) \\ -z^{-n}(\frac{K_s T}{z-1} + \frac{B_s}{z}) & b_s + (\frac{K_s T}{z-1} + \frac{B_s}{z}) \end{bmatrix}$$

Here again, based on Theorem 3.3.1 and using the fact that passivity of $G(z)$ is equal to $G^{-1}(z)$ being passive, for the absolute stability of the delayed sampled-data PEB bilateral teleoperation system it suffices to show the positive realness of $G^{-1}(z)$. Same as before, based on Definition 3.3.3, three conditions are to be satisfied. The first and third conditions are the case here since all poles of each element of $G^{-1}(z)$ lie inside or on the unit circle and the pole at $z = 1$ is simple with the same residue matrix as (4.13), which is clearly positive semidefinite. The third condition which requires $G^{-1}\{j\omega\} + G^{-T}\{-j\omega\}$ to be positive semidefinite, is yet to be checked. Substituting $z = e^{j\omega T} = \cos(\omega T) + j\sin(\omega T)$, the second condition in Definition 3.3.3 for positive realness of $G^{-1}(z)$ will lead to the following conditions:

$$b_m + B_m \cos(\omega T) - \frac{K_m T}{2} > 0 \tag{4.26}$$

$$\begin{aligned} &det(G(e^{j\omega T}) + G^T(e^{-j\omega T})) = \\ &4(b_m + B_m \cos(\omega T) - \frac{K_m T}{2})(b_s + B_s \cos(\omega T) - \frac{K_s T}{2}) - \\ &4(\frac{(K_m + K_s)T}{2}(\cos(\omega t_d) + S_1) - (B_m + B_s)\cos(\omega(T + t_d)))^2 - \\ &4(\frac{(K_m - K_s)T}{2}(\sin(\omega T) - S_2) - (B_m - B_s)\sin(\omega(T + t_d)))^2 > 0 \end{aligned} \tag{4.27}$$

where $S_1 = \frac{\sin(\omega t_d)\sin(\omega T)}{(1-\cos(\omega T))}$ and $S_2 = \frac{\cos(\omega t_d)\sin(\omega T)}{(1-\cos(\omega T))}$. Assuming that $t_d/T = n$ is an integer and for equal controllers $C_m = C_s = K + \frac{B(z-1)}{Tz}$, the worst-case for (4.27) occurs when S has its maximum value. Therefore, solving the $\frac{d}{d\omega}S = 0$ will lead us to $cos(\omega T) = 1$, which is confirmed to give the maximum value of S by checking the sign of the second derivative of S when $cos(\omega T) = 1$. The maximum value of S will therefore be

$$\lim_{\cos(\omega T)\to 1} S = \lim_{\cos(\omega T)\to 1} \frac{\sin(\omega t_d)\sin(\omega T)}{2(1-\cos(\omega T))} = \frac{2t_d}{T}$$

Then, condition (4.27) will simplify to

$$(b_m + B - \frac{K}{2})(b_s + B - \frac{K}{2}) - (\frac{KT}{2} + Kt_d - B)^2 > 0 \tag{4.28}$$

With $b = \min\{b_m, b_s\}$, the absolute stability condition for a delayed sampled-data teleoperation system under passive terminations will be

$$b + 2B > KT + Kt_d \tag{4.29}$$

ACTIVE TERMINATIONS, DELAY Using the same procedure as for the non-delayed bilateral teleoperation system with active terminations the conditions (4.26) and (4.28) will change to

$$b_m - z_a + B_m\cos(\omega T) - \frac{K_m T}{2} > 0 \tag{4.30}$$

$$(b_m - z_a + B - \frac{K}{2})(b_s - z_b + B - \frac{K}{2}) - (\frac{KT}{2} + Kt_d - B)^2 > 0 \tag{4.31}$$

With $b_d = \min\{b_m - z_a, b_s - z_b\}$, the absolute stability condition for a delayed bilateral teleoperation system under active terminations will be

$$b_d + 2B > KT + Kt_d \tag{4.32}$$

4.4 SIMULATION RESULTS

In this section, the stability conditions derived throughout this paper are verified using simulations. Having an operator or an environment with a set amount of shortage of passivity is quite difficult

to robustly realize in practice. For this reason, experimental results could not be provided for conditions that allow operator activity; instead, such cases are tested in simulations. In order to test conditions (4.24) and (4.32), which correspond to active terminations without and with delay, the sampled-data bilateral teleoperation system in Figure 4.2a is simulated in MATLAB/Simulink. To determine the stability of the system, the system outputs are monitored for boundedness at all times -- if any output goes unbounded, the system is unstable.

For the non-delayed bilateral teleoperation system with with $M_m = M_s = 0.015$, $b = 0.02$ and $B = 0$, simulations have been conducted for three cases, where the shortage of passivity of the operator and the environment are either 0, $0.2b$, or $0.5b$. To this end, the operator and the environment models are considered to be $-z_a + \frac{1}{s}$; note that $\Re\{\frac{1}{s}\} = 0$ makes it a least-passive termination corresponding to a worst-case scenario for the coupled system stability. During the simulations, the sampling time is increased by steps of $1ms$. For each sampling time, the controller gain K is changed to find the largest gain value for which the system remains stable. In Figure 4.3a, each of these maximum controller gain values at a given sampling period is represented by a star. Evidently, these simulation data points are very close to the solid lines, which correspond to the theoretical borderline given by (4.24). Therefore, the simulations confirm the theoretical condition (4.24). Also, as expected from (4.24), increase in the shortages of passivity z_a and z_b will cause the stable region to shrink.

For the delayed bilateral teleoperation system with $M_m = M_s = 0.15$, $b = 0.2$ and $B = 0$, the delay t_d is set to $4T$ and again simulations are conducted for the three cases involving shortages of passivity $z_a = z_b$ of 0, $0.2b$, and $0.5b$. The simulation procedure is the same as before. As shown in Figure 4.3b, again the simulation data points represented by stars correspond are very close to the theoretical borderline (4.32). As before, any increase in the shortages of passivity z_a and z_b decreases the stability region as predicted by the theoretical condition (4.32).

4.5 EXPERIMENTAL RESULTS

To verify the stability conditions (4.19) and (4.29), experiments involving a PEB bilateral teleoperation system consisting of a pair of Phantom Premium 1.5A robot (Geomagic, Wilmington, MA) with JR3 force sensors (JR3, Inc., Woodland, CA) at their end-effectors

are conducted. The mass and damping for the Phantom Premium 1.5A robot are $m = 0.015$ and $b = 0.01822$. The robots can move in three Cartesian directions and can be modeled as first-order transfer functions from the end-effector force inputs to the end-effector velocity outputs along each of these directions. Out of the three Cartesian axes, the x axis is used in the experiment while the y and z axes are locked using high-gain controllers. The controllers C_m and C_s have been implemented in discrete-time using the backward-difference method.

With the assumption that $C_m = C_s = K + B\frac{z-1}{z}$, the procedure for experimentally determing the stability/instability region for the bilateral teleoperation system is as follow. The objective of the experiment is to determine the largest and smallest values of the controller gain K with which the system is stable and unstable, respectively. At different sampling times apart by steps of $1ms$ in a given range, the controller gain is altered gradually until the above-mentioned maximum and minimum gains are found. Starting with a value of K close to the value obtained from conditions (4.19) and (4.29), the master robot is shaken intentionally. If after the master robot is released (rendering the human operator to be the free-space, which is passive), the position oscillation amplitude increases over time, it means that the system was unable to reach stability and hence the data point corresponding to that experiment is unstable Figure 4.4b. But if after the master robot is released the oscillations tend to damp, then the corresponding data point will clearly be stable Figure 4.4a. For each unstable data point found in the $K - T$ plane using the aforementioned test, the controller gain K is decreased to find the minimum controller gain value that stabilizes the system despite the initial instability forced on the system by the operator. The corresponding value is then marked on the $K - T$ plane by a circle corresponding to stability. For stable data points on the other hand, the controller gain K is increased untill instability is observed. The largest controller gain value for which the system remains stable is then marked on the $K - T$ plane by a star.

The experimentally-obtained borderlines found for the cases of non-delayed and delayed bilateral teleoperation system with a passive operator are shown in Figure 4.5a and 4.5b, respectively. For each case, the theoretical regions of stability and instability obtained from conditions (4.19) and (4.29) are separated by the theoretical borderline (blue line). As explained before, the result of each experiment is indicated either as a star or a circle, which correspond to largest and the smallest controller gains for which the

system will be stable or unstable, respectively. Note that for each sampling time, many more tests were conducted but they are not shown in Figures 4.5a and 4.5b; only those data points corresponding to the smallest and largest controller gains for unstable and stable systems are shown. From 4.5a and 4.5b, it is seen that the theoretical absolutely stable/potentially unstable borderline is more conservative than that obtained experimentally. As it can be seen in Section 4.4, the data points found via simulations are very close to the theoretical borderline. What explains the distance between the two plots is the methodology used to test stability in the simulations versus that in the experiments. In simulations, the system is excited using a very small, bounded sine-wave F_h^*. In experiments happening in practice, however, this is not an actual physical input that can be manipulated. Therefore, in the experiments, we had no option but to use the method based on initial intentional destabilization (i.e., violently shaking the master followed by releasing it and then observing the outputs), which is a different criterion for detecting instability. Despite this difference, both borderlines exhibit the same trade-offs between the sampling period and the control gain.

4.6 CONCLUSION

This chapter studied the absolute stability of a sampled-data PEB bilateral teleoperation system based on the discrete-time circle criterion. In practice, depending on the task being performed by the human operator, the operator might behave passively or actively. The proposed stability analysis method enabled a unified framework in which both the human operator and the environment are allowed to demonstrate active or passive behavior. The same unified framework was applied to study the stability with or without time delay. Simulation results and experiments confirmed the validity of the proposed stability conditions.

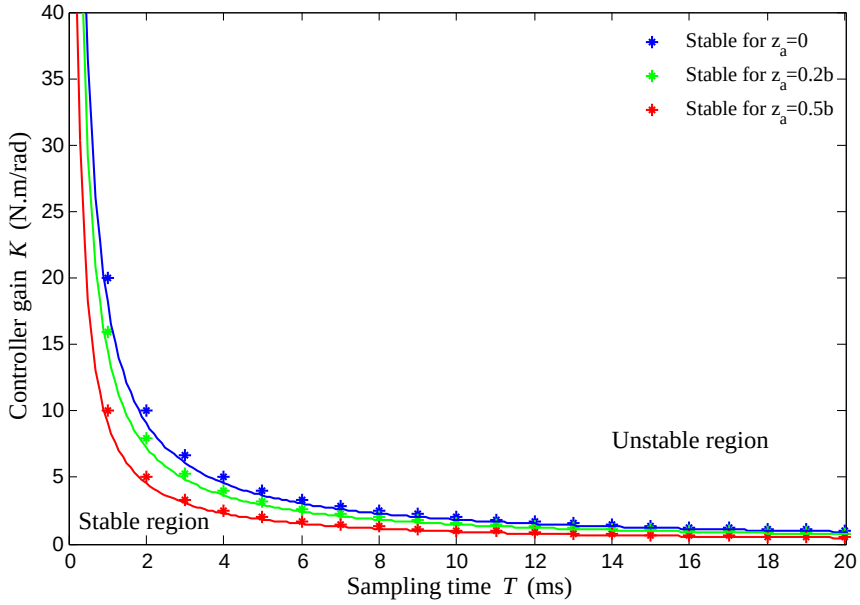

(a)

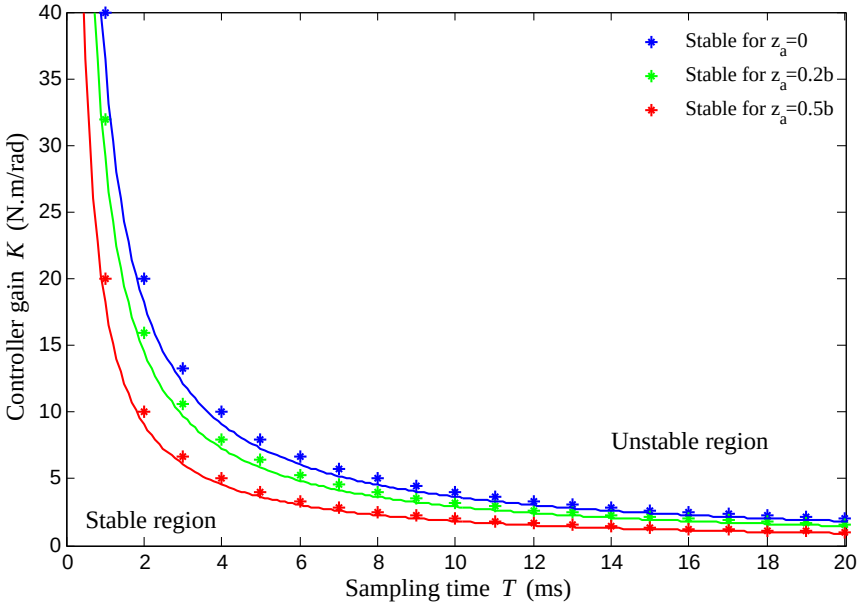

(b)

Figure 4.3: Simulation data points and corresponding theoretical borderlines for (a) a no-delay bilateral teleoepration system, and (b) a delayed ($t_d = 4T$) bilateral teleoepration system.

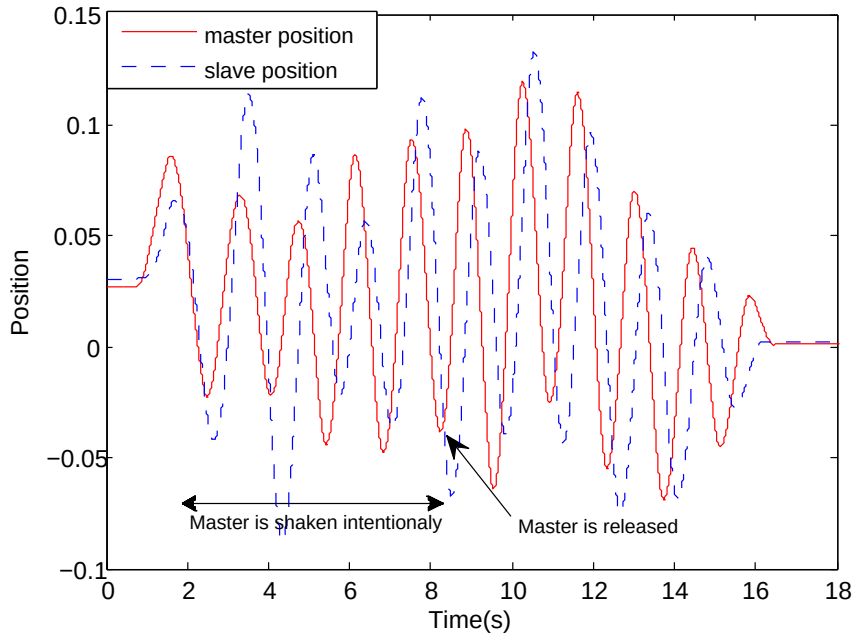

(a)

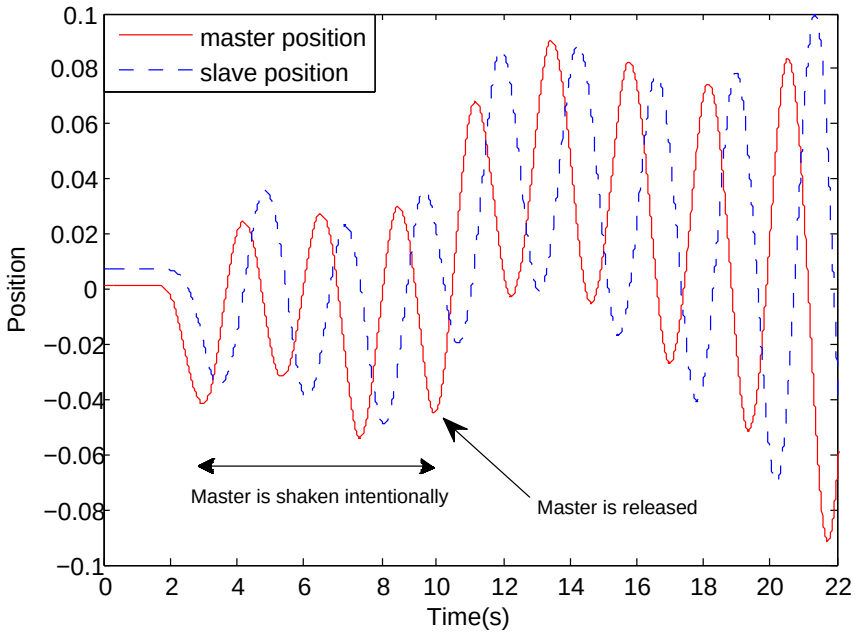

(b)

Figure 4.4: The master and slave position trajectory. (a) A stable system; the operator deliberately de-stabilizes the system by shaking the master robot violently, which injects energy to the system. After releasing the master arm at $t = 8s$, the teleoperation system regains stability. (b) An unstable system; after relasing the master arm at $t = 10s$, the position oscillation amplitude increases and the system goes unstable.

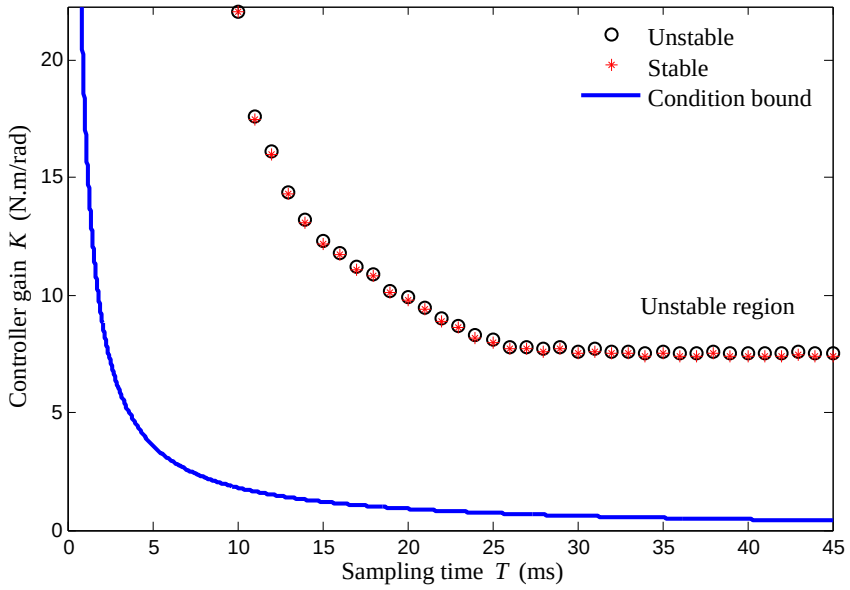

(a)

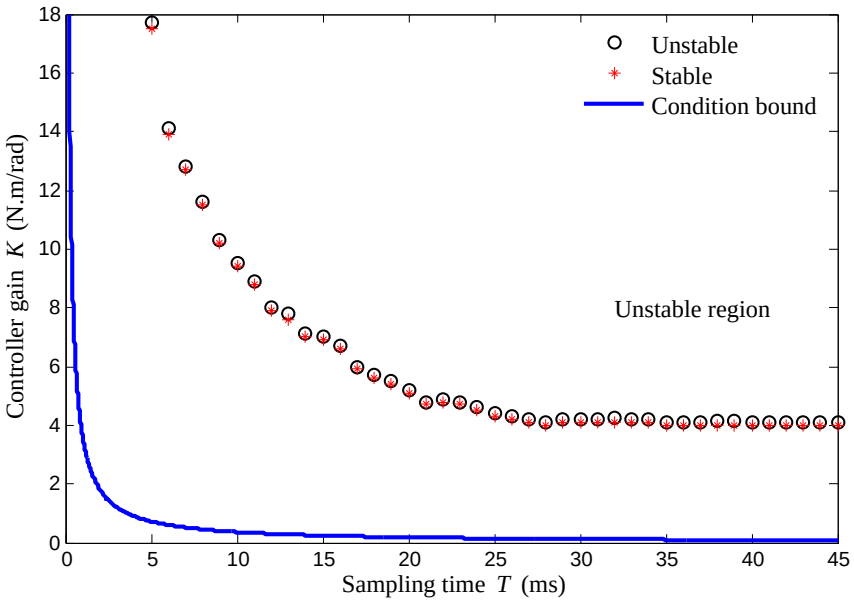

(b)

Figure 4.5: Experimental data points and theoretical borderlines for (a) a non-delayed PEB bilateral teleoperation system, and (b) a delayed ($t_d = 4T$) PEB bilateral teleoperation system.

5

STABILITY ANALYSIS OF DELAYED 4-CHANNEL BILATERAL TELEOPERATION SYSTEMS

5.1 SUMMARY

This chapter studies the stability of a delayed four-channel (4CH) teleoperation system based on the passivity framework. Assuming that the operator and the environment are passive systems, the stability of the teleoperation system is reduced to ensuring the passivity of a master control unit (MCU), a slave control unit (SCU), and the time-delayed communication channel. Each of these blocks is modeled as a 2×2 transfer function matrix and passified using our proposed approach in a multi-loop feedback (MLF) structure. We report conditions on the controllers of the 4CH architecture that are sufficient for passivity of MCU and SCU. Simulation results confirm the validity of these conditions for the stability of the teleoperation system.

5.2 INTRODUCTION

A teleoperation system consists of a two-port network representing a teleoperator (comprising a master robot, a slave robot, their controllers, and a communication channel) coupled to two one-port networks representing a human operator and an environment. A teleoperator's two-port network model can be an impedance matrix relating velocities to forces, a hybrid matrix relating a mixed force-velocity vector to another mixed force-velocity vector, or an admittance matrix relating forces to velocities [27, 56]. Based on this modeling, two-port network theory can be used to analyze the teleoperator's passivity and, therefore, the teleoperation system's stability.

Passivity-based stability analysis of bilateral teleoperation systems was first introduced in [1] through scattering theory, and then presented in the wave variables framework in [55]. A review of time delay compensation techniques for teleoperation systems can be found in [3]. In [1,55], the emphasis is on passifying the communication channel *assuming that the master and the slave when combined with their respective controllers are passive systems*. Although the mas-

ter and the slave robots may be assumed loosely to be passive [30], there is no guarantee that the master control unit (MCU) and the slave control unit (SCU), which result from combining the master and the slave with their controllers, are also passive. To the best of the authors' knowledge, the conditions under which the MCU and the SCU remain passive have not been reported before. In this chapter, we derive conditions for passivity of the MCU and the SCU while also passifying the delayed communication channel.

Wave transformation for passifying a delayed communication channel were developed for a channel that can be modeled as a 2-port network [55]. In order to apply the wave variables method to a delayed 4CH teleoperation system, in which the communication channel has 4 inputs and 4 outputs, similar to the method in [8], a weighted sum of force and velocity at each side of the teleoperation system can be sent through the channel making the communication channel appear as a 2-port network. However, this approach to delay compensation in the 4CH teleoperation system introduces non-physical variables that complicate the teleoperator's passivity analysis. In this chapter, without any need for physical interpretation of the signals that are involved in a delay-compensated 4CH teleoperation system, a transfer matrix based approach to modeling and stability analysis is presented that is easier to follow compared to traditional two-port network based passivity analyses. The stability analysis introduced in this chapter has been also extended to trilateral teleoperation system with the 4CH structure introduced in [39]. In recent years, multilateral teleoperation systems have been studied extensively in literature [38, 39, 41–43, 66, 67, 71].

The rest of the chapter is organized as follows. Section 5.3 provides mathematical preliminaries required for this chapter. In Section 5.4, the 4CH teleoperation system is modeled. In Section 5.5, the passification procedure for the delayed communication channel within the 4CH architecture is presented. Section 5.6 finds a condition for stability of the delay-compensated 4CH teleoperation system in terms of passivity of the MCU and the SCU. Simulation results are presented in Section 5.8 and Section 5.9 presents the conclusions.

5.3 MATHEMATICAL PRELIMINARIES

Definition 5.3.1. *[27] The M-port network N_M shown in Figure 5.1 with zero initial energy is passive if and only if*

$$\int_0^t \sum_{i=1}^{M} f_i(\tau) v_i(\tau) d\tau \geq 0, \quad \forall t \geq 0 \tag{5.1}$$

for all admissible forces f_i's and velocities v_i's, $i = 1, ..., m$.

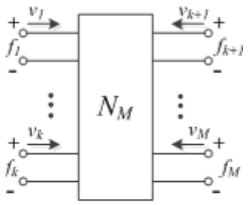

Figure 5.1: An M-port network

Definition 5.3.2. *[44] The system*

$$\dot{x} = f(x, u) \tag{5.2}$$
$$y = h(x, u) \tag{5.3}$$

is said to be passive if there exists a continuously differentiable positive semidefinte function $V(x)$ (called storage function) such that

$$u^T y \geq \dot{V} = \frac{\partial V}{\partial x} f(x, u), \forall (x, u) \in R^n \times R^m \tag{5.4}$$

Moreover, it is said to be strictly passive if $u^T y > \dot{V}$.

Lemma 5.3.1. *[44] The LTI minimal realization*

$$\dot{x} = Ax + Bu \tag{5.5}$$
$$y = Cx + Du \tag{5.6}$$

with $G(s) = C(sI - A)^{-1}B + D$ is

- *passive if $G(s)$ is positive real;*
- *strictly passive if $G(s)$ is strictly positive real.*

Definition 5.3.3. *[44] An $n \times n$ proper rational transfer function matrix $G(s)$ is positive real if*

- *poles of all elements of* $G(s)$ *are in* $Re[s] \leq 0$,
- *for all real* ω *for which* $j\omega$ *is not a pole of any element of* $G(s)$, *the matrix* $G(j\omega) + G^T(-j\omega)$ *is positive semidefinite, and*
- *any pure imaginary pole of* $j\omega$ *of any element of* $G(s)$ *is a simple pole and the residue matrix* $lim_{s \to j\omega}(s - j\omega)G(s)$ *is positive semidefinite Hermitian.*

Applying Definition 5.3.3 and Lemma 5.3.1 to a 2×2 transfer matrix $G(s)$, which can represent a two-port network, leads to Raisbeck's passivity criterion (see Appendix A.1 for details).

5.4 SYSTEM MODELING

The LTI dynamics of the operator and the environment are assumed to be

$$F_h = F_h^* - Z_h V_m \tag{5.7}$$
$$F_e = F_e^* - Z_e V_s \tag{5.8}$$

where F_h and F_e are the operator force applied to the master robot and the environment force applied to the slave robot [1], Z_h and Z_e are the operator and the environment impedances, V_m and V_s are the operator and the environment velocities, and F_h^* and F_e^* are the exogenous force inputs from the operator and the environment, respectively. The LTI models of the master and the slave robots are assumed to be

$$Z_m V_m = F_h + F_{cm} \tag{5.9}$$
$$Z_s V_s = F_e + F_{cs} \tag{5.10}$$

where $Z_m = M_m s$ and $Z_s = M_s s$ are the impedances of 1-DOF master and salve robots, respectively. Also, F_{cm} and F_{cs} are the control signals for the master and the slave robots, respectively. In the 4CH teleoperation architecture in Figure 5.2, the control signals are

$$F_{cm} = -C_m V_m - C_4 V_{md} + C_6 F_h - C_2 F_{hd} \tag{5.11}$$
$$F_{cs} = -C_s V_s + C_1 V_{sd} + C_5 F_e + C_3 F_{ed} \tag{5.12}$$

where $C_m = (K_{dm} + \frac{K_{pm}}{s})$ and $C_s = (K_{ds} + \frac{K_{ps}}{s})$ represent local PD position controllers, C_6 and C_5 are local force controllers, C_2 and C_3

1 In this chapter F_e is considered as the environment force applied to the slave where in literature it is defined as the slave's force applied upon the environment. This change of notation is made to preserve symmetric structure of the 4CH teleoperation system.

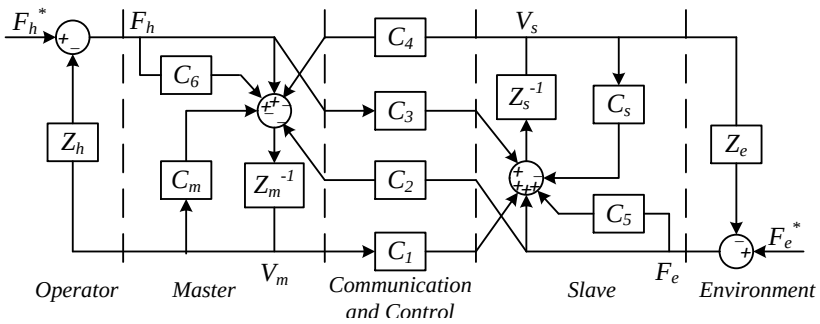

Figure 5.2: A 4CH bilateral teleoperation system structure

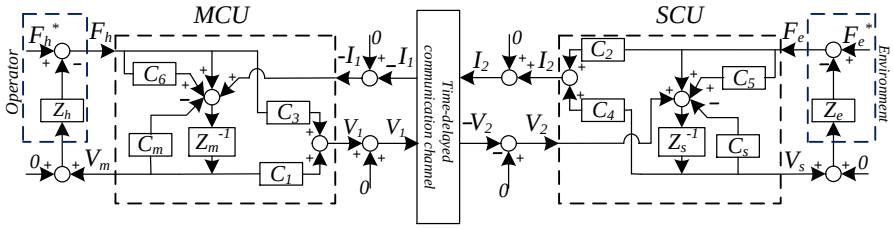

Figure 5.3: A 4CH bilateral teleoperation system in which the communication channel has been re-modeled as a two-port network

are force feedback and feed-forward controllers, and C_1 to C_4 are position compensators working in conjunction with C_s and C_m, V_{md} and V_{sd} are desired velocities, and F_{hd} and F_{ed} are desired forces for the master and the slave, respectively.

5.5 CHANNEL DELAY COMPENSATION IN 4CH TELEOPERATION

Inspired by [8], for compensating for the communication delay in a 4CH teleoperation system, a weighted sum of force and velocity at each side of the teleoperation system must be considered as incoming signals such that the communication channel appears as a 2-port network system. Once we do so, the 4CH teleoperation system in Figure 5.2 is re-modeled as shown in Figure 5.3. The 2×2 transfer matrix relating the outputs of the delayed communication channel to its inputs are

$$\begin{bmatrix} I_1 \\ -V_2 \end{bmatrix} = \begin{bmatrix} 0 & e^{-sT} \\ -e^{-sT} & 0 \end{bmatrix} \begin{bmatrix} V_1 \\ I_2 \end{bmatrix} \tag{5.13}$$

Based on Definition 5.3.3, the channel transfer matrix is not positive real and thus the delayed communication channel is not pas-

sive. Realizing a passive communication channel can be carried out through two methods. The first method is based on the wave variables formulation [55]. In Figure 5.4, the outputs of the wave transformation block at the master side are

$$I_1 = bV_1 + \sqrt{2b}u_m; v_m = \sqrt{2b}V_1 + u_m \tag{5.14}$$

and at the slave side they are

$$-V_2 = -\frac{1}{b}(-I_2 + \sqrt{2b}v_s); u_s = \frac{1}{b}(\sqrt{2b}I_2 - bv_s) \tag{5.15}$$

Since $u_m(t) = u_s(t-T)$ and $v_s(t) = v_m(t-T)$, we get

$$I_1 = e^{-sT}I_2 - be^{-sT}V_2 + bV_1 \tag{5.16}$$

$$-V_2 = -e^{-sT}V_1\frac{1}{b}e^{-sT}I_1 + \frac{1}{b}I_2 \tag{5.17}$$

This will change the channel transfer function matrix from (5.13) to

$$C(s) = \begin{bmatrix} b\frac{e^{sT}-e^{-sT}}{(e^{sT}+e^{-sT})} & \frac{2}{(e^{sT}+e^{-sT})} \\ -\frac{2}{(e^{sT}+e^{-sT})} & \frac{e^{sT}-e^{-sT}}{b(e^{sT}+e^{-sT})} \end{bmatrix} \tag{5.18}$$

which is positive real according to Definition 5.3.3, and therefore is passive. The second method follows a purely transfer function based approach. The objective here is to change the original delayed channel (5.13) to become a passive transfer matrix. Thus, the problem boils down to solving the following equations for unknown coefficients a_1, a_2, b_1, b_2, c_1 and c_2, so that the resulting transfer matrix satisfies the positive-realness requirements.

$$I_1 = aV_1 + be^{-sT}(-V_2) + ce^{-sT}I_2 \tag{5.19}$$

$$-V_2 = a^{'}I_2 + b^{'}e^{-sT}V_1 + c^{'}e^{-sT}I_1 \tag{5.20}$$

Note that if $T = 0$, we need to get $I_1 = I_2$ and $V_2 = V_1$. To satisfy this, it is necessary that

$$a = b, c = 1, a^{'} = -c^{'}, b^{'} = -1$$

Substituting these in (5.19)-(5.20), the new channel will be positive real if

$$c^{'} = \frac{-1}{b}$$

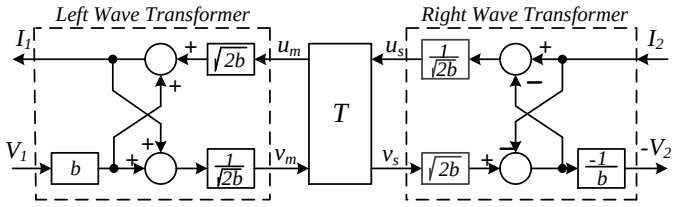

Figure 5.4: A delay-compensated communication channel

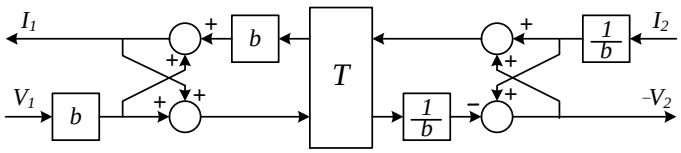

Figure 5.5: Another delay compensated communication channel

Thus, the new channel (5.19)-(5.20) will have only one free parameter b. Finally, the transfer matrix of this delay-compensated channel will turn out to be the same as (5.18), which meets the positive-realness conditions according to Definition 5.3.3 and is passive.

5.6 STABILIZATION OF A DELAY-COMPENSATED 4CH BILATERAL TELEOPERATION SYSTEM

A mathematically involved and intractable approach to stabilizing the delayed 4CH teleoperation system is to consider the teleoperator as a whole

$$\begin{bmatrix} V_m \\ V_s \end{bmatrix} = G_{total} \begin{bmatrix} F_h \\ F_e \end{bmatrix} \tag{5.21}$$

where $G_{total}(s)$ is to be passified through the design of the controllers. This transfer matrix is far too complicated to analyze for passivity. In the context of bilateral teleoperation systems in the presence of constant time-delay, passivity-based stability methods are attempt to passify the communication channel *assuming that both the MCU and the SCU are passive*. However, the passivity of the MCU and the SCU needs to be guaranteed via proper choice of control systems. Here, it is shown that there are certain conditions involving the values of the gains of the master and slave controllers in order for the passivity of the MCU and SCU to be guaranteed.

Three different approaches to the passivity analysis are presented below. The first two approaches, the 2-port network (2PN) and

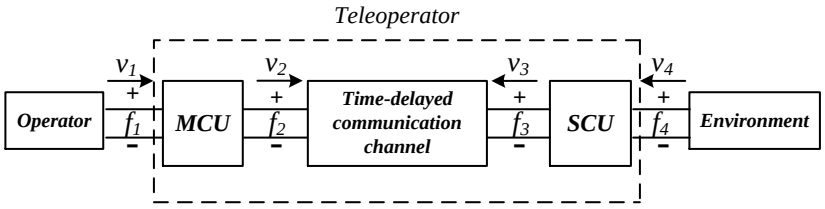

Figure 5.6: 2PN structure: passivity of the human operator, MCU, time-delayed communication channel, SCU, and environment is sufficient for passivity (and stability) of the teleoperation system.

single-loop feedback (SLF) structures, are previously introduced in literature and we show that they cannot stabilize the 4CH teleoperation system. However, using the third approach, multi-loop feedback (MLF) structure proposed in this chapter, the stability of the system will be guaranteed.

5.6.1 *Approach 1: 2-Port Network (2PN) Structure*

Theorem 5.6.1. *The teleoperator, i.e., the teleoperation system excluding the operator and the environment as shown in Figure 5.6, is passive if the MCU, the time delayed communication channel and the SCU are passive.*

Proof. If the MCU, the time delayed communication channel and the SCU are passive, then based on Definition 5.3.1 we get

$$\int f_1 v_1 + \int f_2(-v_2) \geq 0 \tag{5.22}$$

$$\int f_2 v_2 + \int f_3 v_3 \geq 0 \tag{5.23}$$

$$\int f_3(-v_3) + \int f_4 v_4 \geq 0 \tag{5.24}$$

The sum of (5.22) - (5.24) gives

$$\int f_1 V_1 + \int f_4 V_4 \geq 0 \tag{5.25}$$

which implies the passivity of the teleoperator. □

The problem faced in practice with the 2PN structure in the context of 4CH teleoperation is that since a weighted sum of both force and velocity are exchanged between the MCU, the channel, and the SCU, physical interpretation of these signals is not easy, which means that writing the two-port network models based on immitance parameters is rather difficult. It is preferable to pursue

a solely transfer function based approach that deals with system inputs and outputs regardless of their physical interpretation (or lack thereof).

5.6.2 *Approach 2: Single-Loop Feedback (SLF) Structure*

In this section, the stability analysis method proposed in [8], the SLF structure, is further investigated. As seen in Figure 5.3, we have

$$\frac{F_h(1+C_6)}{Z_{tm}} - \frac{I_1}{Z_{tm}} = V_m \quad , \quad \frac{F_e(1+C_5)}{Z_{ts}} + \frac{V_2}{Z_{ts}} = V_s \tag{5.26}$$

$$C_3F_h + C_1V_m = V_1 \quad , \quad C_2F_e + C_4V_s = I_2 \tag{5.27}$$

where $Z_{tm} = Z_m + C_m$ and $Z_{ts} = Z_s + C_s$. Manipulating (5.26)-(5.27) will result in the single-loop feedback structure equivalent of the teleoperation system shown in Figure 5.7, where $C(s)$ is the transfer matrix (5.18) of the delay-compensated communication channel and

$$G(s) = \begin{bmatrix} C_1 Z_{tm}^{-1} & 0 \\ 0 & C_4 Z_{ts}^{-1} \end{bmatrix} \tag{5.28}$$

Theorem 5.6.2. *[8] Assume that a teleoperation system is coupled to an environment and a human operator that are passive but otherwise arbitrary. If $G(s)$ is strictly positive real, then for inputs with finite norms, the outputs in the system shown in Figure 5.7 will have finite norms. (Note that the delay has been compensated for in the channel)*

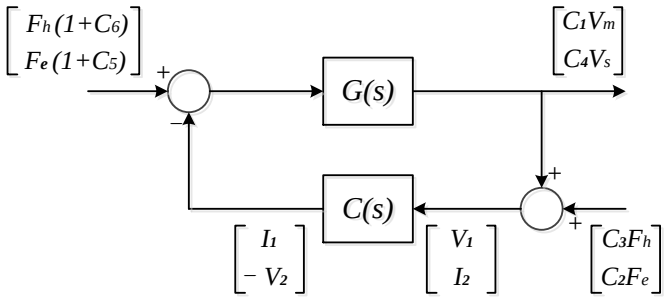

Figure 5.7: SLF structure: equivalent single-loop feedback structure of the 4CH teleoperator (i.e., not including the human operator and the environment).

A major drawback of the SLF structure is that it guarantees input-output stability from the inputs involving F_h and F_e to the outputs

involving V_m and V_s. However, we know that there are two more feedback loops involving Z_h and Z_e in a teleoperation system (not shown in Figure 5.7) namely (5.7)-(5.8), that can affect the stability of the closed-loop system. In other words, only F_h^* and F_e^* are true inputs to the system. Incorporating the dynamics of the human operator and the environment into Figure 5.7 results in a complicated structure that cannot easily be analyzed for passivity using the tools listed in Section 5.3.

5.6.3 *Approach 3: Multi-Loop Feedback (MLF) Structure*

MLF structure, which is the proposed approach of this thesis, will enable us to study the passivity of the 4CH teleoperation system easily compared to 2-PN or SLF structures. The 4CH bilateral teleoperation system in Figure 5.3 can be represented through an MLF structure as shown in Figure 5.8, where $e_1 = V_m$, $e_2 = \begin{pmatrix} F_h \\ -I_1 \end{pmatrix}$, $e_3 = \begin{pmatrix} V_1 \\ I_2 \end{pmatrix}$, $e_4 = \begin{pmatrix} V_2 \\ F_e \end{pmatrix}$, $e_5 = V_s$, $u_1 = 0$, $u_2 = \begin{pmatrix} F_h^* \\ 0 \end{pmatrix}$, $u_3 = \begin{pmatrix} 0 \\ 0 \end{pmatrix}$, $u_4 = \begin{pmatrix} 0 \\ F_e^* \end{pmatrix}$, $u_5 = 0$, $y_1 = V_m Z_h$, $y_2 = \begin{pmatrix} V_m \\ V_1 \end{pmatrix}$, $y_3 = \begin{pmatrix} I_1 \\ -V_2 \end{pmatrix}$, $y_4 = \begin{pmatrix} I_2 \\ V_s \end{pmatrix}$ and $y_5 = V_s Z_e$.

Theorem 5.6.3. *The system in Figure 5.8 is passive if Z_e, SCU, time-delayed communication channel, MCU, and Z_h, respectively blocks are passive.*

Proof. Let $V_1(x_1), V_2(x_2), V_3(x_3), V_4(x_4)$ and $V_5(x_5)$ be the storage functions of Z_e, the SCU, the time-delayed communication channel, the MCU and Z_h, respectively. Assume the initial stored energy in each of these systems is zero. Based on Definition 5.3.2,

$$e_i^T y_i \geq \dot{V}_i \tag{5.29}$$

From the feedback loops in Figure 5.8, it can be seen that

$$e_1 = u_1 + \begin{bmatrix} 1 & 0 \end{bmatrix} y_2 \tag{5.30}$$

$$e_2 = \begin{bmatrix} \begin{bmatrix} 1 & 0 \end{bmatrix} u_2 - y_1 \\ \begin{bmatrix} 0 & 1 \end{bmatrix} u_2 - \begin{bmatrix} 1 & 0 \end{bmatrix} y_3 \end{bmatrix} \tag{5.31}$$

$$e_3 = \begin{bmatrix} \begin{bmatrix} 1 & 0 \end{bmatrix} u_3 + \begin{bmatrix} 0 & 1 \end{bmatrix} y_2 \\ \begin{bmatrix} 0 & 1 \end{bmatrix} u_3 + \begin{bmatrix} 1 & 0 \end{bmatrix} y_4 \end{bmatrix} \tag{5.32}$$

$$e_4 = \begin{bmatrix} \begin{bmatrix} 1 & 0 \end{bmatrix} u_4 - \begin{bmatrix} 0 & 1 \end{bmatrix} y_3 \\ \begin{bmatrix} 0 & 1 \end{bmatrix} u_4 - y_5 \end{bmatrix} \tag{5.33}$$

$$e_5 = u_5 + \begin{bmatrix} 0 & 1 \end{bmatrix} y_4 \tag{5.34}$$

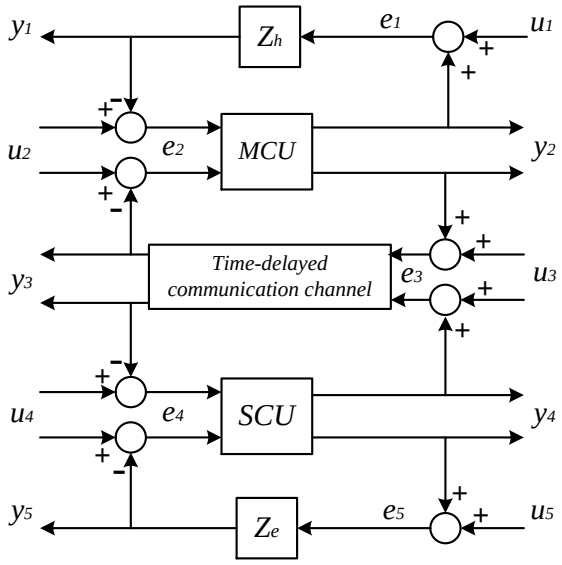

Figure 5.8: MLF structure: Equivalent multi-loop feedback structure of the 4CH teleoperation system.

Therefore, it is easy to show that

$$e_1^T y_1 + e_2^T y_2 + e_3^T y_3 + e_4^T y_4 + e_5^T y_5 = u_1^T y_1 + u_2^T y_2 + u_3^T y_3 + u_4^T y_4 + u_5^T y_5$$

For the entire teleoperation system, let us define $u = \begin{bmatrix} u_1 & u_2 & u_3 & u_4 & u_5 \end{bmatrix}^T \quad y = \begin{bmatrix} y_1 & y_2 & y_3 & y_4 & y_5 \end{bmatrix}^T$ Thus,

$$u^T y = u_1^T y_1 + u_2^T y_2 + u_3^T y_3 + u_4^T y_4 + u_5^T y_5 \geq \dot{V}_1 + \dot{V}_2 + \dot{V}_3 + \dot{V}_4 + \dot{V}_5$$

Taking $V(x) = V_1(x_1) + V_2(x_2) + V_3(x_3) + V_4(x_4) + V_5(x_5)$, we obtain

$$u^T y \geq \dot{V} \tag{5.35}$$

This concludes the proof. □

5.6.3.1 *Passification of MCU and SCU*

With Z_h and Z_e assumed passive, because of Theorem 5.6.3, the teleoperation system stabilization problem will be reduced to passifying the communication channel, the MCU and the SCU. As ex-

plained in Section 5.5, the communication channel can be passified using either of the methods that were previously described, i.e., the wave variables method in Figure 5.4 or the transfer matrix based method in Figure 5.5. For ensuring passivity of the MCU and the SCU, controllers need to be designed such that they meet the definition of positive realness. Relating inputs to corresponding outputs, the transfer matrices of the MCU and the SCU satisfy

$$\begin{bmatrix} V_m \\ V_1 \end{bmatrix} = G_{MCU} \begin{bmatrix} F_h \\ -I_1 \end{bmatrix} \quad , \quad \begin{bmatrix} I_2 \\ V_s \end{bmatrix} = G_{SCU} \begin{bmatrix} V_2 \\ F_e \end{bmatrix} \tag{5.36}$$

where

$$G_{MCU} = \begin{bmatrix} \frac{1+C_6}{Z_m+C_m} & \frac{1}{Z_m+C_m} \\ C_3 + \frac{C_1(1+C_6)}{Z_m+C_m} & \frac{C_1}{Z_m+C_m} \end{bmatrix} \tag{5.37}$$

$$G_{SCU} = \begin{bmatrix} \frac{C_4}{Z_s+C_s} & C_2 + \frac{C_4(1+C_5)}{Z_s+C_s} \\ \frac{1}{Z_s+C_s} & \frac{1+C_5}{Z_s+C_s} \end{bmatrix} \tag{5.38}$$

Assuming that C_2, C_3, C_5, C_6 (but not C_1 and C_4) are scalar gains and C_1 to C_6 are to be designed, based on Theorem 5.6.3, G_{MCU} and G_{SCU} need to be passive. Passivity of G_{MCU} and G_{SCU} requires them to be positive-real (Lemma 5.3.1). Based on Definition 5.3.3, for positive-realness of each transfer matrix, three conditions are to be satisfied. The first and third conditions are obviously the case here since all poles are on the left hand side of $j\omega$ axis. Assuming that C_2, C_3, C_5, C_6 (but not C_1 and C_4) are scalar gains and they all are to be designed, applying the second part of the Definition 5.3.3 leads to

$$(1+C_6)K_{dm}\omega^2 > 0, \quad (1+C_5)K_{ds}\omega^2 > 0 \tag{5.39}$$

$$\Re[C_1(j\omega)((K_{pm} - M_m\omega^2)j - K_{dm}\omega)] > 0 \tag{5.40}$$

$$\Re[C_4(j\omega)((K_{ps} - M_s\omega^2)j - K_{ds}\omega)] > 0 \tag{5.41}$$

$$\begin{aligned} &[(K_{pm} - M_m\omega^2) - C_3K_M](1+C_6)K_{dm}[(2\Re C_1)(K_{pm} \\ &- M_m\omega^2) + (2\Im C_1)K_{dm}\omega] - [(K_{pm} - M_m\omega^2) + C_3K_M]^2 \\ &- (1+C_6)^2((\Re C_1)^2 + (\Im C_1)^2)K_M + K_{dm}^2\omega^2 - 2(1+C_6) \\ &(\Im C_1)(K_{pm} - M_m\omega^2)K_{dm}\omega + 2(1+C_6)(\Re C_1)K_{dm}^2\omega^2 > 0 \end{aligned} \tag{5.42}$$

$$
\begin{aligned}
&[(K_{ps} - M_s\omega^2) - C_2K_S](1+C_5)K_{ds}[(2\Re C_4)(K_{ps} \\
&- M_s\omega^2) + (2\Im C_4)K_{ds}\omega] - [(K_{ps} - M_s\omega^2) + C_2K_S]^2 \\
&- (1+C_5)^2((\Re C_4)^2] + (\Im C_4)^2)K_S + K_{ds}^2\omega^2 - 2(1+C_5) \\
&(\Im C_4)(K_{ps} - M_s\omega^2)K_{ds}\omega + 2(1+C_5)(\Re C_4)K_{ds}^2\omega^2 > 0 \quad (5.43)
\end{aligned}
$$

where $K_M = (K_{pm} - M_m\omega^2)^2 + K_{dm}^2\omega^2$ and $K_S = (K_{ps} - M_s\omega^2)^2 + K_{ds}^2\omega^2$. Inequalities (5.39)-(5.43) are general sufficient conditions for ensuring passivity of the delayed 4CH teleoperation system in the sense that any given set of controllers ($C_1, \cdots, C_6$ and proportional-derivative C_m and C_s) for any given system (M_m and M_s) can be checked for passivity, and are reported for the first time in this thesis. The transparency conditions for the 4CH teleoperation system (without delay) shown in Figure 5.2 are

$$
\begin{aligned}
C_1 = C_s + Z_s, C_4 = -(C_m + Z_m) \\
C_2 = 1 + C_6, C_3 = -(1 + C_5) \quad (5.44)
\end{aligned}
$$

It is easy to see that (5.44) and (5.39)-(5.43) are incompatible. This means that using the controllers (5.44), which guarantee transparency under zero delay, may not result in a stable teleoperation system when there exists time delay. Though the controllers (5.44) could not ensure passivity, let us assume that C_1 and C_4 have similar structures to $C_s + Z_s$ and $C_m + Z_m$, respectively. This results in PID-like controllers $C_1 = K_{m1}s + \frac{K_{p1}}{s} + K_{d1}$ and $C_4 = K_{m4}s + \frac{K_{p4}}{s} + K_{d4}$ with free parameters K_{mi}, K_{pi}, K_{di}, $i = 1, 4$. Applying Definition 5.3.3, we get the following conditions to ensure the stability of the 4CH delayed teleoperation system:

$$K_{mi}, K_{pi}, K_{di} > 0, \quad for \quad i = 1, 4 \quad (5.45)$$

$$C_2 < 0, \quad C_3 < 0, \quad 1 + C_6 > 0, \quad 1 + C_5 > 0 \quad (5.46)$$

$$\frac{K_{m1}}{M_m} = \frac{K_{p1}}{K_{pm}} = \frac{K_{d1}}{K_{dm}} = \frac{-C_3}{1 + C_6} \quad (5.47)$$

$$\frac{K_{m4}}{M_s} = \frac{K_{p4}}{K_{ps}} = \frac{K_{d4}}{K_{ds}} = \frac{-C_2}{1 + C_5} \quad (5.48)$$

In the simulation study that follows, the above controllers for the 4CH teleoperation system are used. However, as mentioned before, conditions (5.39)-(5.43) are general and can be tested for any given set of controllers.

Remark Figure 5.9 depicts a 2-loop feedback variant of the 4CH teleoperation system. It can be shown that it is passive if the time-delayed communication channel and G_{MS} are passive (note that

since the operator and the environment are assumed passive, based on Definition 5.3.3 the matrix $\begin{bmatrix} Z_s & 0 \\ 0 & Z_e \end{bmatrix}$ will be passive as well). The combination of the MCU and SCU is given by

$$G_{MS} = \begin{bmatrix} \frac{1+C_6}{Z_{tm}} & 0 & \frac{1}{Z_{tm}} & 0 \\ 0 & \frac{1+C_5}{Z_{ts}} & 0 & \frac{1}{Z_{ts}} \\ C_3 + \frac{C_1(1+C_6)}{Z_{tm}} & 0 & \frac{C_1}{Z_{tm}} & 0 \\ 0 & C_2 + \frac{C_4(1+C_5)}{Z_{ts}} & 0 & \frac{C_4}{Z_{ts}} \end{bmatrix} \tag{5.49}$$

Again, the communication channel can be passified using either of

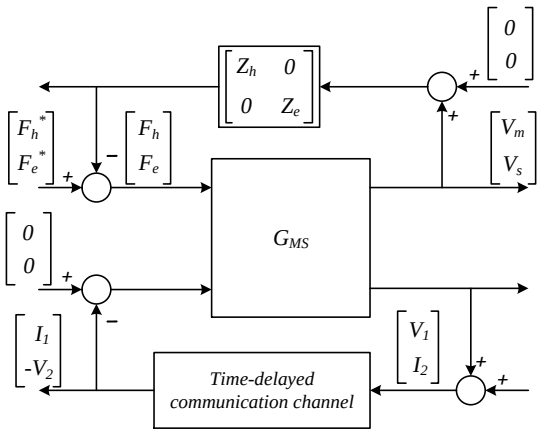

Figure 5.9: 2-loop structure of a 4CH teleoperation system

the methods in Section 5.5. It is easy to show that the passivity of G_{MS} is equivalent to the passivity of *MCU* and *SCU* in the structure shown in Figure 5.8.

5.7 STABILIZATION OF A DELAY-COMPENSATED 4CH TRILATERAL TELEOPERATION SYSTEM

Khademian et al. [39] has introduced a 4CH trilateral (dual-user) shared control structure, where adjustable interaction between the two users as well as between each user and the environment is obtained through introducing a dominance factor α (Figure 5.10). The following represents the dynamics of the teleoperation system in

Figure 5.10. For $i = 1, 2$, the LTI dynamics of the human operators and the environment are

$$F_{hi} = F_{hi}^* - Z_h V_{mi} \tag{5.50}$$
$$F_e = F_e^* - Z_e V_s \tag{5.51}$$

where F_{hi} and F_e are the operator forces applied to the master robots and the environment force applied to the slave robot, Z_{hi} and Z_e are the operators and the environment impedances, V_{mi} and V_s are the operators and the environment velocities, and F_{hi}^* and F_e^* are the exogenous force inputs from the operators and the environment, respectively. The LTI dynamics of the master and slave robots in the Laplace domain are expressed as

$$Z_{m1} V_{m1} = F_{h1} + F_{cm12} + F_{cm1s} \tag{5.52}$$
$$Z_{m2} V_{m2} = F_{h2} + F_{cm12} + F_{cm2s} \tag{5.53}$$
$$Z_s V_s = F_e + F_{cs1} + F_{cs2} \tag{5.54}$$

where $Z_{m1} = M_{m1}s$, $Z_{m1} = M_{m1}s$ and $Z_s = M_s s$ represent the dynamic models of the masters and the slave. Moreover, F_{cm12}, F_{cm1s}, F_{cm21}, F_{cm2s}, F_{cs1} and F_{cs2} are the 4CH control signals expressed as

$$\begin{aligned} F_{cm12} = &- C_{m1} V_{m1} - (1-\alpha) C_{4m1} V_{m2} + C_{6m1} F_{h1} \\ &- (1-\alpha) C_{2m1} F_{h2} \end{aligned} \tag{5.55}$$
$$\begin{aligned} F_{cm1s} = &- C_{m1} V_{m1} - \alpha C_{4m1} V_s + C_{6m1} F_{h1} \\ &- \alpha C_{2m1} F_e \end{aligned} \tag{5.56}$$

$$\begin{aligned} F_{cm21} = &- C_{m2} V_{m2} - \alpha C_{4m2} V_{m1} + C_{6m2} F_{h2} \\ &- \alpha C_{2m2} F_{h1} \end{aligned} \tag{5.57}$$
$$\begin{aligned} F_{cm2s} = &- C_{m2} V_{m2} - (1-\alpha) C_{4m2} V_s + C_{6m2} F_{h2} \\ &- (1-\alpha) C_{2m2} F_e \end{aligned} \tag{5.58}$$
$$F_{cs1} = - C_s V_s - \alpha C_1 V_{m1} + C_5 F_e - \alpha C_3 F_{h1} \tag{5.59}$$
$$\begin{aligned} F_{cs2} = &- C_s V_s - (1-\alpha) C_1 V_{m2} + C_5 F_e \\ &- (1-\alpha) C_3 F_{h2} \end{aligned} \tag{5.60}$$

In the above, $C_{mi} = (K_{dmi} + \frac{K_{pmi}}{s})$ and $C_s = (K_{ds} + \frac{K_{ps}}{s})$ are local PD position controllers, C_{6mi} and C_5 are local force controllers, C_{2mi} and C_3 are force feedback and feed-forward controllers, and C_1 and C_{4mi} are position compensators working in conjunction with C_s and C_{mi} and α is the dominance factor which can hold a value in $[0, 1]$. When α is zero, operator 1 has the full control over the slave robot

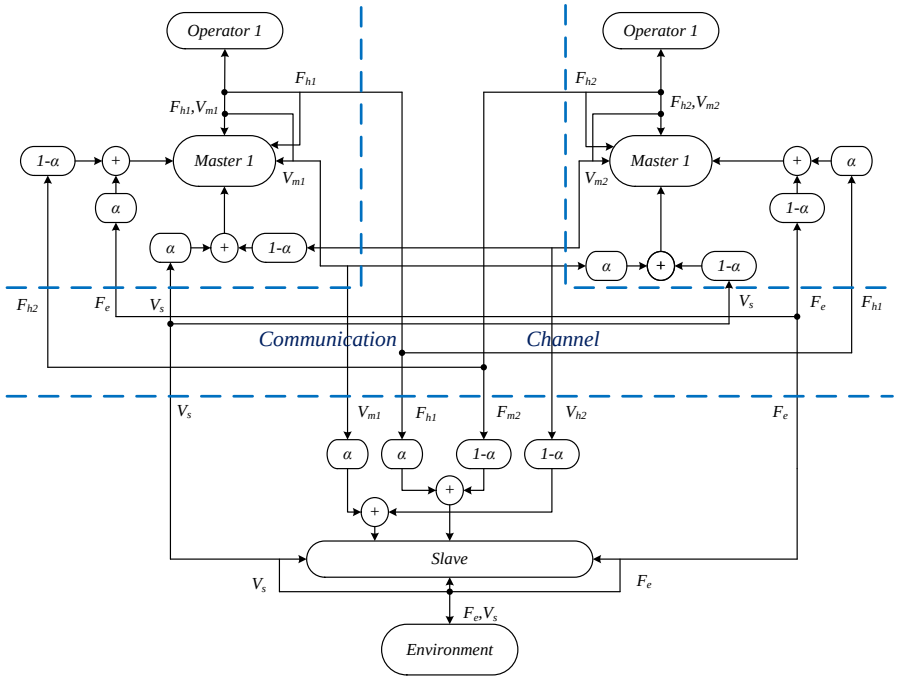

Figure 5.10: A 4CH trilateral teleoperation system structure

and operator 2 is follwoing operator 1. When α is equal to 1 the dominance in controlling the slave's position is transferred to operator 2. With simple manipulation, the system in Figure 5.10 can be presented as in Figure 5.11, where $CC_{1,2}$, $CC_{1,s}$ and $CC_{2,s}$ are the communication channels between master 1 and master 2, between master 1 and slave and between master 2 and slave, respectively. MCU_1, MCU_2 and SCU are the master 1 control unit, master 2 control unit, and slave control unit, respectively. The detailed model of control units are shown in Figures 5.12, 5.13 and 5.14.

5.7.1 *Stability Analysis of a Trilateral Teleoperation System*

The trilateral teleoperation system in Figure 5.11 can be represented through an MLF structure as shown in Figure 5.15, where $e_1 = V_s$, $e_2 = \begin{pmatrix} F_s \\ V_{s1} \\ V_{s2} \end{pmatrix}$, $e_3 = \begin{pmatrix} I_{s2} \\ V_{2s} \end{pmatrix}$, $e_4 = V_{m2}$, $e_5 = \begin{pmatrix} F_{h2} \\ V_{21} \\ -I_{2s} \end{pmatrix}$, $e_6 = \begin{pmatrix} I_{s1} \\ V_{1s} \end{pmatrix}$, $e_7 = \begin{pmatrix} I_{21} \\ V_{12} \end{pmatrix}$, $e_8 = V_{m2}$, $e_9 = \begin{pmatrix} F_{h1} \\ -I_{12} \\ -I_{1s} \end{pmatrix}$, $u_1 = 0$, $u_2 = \begin{pmatrix} F_e^* \\ 0 \\ 0 \end{pmatrix}$, $u_3 = \begin{pmatrix} 0 \\ 0 \end{pmatrix}$, $u_4 = 0$, $u_5 = \begin{pmatrix} F_{h2}^* \\ 0 \\ 0 \end{pmatrix}$, $u_6 = \begin{pmatrix} 0 \\ 0 \end{pmatrix}$, $u_7 = \begin{pmatrix} 0 \\ 0 \end{pmatrix}$, $u_8 = 0$, $u_9 = \begin{pmatrix} F_{h1}^* \\ 0 \\ 0 \end{pmatrix}$, $y_1 = V_s Z_e$, $y_2 = \begin{pmatrix} V_s \\ I_{s1} \\ I_{s2} \end{pmatrix}$, $y_3 = \begin{pmatrix} -V_{s2} \\ I_{2s} \end{pmatrix}$, $y_4 = Z_{h2} V_{m2}$, $y_5 = \begin{pmatrix} V_{h2} \\ I_{21} \\ V_{2s} \end{pmatrix}$

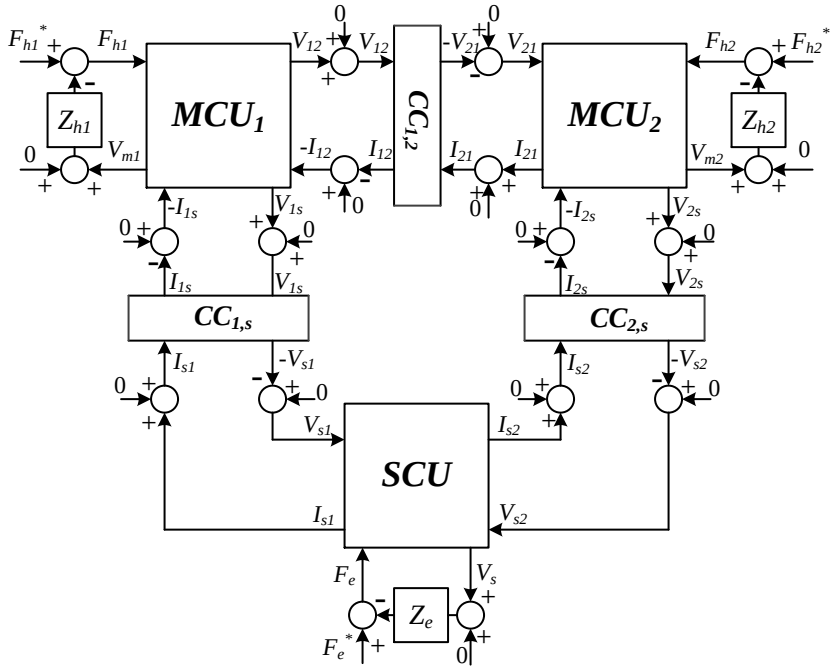

Figure 5.11: The model of a 4CH trilateral teleoperation system

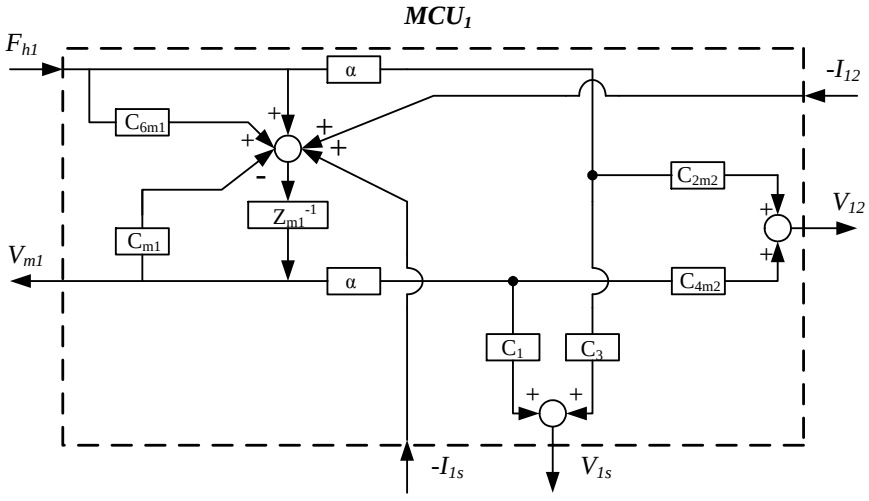

Figure 5.12: The model of master 1 control unit

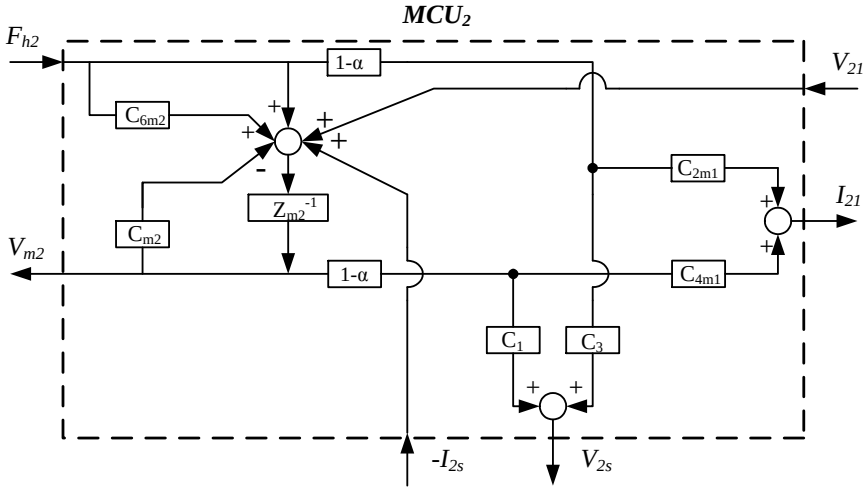

Figure 5.13: The model of master 2 control unit

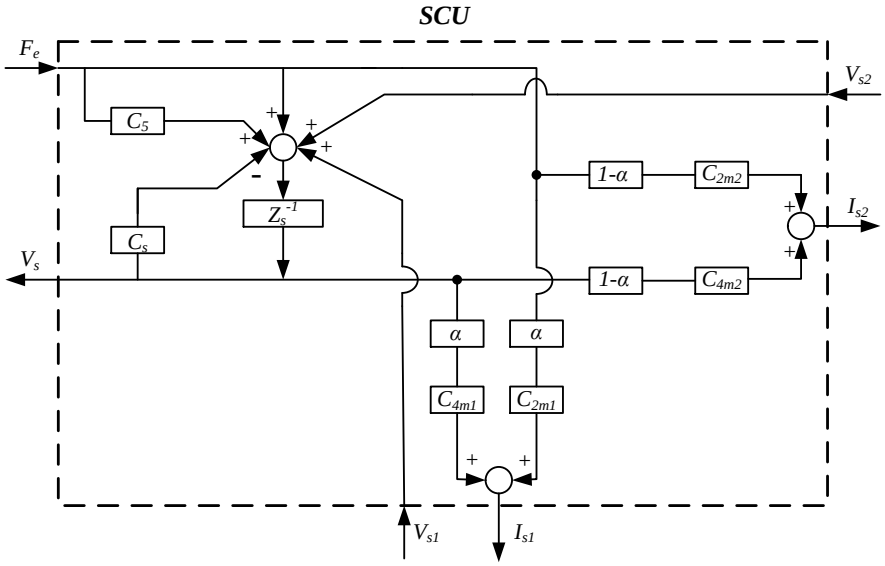

Figure 5.14: The model of slave control unit

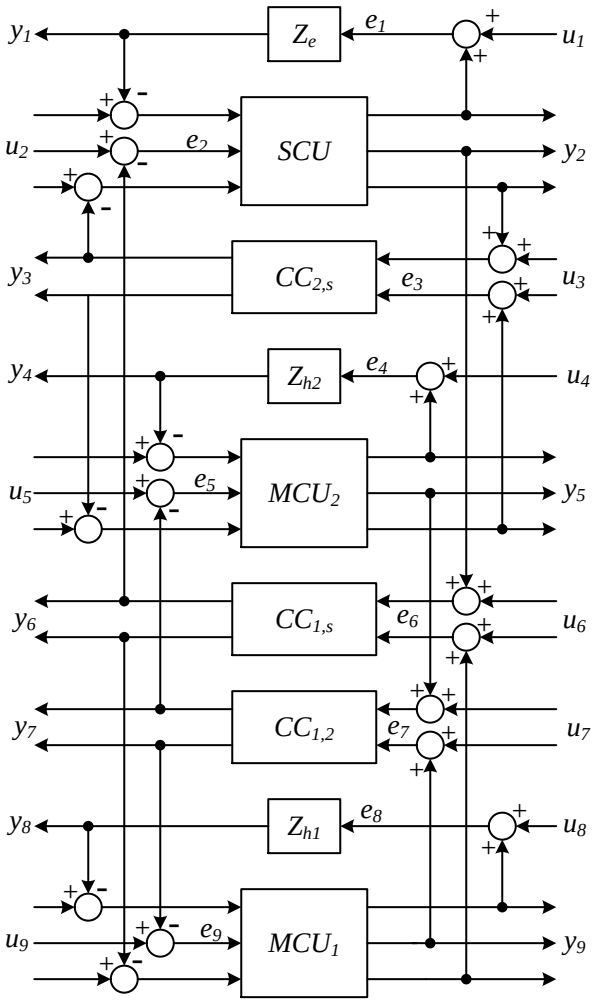

Figure 5.15: MLF structure: equivalent multi-loop feedback structure for a 4CH trilateral teleoperation system

and $y_6 = \begin{pmatrix} -V_{s1} \\ I_{1s} \end{pmatrix}$, $y_7 = \begin{pmatrix} -V_{21} \\ I_{12} \end{pmatrix}$, $y_8 = V_{m1} Z_{h1}$, $y_9 = \begin{pmatrix} V_{h1} \\ V_{12} \\ V_{1s} \end{pmatrix}$. Thus, using a approach similar to that for the 4CH bilateral teleopration system in Section 5.6.3, the stability of 4CH trilateral system can be addressed.

Theorem 5.7.1. *The system modeled in Figure 5.15 is stable if each of Z_{h1}, Z_{h2}, Z_e, MCU_1, MCU_2, MCU_3, $CC_{1,2}$, $CC_{1,s}$ and $CC_{2,s}$ are passive.*

The proof of this theorem is provided in Appendix A.2.

With the assumption that for each communication channel ($CC_{1,2}$, $CC_{1,s}$ and $CC_{2,s}$), the corresponding delay has been compensated for using one of the two techniques explained in Section 5.5 and assuming that each termination (Z_{h1}, Z_{h2} or Z_e) is passive, the sta-

bility problem of a 4CH trilateral teleoperation system will reduce to ensuring the passivity of each control unit.

The input-output mapping for each control unit is

$$\begin{bmatrix} V_{m1} \\ V_{12} \\ V_{1s} \end{bmatrix} = G_{MCU_1}(s) \begin{bmatrix} F_{h1} \\ -I_{12} \\ -I_{1s} \end{bmatrix} \tag{5.61}$$

$$\begin{bmatrix} V_{m2} \\ I_{21} \\ V_{2s} \end{bmatrix} = G_{MCU_2}(s) \begin{bmatrix} F_{h2} \\ V_{21} \\ -I_{2s} \end{bmatrix} \tag{5.62}$$

$$\begin{bmatrix} V_s \\ I_{s1} \\ I_{s2} \end{bmatrix} = G_{SCU}(s) \begin{bmatrix} F_e \\ V_{1s} \\ V_{2s} \end{bmatrix} \tag{5.63}$$

where

$$G_{MCU_1}(s) = \tag{5.64}$$
$$\begin{bmatrix} \frac{1+C_{6m1}}{Z_{m1}+C_{m1}} & \frac{1}{Z_{m1}+C_{m1}} & \frac{1}{Z_{m1}+C_{m1}} \\ \alpha(C_{2m2} + \frac{C_{4m2}(1+C_{6m1})}{Z_{m1}+C_{m1}}) & \frac{\alpha C_{4m2}}{Z_{m1}+C_{m1}} & \frac{\alpha C_{4m2}}{Z_{m1}+C_{m1}} \\ \alpha(C_3 + \frac{C_1(1+C_{6m1})}{Z_{m1}+C_{m1}}) & \frac{\alpha C_1}{Z_{m1}+C_{m1}} & \frac{\alpha C_1}{Z_{m1}+C_{m1}} \end{bmatrix}$$

$$G_{MCU_2}(s) = \tag{5.65}$$
$$\begin{bmatrix} \frac{1+C_{6m2}}{Z_{m2}+C_{m2}} & \frac{1}{Z_{m2}+C_{m2}} & \frac{1}{Z_{m2}+C_{m2}} \\ (1-\alpha)(C_{2m1} + \frac{C_{4m1}(1+C_{6m2})}{Z_{m2}+C_{m2}}) & \frac{(1-\alpha)C_{4m1}}{Z_{m2}+C_{m2}} & \frac{(1-\alpha)C_{4m1}}{Z_{m2}+C_{m2}} \\ (1-\alpha)(C_3 + \frac{C_1(1+C_{6m2})}{Z_{m2}+C_{m2}}) & \frac{(1-\alpha)C_1}{Z_{m2}+C_{m2}} & \frac{(1-\alpha)C_1}{Z_{m2}+C_{m2}} \end{bmatrix}$$

$$G_{SCU}(s) = \tag{5.66}$$
$$\begin{bmatrix} \frac{1+C_5}{Z_s+C_s} & \frac{1}{Z_s+C_s} & \frac{1}{Z_s+C_s} \\ \alpha(C_{2m1} + \frac{C_{4m1}(1+C_5)}{Z_s+C_s}) & \frac{\alpha C_{4m1}}{Z_s+C_s} & \frac{\alpha C_{4m1}}{Z_s+C_s} \\ (1-\alpha)(C_{2m2} + \frac{C_{4m2}(1+C_5)}{Z_s+C_s}) & \frac{(1-\alpha)C_{4m2}}{Z_s+C_s} & \frac{(1-\alpha)C_{4m2}}{Z_s+C_s} \end{bmatrix}$$

Based on Definition 5.3.3, for passivity of each of the above transfer matrices three conditions are to be satisfied. The first and third conditions are obviously the case here since all poles are in $j\omega < 0$. The second condition in Definition 5.3.3 still needs to be checked. Assuming that C_{2mi}, C_3, C_5, C_{6mi} (but not C_1 and C_{4mi}) are scalar gains and they all are to be designed, applying the second part of the Defintion 5.3.3 leads to

$$1 + C_{6m1} > 0, \quad 1 + C_{6m2} > 0, \quad 1 + C_5 > 0 \tag{5.67}$$

$$C_{2m1} < 0, \quad C_{2m2} < 0, \quad C_3 < 0 \tag{5.68}$$

$$\frac{C_{4m2}}{C_{m1} + Z_{m1}} = \frac{-C_{2m2}}{1 + C_{6m1}} \tag{5.69}$$

$$\frac{C_1}{C_{m1} + Z_{m1}} = \frac{-C_3}{1 + C_{6m1}} \tag{5.70}$$

$$\frac{C_{4m1}}{C_{m2} + Z_{m2}} = \frac{-C_{2m1}}{1 + C_{6m2}} \tag{5.71}$$

$$\frac{C_1}{C_{m2} + Z_{m2}} = \frac{-C_3}{1 + C_{6m2}} \tag{5.72}$$

$$\frac{C_{4m1}}{C_s + Z_s} = \frac{-C_{2m1}}{1 + C_5} \tag{5.73}$$

$$\frac{C_{4m2}}{C_s + Z_s} = \frac{-C_{2m2}}{1 + C_5} \tag{5.74}$$

$$\frac{C_{2m1}}{C_{2m2}} = \frac{C_{4m1}}{C_{4m2}} = \frac{1 - \alpha}{\alpha} \tag{5.75}$$

Here, it is assumed that C_{4m1}, C_{4m2} and C_1 have similar structures to $C_{m1} + Z_{m1}$, $C_{m2} + Z_{m2}$ and $C_s + Z_s$, respectively. This results in PID-like controllers $C_1 = K_{m1}s + \frac{K_{p1}}{s} + K_{d1}$ and $C_{4mi} = K_{m4i}s + \frac{K_{p4i}}{s} + K_{d4i}$ with free positive parameters K_{m1}, K_{p1}, K_{d1},K_{m4i}, K_{p4i}, K_{d4i}, $i = 1, 4$. Note that these results are only valid if $0 < \alpha < 1$; when $\alpha = 0$ or 1 the structure is no longer considered trilateral since there will not be any feedback connection from operator 1 or operator 2, respectively. As it can be seen in the above conditions, the stability of the 4CH trilateral teleoperation system is dependent on the value of the dominance factor α. In the special case where the dominance is equally distributed between two operators ($\alpha = 0.5$), (5.75) will become:

$$C_{2m1} = C_{2m2}, \quad C_{4m1} = C_{4m2} \tag{5.76}$$

(A)	M_m	0.3	K_{pm}	100	K_{dm}	10	C_2	-2	C_6	1	C_4 $0.3s+10+100/s$
	M_s	0.6	K_{ps}	200	K_{ds}	20	C_3	-4	C_5	3	C_1 $0.6s+20+200/s$
(B)	M_m	0.3	K_{pm}	100	K_{dm}	10	C_2	-10	C_6	1	C_4 $0.3s+10+100/s$
	M_s	0.7	K_{ps}	300	K_{ds}	30	C_3	2	C_5	3	C_1 $0.35s+30+300/s$

Table 5.1: The masses and controllers gains used in the simulation: (A) passive case and (B) non-passive case

5.8 SIMULATION RESULTS

In this section, the passivity conditions derived in this chapter, (5.45)-(5.48) found in section 5.6.3.1 and (5.67)-(5.75) found in section 5.7.1, will be verified via simulations. For checking the passivity of the 4CH teleoperation system, a passivity observer [61] has been incorporated into the simulation to calculate the dissipated energy in the teleoperator. This dissipated energy is given by

$$E_{dissipated} = \int_0^t F_h(\tau)V_m(\tau)d\tau + \int_0^t F_e(\tau)V_s(\tau)d\tau \geq 0 \qquad (5.77)$$

The teleoperator is passive if this integral is non-negative at all times. The 4CH teleoperation system in Figure 5.3 has been simulated in MATLAB/Simulink. The time delay in the communication channel is set to 0.5 sec. A pair of 1-DOF master and slave robots modeled by point masses is considered. Both the master and the slave are connected to LTI terminations with transfer functions $\frac{1}{s+1}$. This termination is passive as for $s = j\omega$ we have $Re(\frac{1}{s+1}) = \frac{1}{\omega^2+1} > 0$ when $\omega > 0$. For F_h^*, a sine-wave with unit amplitude and 1 Hz frequency is used. According to (5.45)-(5.48), it is expected that the

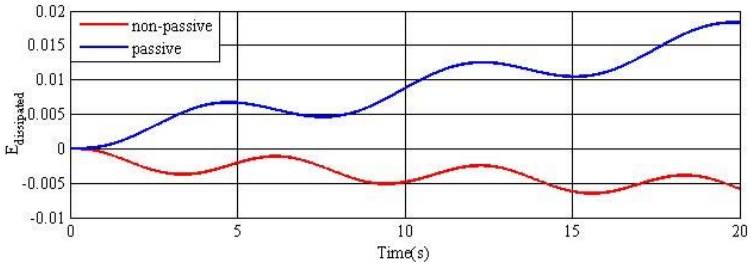

Figure 5.16: Passivity observer $E_{dissipated}$ used for the teleoperator's passivity analysis

passivity of the 4CH teleoperator should depend on the controller gains. Figure 5.16 shows that when the controller gains are chosen to meet conditions (5.45)-(5.48), e.g., as listed in Table 5.1(A),

(A)	Z_{m1}	0.6s	C_{m1}	1+1/s	C_{2m1}	-4	C_{6m1}	1	C_{4m1}	$1.2s+2+2/s$
	Z_{m2}	0.6s	C_{m2}	1+1/s	C_{2m2}	-4	C_{6m2}	1	C_{4m2}	$1.2s+2+2/s$
	Z_s	0.6s	C_s	0.6s+1+1/s	C_3	-4	C_5	3	C_1	$0.6s+1+1/s$
(A)	Z_{m1}	0.5s	C_{m1}	1+1/s	C_{2m1}	-4	C_{6m1}	1	C_{4m1}	$1.2s+2+2/s$
	Z_{m2}	0.6s	C_{m2}	1+1/s	C_{2m2}	-4	C_{6m2}	1	C_{4m2}	$1.2s+2+2/s$
	Z_s	0.3s	C_s	0.6s+1+1/s	C_3	1	C_5	2	C_1	$0.6s+1+1/s$

Table 5.2: The masses and controllers gains used in the simulation: (A) passive case and (B) non-passive case.

the teleoperator is passive. However, for a set of masses and controller gains that do not satisfy (5.45)-(5.48), e.g., as listed in Table 5.1(B), the teleoperator will become non-passive. Similarly, in order to check the validity of the passivity conditions (5.67)-(5.75) for the 4CH trilateral teleoperation system in Figure 5.10, a passivity observer has been incorporated into the simulation to calculate the dissipated energy in the teleoperator. This dissipated energy is given by

$$E_{dissipated} = \int_0^t F_{h1}(\tau)V_{m1}(\tau)d\tau + \int_0^t F_{h2}(\tau)V_{m2}(\tau)d\tau + \int_0^t F_e(\tau)V_s(\tau)d\tau \geq 0 \tag{5.78}$$

The trilateral teleoperator is passive if this integral is non-negative at all times. The 4CH trilateral teleoperation system in Figure 5.10 has been simulated in MATLAB/Simulink. The time delay is set to 0.5 sec. Two 1-DOF, point mass master and one slave robots modeled by their point masses are considered. The master 1 and master 2 and the slave are connected to passive LTI terminations with transfer functions $\frac{1}{s+1}$. Sine-wave (with unit amplitude and 1 Hz frequency) F^*_{h1} and F^*_{h2} are used. According to (5.67)-(5.75), it is expected that the passivity of the 4CH trilateral teleoperator should depend on the controller gains. Figure 5.17 shows that when the controller gains are chosen to meet conditions (5.67)-(5.75), e.g., as listed in Table 5.2(A), the trilateral teleoperator is passive. However, for a set of masses and controllers gain that do not satisfy (5.67)-(5.75), e.g., as listed in Table 5.2(B), the teleoperator will become non-passive. Note that it is assumed that $\alpha = 0.5$.

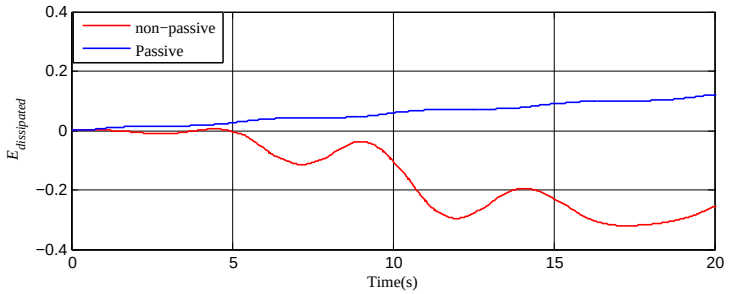

Figure 5.17: Passivity observer $E_{dissipated}$ used for the trilateral teleoperator's passivity analysis

5.9 CONCLUSION AND FUTURE WORK

In this chapter, the stability of 4CH bilateral and trilateral teleoperation systems in the presence of time delay is studied. When delay exists in the communication channel, addressing the passivity (and stability) of the teleoperation system as a whole is too complicated and computationally intractable. Modifying the structure of the 4CH teleoperation system as shown in Figure 5.8 (or Figure 5.9) will enable us to study the requirements of passivity on a modular and tractable basis. It was discussed that passifying the communication channel alone will not guarantee the stability of the entire teleoperation system. Assuming that the operator(s) and the environment are passive, controllers for the master(s) and the slave still need to satisfy a set of requirements found in this chapter.

6 CONCLUSIONS AND FUTURE DIRECTIONS

6.1 CONCLUSIONS

This thesis addressed the stability problem in the context of sampled-data HVE systems and sampled-data and continuous-time teleoperation systems. The major contributions of this thesis are summarized as follows:

- A unified framework to study the stability of sampled-data HVE and sampled-data PEB bilateral teleoperation systems in the presence of three main de-stabilizing factors: (a) delayed communication channel, (b) controller discretization and (c) active operator/environment. Although the stability of HVE systems had been studied extensively in literature, the effect of active operator was neglected assuming that the operator behaves passively. However, this assumption is not always valid, and depending on the task being performed by the operator, the passivity assumption may be violated. Our proposed framework enables us to study the stability of both HVE and bilateral teleoperation systems in the presence of active terminations (operator or environment). Another advantage of this framework over previously proposed methods in the literature is that it can be easily applied to m-user HVE systems where $m \geq 2$. This framework also enables us to compare the relative effects of delay, controller discretization and active terminations on the stability of both HVE and bilateral teleoperation systems.

- A framework to study the stability of delayed 4CH bilateral teleoperation systems is proposed. While previous studies in the literature tend to model the teleoperation systems via 2-port (teleoperator) and 1-port (operator and environment) networks to address the stability using the physical definition of passivity, in our proposed method a transfer matrix based approach to modeling and stability analysis is presented that is easier to follow. Also, in the literature the passivity-based stability analysis for a delayed teleoperation system under 4CH architecture has mostly been narrowed to only compensating for the delay in the communication channel while as-

suming the rest of the system will be passive. We show that although the master(s) and slave robots are passive systems, when combined with their controllers the passivity can be jeopardized, thus a set of conditions involving the controllers' parameters need to be satisfied. For the case of 4CH trilateral teleoperation system it has been shown that the passivity-based analysis results in a set of conditions where the controller values are dependent on the dominance factor involved in the architecture.

6.2 DIRECTIONS FOR FUTURE RESEARCH

In the context of stability analysis of sampled-data HVE systems and sampled-data bilateral teleoperation systems, potential future works include the following:

1. A possible extension to the proposed framework in this thesis is to consider more dexterous robots. Applications of HVE systems under 1-DoF robots are limited but can boost vastly where there is more than one degree-of-freedom in the robot.

2. The nature of the delay in the Internet-based communication channels is time-varying which can jeopardize the stability of the system greatly. A natural extension to the proposed framework comes by allowing time-varying communication delays and studying its effect on the overall system stability in both Chapter 3 and Chapter 4.

3. In this thesis, the stability analysis proposed in Chapter 4 is only applied to bilateral teleoperation systems under PEB architecture. Extending this proposed framework to bilateral teleoperation systems under 4CH and DFR architectures can be considered.

In the context of stability analysis of continuous-time teleoperation systems under 4CH architecture, possible future work includes the following: Since the passivity assumption for terminations in teleoperation systems is not always valid, an immediate extension of the stability analysis method proposed in Chapter 5 is to study the effect of active terminations on the stability of the overall teleoperation system. Considering time-varying communication delay is also another possible future work in this context.

BIBLIOGRAPHY

[1] R. J. Anderson and M. W. Spong. Bilateral control of teleoperators with time delay. In *IEEE Transactions on Automatic Control*, 34(5):494 –501, 1989.

[2] R. J. Anderson and M. W. Spong. Asymptotic Stability for Force Reflecting Teleoperators with Time Delay. In *The International Journal of Robotics Research*, 11(2):135–149, 1992.

[3] P. Arcara and C. Melchiorri. Control schemes for teleoperation with time delay: A comparative study. In *Robotics and Autonomous Systems*, (38):49–64, 2002.

[4] J. Artigas, C. Preusche, G. Hirzinger, G. Borghesan, and C. Melchiorri. Bilateral energy transfer in delayed teleoperation on the time domain. *Proceedings of IEEE International Conference on Robotics and Automation*, 671 –676, Pasadena, CA, USA, 2008.

[5] O. Astley and V. Hayward. Design constraints for haptic surgery simulation. In *Proceedings of IEEE International Conference on Robotics and Automation*, 3:2446–2451, San Francisco, CA, USA, 2000.

[6] K. J. Astrom and B. Wittenmark. *Adaptive Control*. Addison-Wesley Longman Publishing Co., Inc., Boston, MA, USA, 2nd edition, 1994.

[7] S. Atashzar, I. Polushin, and R. Patel. Networked teleoperation with non-passive environment: Application to tele-rehabilitation. In *Proceedings of IEEE/RSJ International Conference on Intelligent Robots and Systems*, 5125–5130, Vilamoura, Portugal, 2012.

[8] A. Aziminejad, M. Tavakoli, R. Patel, and M. Moallem. Transparent time-delayed bilateral teleoperation using wave variables. In *IEEE Transactions on Control Systems Technology*, 16(3):548–555, 2008.

[9] B. Bae, T. Koo, K. Park, and Y. Kim. Design and control of a two degree of freedom haptic device for the application of pc video games. In *Proceedings of IEEE/RSJ International Conference on Intelligent Robots and Systems*, 3:1738–1743, Maui, USA, 2001.

[10] A. K. Bejczy, S. Venema, and W. S. Kim. Role of computer graphics in space telerobotics: preview and predictive displays. In *Proceedings of SPIE Conference on Cooperative Intelligent Robotics in Space*, 1387:365–377, Boston, MA, USA, 1991.

[11] P. Berestesky, N. Chopra, and M. Spong. Discrete time passivity in bilateral teleoperation over the internet. In *Proceedings of International Conference on Robotics and Automation*, 4557–4564, New Orleans, LA, 2004.

[12] S. E. Butner and M. Ghodoussi. Transforming a surgical robot for human telesurgery. In *IEEE Transactions on Robotics and Automation*, 19(5):818–824, 2003.

[13] F. M. Callier. Dissipative systems analysis and control: Theory and applications (2nd edition) In *IEEE Transactions on Automatic Control*, 52(7):1357–1358, 2007.

[14] C. Carignan and H. Krebs. Telerehabilitation robotics: bright lights, big future? In *Journal of Rehabilitation Research and Development*, 43(5):695–710.

[15] J. Colgate and G. Schenkel. Passivity of a class of sampled-data systems: Application to haptic interfaces. In *Journal of Robotic Systems*, 14(1):37–47, 1997.

[16] N. Diolaiti, G. Niemeyer, F. Barbagli, and J. J.K. Salisbury. Stability of haptic rendering: Discretization, quantization, time delay, and coulomb effects. In *IEEE Transactions on Robotics*, 22(2):256– 268, 2006.

[17] M. Dyck, A. Jazayeri, and M. Tavakoli. Is the human operator in a teleoperation system passive? In *Proceedings of IEEE World Haptics Conference*, Daejeon, Korea, 683–688, 2013.

[18] K. Fite, L. Shao, and M. Goldfarb. Loop shaping for transparency and stability robustness in bilateral telemanipulation. In *IEEE Transactions on Robotics and Automation*, 20(3):620–624, 2004.

[19] M. Fotoohi, S. Sirouspour, and D. Capson. A multi-rate control approach to haptic interaction in multi-user virtual environments. In *Proceedings of IEEE International Conference on Robotics and Automation*, 99–104, Rome, Italy, 2007.

[20] J. Funda and R. Paul. A symbolic teleoperator interface for time-delayed underwater robot manipulation. In *Proceedings*

of Ocean Technologies and Opportunities in the Pacific for the 90's, 1526–1533, Honolulu, HI, USA, 1991.

[21] M. Ghodoussi, S. Butner, and Y. Wang. Robotic surgery - the transatlantic case. In *Proceedings of IEEE International Conference on Robotics and Automation*, 2:1882–1888, Washington DC, USA, 2002.

[22] J. Gil, A. Avello, A. Rubio, and J. Florez. Stability analysis of a 1-DoF haptic interface using the Routh-Hurwitz criterion. In *IEEE Transactions on Control Systems Technology*, 12(4):583–588, 2004.

[23] J. Gil, E. Sanchez, T. Hulin, C. Preusche, and G. Hirzinger. Stability boundary for haptic rendering: Influence of damping and delay. In *Proceeding of IEEE International Conference on Robotics and Automation*, 124–129, Rome, Italy, 2007.

[24] R. Gillespie and M. Cutkosky. Stable user-specific rendering of the virtual wall. In *Proceedings of the ASME International Mechanical Engineering Conference and Exposition*, 58:397–406, Atlanta, GA, USA, November 1996.

[25] M. Glencross, C. Jay, J. Feasel, L. Kohli, M. Whitton, and R. Hubbold. Effective cooperative haptic interaction over the internet. In *Proceedings of IEEE Virtual Reality Conference*, 115–122, Charlotte, NC, USA, 2007.

[26] M. Grunwald. *Human Haptic Perception: Basics and Applications*. Birkhäuser Basel, 2008.

[27] B. Hannaford and J.-H. Ryu. Time-domain passivity control of haptic interfaces. In *IEEE Transactions on Robotics and Automation*, 18(1):1 –10, 2002.

[28] S. Haykin. *Active Network Theory*. Addison-Wesley, Reading, MA, 1970.

[29] D. Hill and P. Moylan. Stability results for nonlinear feedback systems. In *Automatica*, 13(4):377 – 382, 1977.

[30] P. F. Hokayem and M. W. Spong. Bilateral teleoperation: An historical survey. In *Automatica*, 42(12):2035 – 2057, 2006.

[31] H. L. Karamanoukian, R. U. Pande, Y. Patel, A. M. Freeman, P. S. Aoukar and G. D'Ancona. Telerobotics, Telesurgery, and Telementoring. In *Pediatric endosurgery and innovative techniques* 7(4):421–425, 2003.

[32] T. Hulin, C. Preusche, and G. Hirzinger. Stability boundary for haptic rendering: Influence of human operator. In *Proceedings of IEEE/RSJ International Conference on Intelligent Robots and Systems*, 3483–3488, Pasadena, CA, USA, 2008.

[33] J. Gil, T. Hulin, C. Preusche, E. Sanchez, and G. Hirzinger. Stability boundary for haptic rendering: Influence of damping and delay. In *Journal of Computing and Information Science in Engineering*, 9(1), 011005–011013, 2009.

[34] D. Jack, R. Boian, A. Merians, M. Tremaine, G. Burdea, S. Adamovich, M. Recce, and H. Poizner. Virtual reality-enhanced stroke rehabilitation. In *IEEE Transactionson Neural Systems and Rehabilitation Engineering*, 9(3):308–318, 2001.

[35] A. Jazayeri, M. Dyck, and M. Tavakoli. Stability analysis of teleoperation systems under strictly passive and non-passive operator. In *Proceedings of IEEE World Haptics Conference*, 695–700, Daejeon, Korea, 2013.

[36] A. Jazayeri and M. Tavakoli. A passivity criterion for sampled-data bilateral teleoperation systems. In *Proceedings of IEEE World Haptics Conference*, 487–492, Istanbul, Turkey, 2011.

[37] A. Jazayeri and M. Tavakoli. Absolute stability analysis of sampled-data scaled bilateral teleoperation systems. In *Control Engineering Practice*, 21(8):1053 – 1064, 2013.

[38] T. Kanno and Y. Yokokohji. Multilateral teleoperation control over time-delayed computer networks using wave variables. In *Proceedings of IEEE Haptics Symposium*, 125–131, Vancouver, Canada, 2012.

[39] B. Khademian and K. Hashtrudi-Zaad. A four-channel multilateral shared control architecture for dual-user teleoperation systems. In *Proceedings of IEEE/RSJ International Conference on Intelligent Robots and Systems*, 2660–2666, San Diego, CA, USA, 2007.

[40] B. Khademian and K. Hashtrudi-Zaad. Kinesthetic performance analysis of dual-user teleoperation systems. In *Proceedings of IEEE International Conference on Systems, Man and Cybernetics*, 228–233, Montreal, QC, Canada, 2007.

[41] B. Khademian and K. Hashtrudi-Zaad. A robust multilateral shared controller for dual-user teleoperation systems. In *Pro-*

ceedings of Canadian Conference on Electrical and Computer Engineering, 001871–001876, Niagara Falls, ON, Canada, 2008.

[42] B. Khademian and K. Hashtrudi-Zaad. Unconditional stability analysis of dual-user teleoperation systems. In *Proceedings of IEEE Haptics Symposium*, 161–166, Waltham, MA, 2010.

[43] B. Khademian and K. Hashtrudi-Zaad. Dual-user teleoperation systems: New multilateral shared control architecture and kinesthetic performance measures. In*IEEE/ASME Transactions on Mechatronics*, 17(5):895–906, 2012.

[44] H. Khalil. *Nonlinear Systems*. Prentice Hall, 2002.

[45] L. Hitz and B. D. O. Anderson. Discrete positive-real functions and their application to system stability. In *Proceedings of the Institution of Electrical and Engineers*, 116(1):153–155, 1969.

[46] D. A. Lawrence. Stability and transparency in bilateral teleoperation. In *IEEE Transactions on Robotics & Automation*, 9:624–637, October 1993.

[47] G. Leung and B. Francis. Bilateral control of teleoperators with time delay through a digital communication channel. In *Proceedings of the Thirtieth Annual Allerton Conference on Communication, Control and Computing*, 692–701, Urbana, IL, USA, 1992.

[48] J. Lim, J. Ko, and J. Lee. Internet-based teleoperation of a mobile robot with force-reflection. In *Proceedings of 2003 IEEE Conference on Control Applications*, 1:680–685, Istanbul, Turkey, 2003.

[49] A. Madhani, G. Niemeyer, and J. K. Salisbury. Jr. The black falcon – a teleoperated surgical instrument for minimally invasive surgery. In *Proceedings of IEEE/RSJ International Conference on Intelligent Robots and Systems*, Victoria, BC, Canada, 1998.

[50] R. McColl, I. Brown, C. Seligman, F. Lim, and A. Alsaraira. Haptic rendering perception studies for laparoscopic surgery simulation. In *Proceedings of International Conference of the IEEE Engineering in Medicine and Biology Society*, 833–836, New York City, NY, USA, 2006.

[51] M. Minsky, O.-y. Ming, O. Steele, F. P. Brooks, Jr., and M. Behensky. Feeling and seeing: Issues in force display. In *Proceedings of the 1990 Symposium on Interactive 3D Graphics*, 235–241, New York, NY, USA, 1990.

[52] C. Nichol and M. Manic. Video game device haptic interface for robotic arc welding. In *Proceedings of 2nd Conference on Human System Interactions*, 648–653, Catania, Italy, 2009.

[53] G. Niemeyer, C. Preusche, and G. Hirzinger. Telerobotics. In B. Siciliano and O. Khatib, editors, *Springer Handbook of Robotics*, 741–757. Springer Berlin Heidelberg, 2008.

[54] G. Niemeyer and J.-J. E. Slotine. *Towards Bilateral Internet Teleoperation*, page 193–213. The MIT Press, Cambridge, MA, 2001.

[55] G. Niemeyer and J. J. E. Slotine. Telemanipulation with time delays. In *International Journal of Robotics Research*, 23(9):873–890, 2004.

[56] G. Niemeyer, G. Verghese, and T. Sheridan. Design issues in 2-port network models of bilateral remote manipulation. In *Proceedings of IEEE International Conference on Robotics and Automation*, 3:1316 –1321, Scottsdale, AZ, USA, 1989.

[57] M. Orozco and A. P. E. Silva, J. El Saddik. The role of haptics in games. In *Haptics Rendering and Application*, 2:1221–1226, 2012.

[58] P. F. Hokayem, D. M. Stipanovic and M. Spong. Suboptimal master-slave teleoperation control with delays. In *Proceedings of the 2006 American Control Conference*, Minnesota, USA, June 2006.

[59] B. Perez-Gutierrez, D. Martinez, and O. Rojas. Endoscopic endonasal haptic surgery simulator prototype: A rigid endoscope model. In *Proceedings of IEEE Virtual Reality Conference*, 297–298, Waltham, MA, USA, 2010.

[60] V. Popescu, G. Burdea, M. Bouzit, and V. Hentz. A virtual-reality-based telerehabilitation system with force feedback. In *IEEE Transactions on Information Technology in Biomedicine*, 4(1):45–51, 2000.

[61] J.-H. Ryu, B. Hannaford, C. Preusche, and G. Hirzinger. Time domain passivity control with reference energy behavior. In *Proceedings of IEEE/RSJ International Conference on Intelligent Robots and Systems*, 3:2932 – 2937, Las Vegas, Nev, USA, 2003.

[62] S. Salcudean. Control for teleoperation and haptic interfaces. In B. Siciliano and K. Valavanis, editors, *Control Problems in Robotics and Automation*, volume 230 of *Lecture Notes in Control and Information Sciences*, 51–66. Springer Berlin Heidelberg, 1998.

[63] G. Sankaranarayanan and B. Hannaford. Experimental internet haptic collaboration using virtual coupling schemes. In *Proceedings of International symposium on Haptic interfaces for virtual environment and teleoperator systems*, 259–266, Reno, Nev, 2008.

[64] J. Sheng and P. Liu. A review of bilateral sampled-data control of teleoperators. In *Proceedings of IEEE International Conference on Robotics and Biomimetics*, 385 –390, Shenyang, China, 2004.

[65] T. Sheridan. Telerobotics. In *Automatica*, 25(4):487 – 507, 1989.

[66] S. Sirouspour. Modeling and control of cooperative teleoperation systems. In *IEEE Transactions on Robotics*, 21(6):1220–1225, 2005.

[67] S. Sirouspour and P. Setoodeh. Multi-operator/multi-robot teleoperation: an adaptive nonlinear control approach. In *Proceedings of IEEE/RSJ International Conference on Intelligent Robots and Systems*, 1576–1581, Edmonton, AB, 2005.

[68] S. Stramigioli, C. Secchi, A. van der Schaft, and C. Fantuzzi. A novel theory for sample data system passivity. In *Proceedings of the IEEE/RSJ International Conference on Intelligent Robots and Systems*, 1936–1941, Lausanne, Switzerland, 2002.

[69] M. Tavakoli, A. Aziminejad, R. Patel, and M. Moallem. Discrete-time bilateral teleoperation: modelling and stability analysis. In *IET Control Theory and Applications*, 2(6):496–512, June 2008.

[70] M. Tavakoli, A. Aziminejad, R. V. Patel, and M. Moallem. Stability of discrete-time bilateral teleoperation control. In *Proceedings of International Conference on Intelligent Robots and Systems*, 1624–1630, San Diego, CA, USA, October 2007.

[71] U. Tumerdem and K. Ohnishi. Delay independent L2 stable multilateral teleoperation with damping injection. In *Proceedings of IEEE International Conference on Industrial Technology*, 88–93, Valparaiso, Chile, 2010.

[72] S. Ullrich and T. Kuhlen. Haptic palpation for medical simulation in virtual environments. In *IEEE Transactions on Visualization and Computer Graphics*, 18(4):617–625, 2012.

[73] W. Wei and Y. Kui. Teleoperated manipulator for leak detection of sealed radioactive sources. In *Proceedings of IEEE International Conference on Robotics and Automation*, 2:1682–1687, New Orleans, LA, USA, 2004.

[74] N. Yasrebi and D. Constantinescu. Centralized multi-user multi-rate haptic cooperation using wave transformation. In *Proceedings of International Conference on Mechatronics and Automation*, 3816–3821, Changchun, China, 2009.

[75] Y. Yokokohji and T. Yoshikawa. Bilateral control of master-slave manipulators for ideal kinesthetic coupling-formulation and experiment. In *Proceedings of IEEE International Conference on Robotics and Automation*, 2:849–858, Nice, France, 1992.

[76] W.-K. Yoon, T. Goshozono, H. Kawabe, M. Kinami, Y. Tsumaki, M. Uchiyama, M. Oda, and T. Doi. Model-based space robot teleoperation of ets-vii manipulator. In *IEEE Transactions on Robotics and Automation*, 20(3): 602–612, 2004.

[77] C. Basdogan, S. De, J. Kim, M. Muniyandi, H. Kim, and M. Srinivasan, Haptics in minimally invasive surgical simulation and training. In *IEEE Transactions on Computer Graphics and Applications*, 24:(2):56–64, 2004.

[78] B. Chebbi, D. Lazaroff, F. Bogsany, P. X. Liu, L. Niy, and M. Rossi, Design and implementation of a collaborative virtual haptic surgical training system. In *Proceedings of IEEE International Conference Mechatronics and Automation*, 1:315–320, 2005.

[79] C. R. Carignan, and P. A. Olsson, Cooperative control of virtual objects over the Internet using force-reflecting master arms. In Proceedings of International Conference on Robotics and Automation, 2:1221–1226, New Orleans, LA, USA, 2004.

[80] M. Johnson, R. Loureiro, and W. Harwin, Collaborative tele-rehabilitation and robot-mediated therapy for stroke rehabilitation at home or clinic. In *Intelligent Service Robotics*, 2(2):109–121, 2008.

[81] I. Goncharenko, M. Svinin, S. Matsumoto, Y. Masui, Y. Kanou, and S. Hosoe, Cooperative control with haptic visualization in shared virtual environments. In *Proceedings of International Conference on Information Visualisation*, 533–538, London, UK, 2004.

[82] C. Ho, C. Basdogan, M. Slater, N. Durlach, and M. A. Srinivasan, An Experiment on the Influence of Haptic Communication on the Sense of Being Together. In *Proceedings of the British Telecom Workshop on Presence in Shared Virtual Environments*, 525–532, Ipswich, UK, 1998.

A

APPENDIX

A.1 PROOF OF RAISBECK'S PASSIVITY CRITERION

Raisbeck's passivity criterion [28]. The necessary and sufficient condition for passivity of a 2-port network with immitance parameters p are

1. The p-parameters have no RHP poles
2. Any poles of the p-parameters on the imaginary axis are simple, and the residues of the p-parameters at these poles satisfy the following conditions (k_{ij} denotes the residue of p_{ij} and k_{ij}^* is the complex conjugate of k_{ji}):

$$\begin{aligned} &k_{11} \geq 0 \\ &k_{22} \geq 0 \\ &k_{11}k_{22} - k_{12}k_{21} \geq 0, \quad \textit{with} \quad k_{21} = k_{12}^* \end{aligned}$$

3. The real and imaginary part of the p parameters satisfy

$$\begin{aligned} &\Re p_{11} \geq 0 \\ &\Re p_{22} \geq 0 \\ &4\Re p_{11}\Re p_{22} - (\Re p_{12} + \Re p_{21})^2 - (\Im p_{12} - \Im p_{21})^2 \geq 0 \end{aligned}$$

Proof.

$$G(j\omega) = \begin{bmatrix} p_{11}(j\omega) & p_{12}(j\omega) \\ p_{21}(j\omega) & p_{22}(j\omega) \end{bmatrix}$$

is positive real if

$$\begin{aligned} &G(j\omega) + G^T(-j\omega) = \\ &\begin{bmatrix} p_{11}(j\omega) + p_{11}(-j\omega) & p_{12}(j\omega) + p_{21}(-j\omega) \\ p_{21}(j\omega) + p_{12}(-j\omega) & p_{22}(j\omega) + p_{22}(-j\omega) \end{bmatrix} = \\ &\begin{bmatrix} \Re P_{11} & ((\Re P_{12} + \Re P_{21}) + j(\Im P_{12} - \Im P_{21})) \\ ((\Re P_{12} + \Re P_{21}) - j(\Im P_{12} - \Im P_{21})) & 2\Re P_{22} \end{bmatrix} \end{aligned}$$

is positive semidefinite. Since positive semi-definiteness is equivalent to having non-negative leading principle minors, the conditions in 3 will be met. Also the following matrix must be positive semidefinite Hermitian (k_{ij} denotes the residue of p_{ij} and k^*ij is the complex conjugate of k_{ij}):

$$lim_{s\to\ j\omega}(s - j\omega)G(s) = \begin{bmatrix} k_{11} & k_{12} \\ k_{21} & k_{22} \end{bmatrix}$$

Applying the positive semidefinite Hermitian conditions will leave us with the same conditions in 2. This concludes the proof.

□

A.2 EXTENSION OF PASSIVITY THEOREM TO 4CH TRILATERAL TELEOPERATION SYSTEMS

Theorem A.2.1. *The system modeled in Figure 5.15 is stable if each of Z_{h1}, Z_{h2}, Z_e, MCU_1, MCU_2, MCU_3, $CC_{1,2}$, $CC_{1,s}$ and $CC_{2,s}$ are passive.*

Proof. Let $V_1(x_1)$, $V_2(x_2)$, $V_3(x_3)$, $V_4(x_4)$, $V_5(x_5)$, $V_6(x_6)$, $V_7(x_7)$, $V_8(x_8)$ and $V_9(x_9)$ be the storage functions of Z_e, the SCU, CC_2, s, Z_{h2}, the MCU_2, $CC_{1,s}$, $CC_{1,2}$, Z_{h1} and the MCU_1. Assume the initial stored energy in each of these systems is zero. Based on Definition 5.3.2

$$e_i^T y_i \geq \dot{V}_i \tag{A.1}$$

Fom the feedback loops in Fig. 5.15, it can be seen that

$$e_1 = u_1 + \begin{bmatrix} 1 & 0 & 0 \end{bmatrix} y_2 \tag{A.2}$$

$$e_2 = \begin{bmatrix} \begin{bmatrix} 1 & 0 & 0 \end{bmatrix} u_2 - y_1 \\ \begin{bmatrix} 0 & 1 & 0 \end{bmatrix} u_2 - \begin{bmatrix} 1 & 0 \end{bmatrix} y_6 \\ \begin{bmatrix} 0 & 0 & 1 \end{bmatrix} u_2 - \begin{bmatrix} 1 & 0 \end{bmatrix} y_3 \end{bmatrix} \tag{A.3}$$

$$e_3 = \begin{bmatrix} \begin{bmatrix} 1 & 0 \end{bmatrix} u_3 + \begin{bmatrix} 0 & 0 & 1 \end{bmatrix} y_2 \\ \begin{bmatrix} 0 & 1 \end{bmatrix} u_3 + \begin{bmatrix} 0 & 0 & 1 \end{bmatrix} y_5 \end{bmatrix} \tag{A.4}$$

$$e_4 = u_4 + \begin{bmatrix} 1 & 0 & 0 \end{bmatrix} y_5 \tag{A.5}$$

$$e_5 = \begin{bmatrix} \begin{bmatrix} 1 & 0 & 0 \end{bmatrix} u_5 - y_4 \\ \begin{bmatrix} 0 & 1 & 0 \end{bmatrix} u_5 - \begin{bmatrix} 1 & 0 \end{bmatrix} y_7 \\ \begin{bmatrix} 0 & 0 & 1 \end{bmatrix} u_5 - \begin{bmatrix} 0 & 1 \end{bmatrix} y_3 \end{bmatrix} \tag{A.6}$$

$$e_6 = \begin{bmatrix} \begin{bmatrix} 1 & 0 \end{bmatrix} u_6 + \begin{bmatrix} 0 & 1 & 0 \end{bmatrix} y_2 \\ \begin{bmatrix} 0 & 1 \end{bmatrix} u_6 + \begin{bmatrix} 0 & 0 & 1 \end{bmatrix} y_9 \end{bmatrix} \tag{A.7}$$

$$e_7 = \begin{bmatrix} \begin{bmatrix} 1 & 0 \end{bmatrix} u_7 + \begin{bmatrix} 0 & 1 & 0 \end{bmatrix} y_5 \\ \begin{bmatrix} 0 & 1 \end{bmatrix} u_7 + \begin{bmatrix} 0 & 1 & 0 \end{bmatrix} y_9 \end{bmatrix} \tag{A.8}$$

$$e_8 = u_8 + \begin{bmatrix} 1 & 0 & 0 \end{bmatrix} y_9 \tag{A.9}$$

$$e_9 = \begin{bmatrix} \begin{bmatrix} 1 & 0 & 0 \end{bmatrix} u_9 - y_8 \\ \begin{bmatrix} 0 & 1 & 0 \end{bmatrix} u_9 - \begin{bmatrix} 0 & 1 \end{bmatrix} y_7 \\ \begin{bmatrix} 0 & 0 & 1 \end{bmatrix} u_9 - \begin{bmatrix} 0 & 1 \end{bmatrix} y_6 \end{bmatrix} \tag{A.10}$$

Therefore, it is easy to show that

$$\sum_i^9 e_i^T y_i = \sum_i^9 u_i^T y_i$$

For the entire teleoperation system, let us define

$$u = \begin{bmatrix} u_1 & u_2 & u_3 & u_4 & u_5 & u_6 & u_7 & u_8 & u_9 \end{bmatrix}^{\mathrm{T}}$$
$$y = \begin{bmatrix} y_1 & y_2 & y_3 & y_4 & y_5 & y_6 & y_7 & y_8 & y_9 \end{bmatrix}^{\mathrm{T}}$$

Thus,

$$u^T y = \sum_i^9 u_i^T y_i \geq \sum_i^9 \dot{V}_i$$

Taking $V(x) = V_1(x_1) + V_2(x_2) + V_3(x_3) + V_4(x_4) + V_5(x_5) + V_6(x_6) + V_7(x_7) + V_8(x_8) + V_9(x_9)$, we obtain

$$u^T y \geq \dot{V} \tag{A.11}$$

This concludes the proof. □

COLOPHON

This document was typeset using the typographical look-and-feel `classicthesis` developed by André Miede. The style was inspired by Robert Bringhurst's seminal book on typography "*The Elements of Typographic Style*". `classicthesis` is available for both LaTeX and LyX:

http://code.google.com/p/classicthesis/

Happy users of `classicthesis` usually send a real postcard to the author, a collection of postcards received so far is featured here:

http://postcards.miede.de/

Final Version as of August 28, 2013 (`classicthesis`).